Aus dem Institut für Immunologie
im Biomedizinischen Centrum (BMC)
der Ludwig-Maximilians-Universität München
Medizinische Fakultät

Vorstand: Prof. Dr. Thomas Brocker

The role of cathepsin L in shaping a functional CD4 T cell repertoire

Dissertation
zum Erwerb des Doktorgrades der Naturwissenschaften
an der Medizinischen Fakultät der
Ludwig-Maximilians-Universität München

Vorgelegt von
Elisabetta Petrozziello

aus
Ravenna

2019

Mit Genehmigung der Medizinischen Fakultät
der Universität München

Betreuer:	Prof. Dr. Ludger Klein
Zweitgutachterin:	Prof. Dr. Gerhild Wildner
Dekan:	Prof. Dr. med. dent. Reinhard Hickel

Tag der mündlichen Prüfung: 09.09.2019

Ai miei genitori, a cui devo tutto.

"Don't be afraid of hard work. Nothing worthwhile comes easily.
Don't let others discourage you or tell you that you can't do it.
In my day I was told women didn't go into chemistry.
I saw no reason why we couldn't." — Gertrude B. Elion

Abstract

The generation of the fittest T cell repertoire is accomplished through thymic positive selection. During this process, cortical thymic epithelial cells (cTECs) present self-peptides on major histocompatibility complex (self-pMHC) to developing T cells, in order to test their T cell receptor (TCR) reactivity. Since cTECs possess a unique antigen-processing machinery for the generation of self-pMHC, it is likely that these peculiar peptides are optimized to mediate positive selection and are not found elsewhere in the body. In the thymic cortex, only the T cells expressing a TCR with low affinity to the positively-selecting self-pMHC molecules will survive, so that the mature repertoire will be eventually composed of T cells bearing the right MHC-restriction and a functional TCR.

With our project, we aimed at unraveling the importance of cTEC-specific antigen-processing pathways in shaping a functional T cell repertoire. In particular, we focused on a cortical protease involved in the generation of peptides for the loading of MHCII, namely cathepsin L (CTSL). In order to investigate the impact of this single cortex-specific protease on the quality of the selected $CD4^+$ T cell compartment, we took advantage of a conditional knock-out mouse model where the expression of CTSL is ablated in the thymic epithelium. Using this mouse model, we analyzed $CD4^+$ T cell development in three parallel settings, i. e. in bulk polyclonal $CD4^+$ T cells, as well as in a subset of $CD4^+$ T cells specific for the listeriolysin O (LLO) antigen and in a TCR-oligoclonal $CD4^+$ T cell repertoire. In all cases, deficiency of CTSL during positive selection led to a severe impairment of the $CD4^+$ T cell compartment, affecting both T cell numbers and TCR diversity, although we could identify some TCRs that are selected regardless of CTSL expression. Furthermore, polyclonal TCR stimulation and LLO immunization revealed defective T cell responses in CTSL-deficient mice, which could derive from a decreased functionality of TCRs *per* se or from the lack of some specific TCR clones.

In order to test if the very same TCR – selected in the presence or absence of CTSL – can be equally functional, we are currently re-expressing some putative "CTSL-independent" TCRs in retrogenic mice. These experiments will clarify if the positively-selecting peptides produced by CTSL play a direct role in the generation of a functional $CD4^+$ T cell compartment.

Zusammenfassung

Die Schaffung des tauglichsten T-Zell-Repertoires wird durch die positive Selektion im Thymus gewährleistet. Während dieses Prozesses werden den entwickelnden T-Zellen körpereigene Peptide auf dem Haupthistokompatibilitätskomplex (self-pMHC) von kortikalen Thymusepithelzellen (cTECs) präsentiert, um die Reaktivität des T-Zell-Rezeptors (TCR) zu testen. Da cTECs für die Erzeugung von self-pMHC über einen einzigartigen Mechanismus der Antigen Verarbeitung verfügen, ist es naheliegend, dass diese speziellen Peptide für die Vermittlung der positiv Selektion optimiert und sonst nicht im Körper zu finden sind. Im thymischen Cortex werden nur die T-Zellen überleben die einen TCR mit geringer Affinität gegenüber den positiv-selektierenden self-pMHC Molekülen exprimieren, dass letztendlich das reife Repertoire aus T-Zellen besteht, welche die richtige MHC-Restriktion und einen funktionellen TCR besitzen.

Mit unserem Projekt wollen wir daher die Bedeutung von cTEC-spezifischen Mechanismen der Antigen-Prozessierung für die Bildung eines funktionellen T-Zell-Repertoires herausfinden. Insbesondere haben wir uns auf eine kortikale Protease, Cathepsin L (CTSL), fokussiert, welche bei der Generation von Peptiden für den MCHII involviert ist. Um den Einfluss dieser einzelnen cortexspezifischen Protease auf die Qualität des ausgewählten $CD4^+$ T-Zell-Kompartiments zu untersuchen, nutzten wir die Vorteile eines konditionalen Knockout Mausmodells, bei dem CTSL im Thymusepithel nicht exprimiert ist. In diesem Mausmodell analysierten wir die Entwicklung von $CD4^+$ T-Zellen in drei unterschiedlichen Szenarien, d.h. in allen polyklonale $CD4^+$ T-Zellen, sowie in einer Listeriolysin O (LLO) spezifischen $CD4^+$ T-Zellen Fraktion und in einem TCR oligoklonalen $CD4^+$ T-Zell-Repertoire.

In allen Fällen führte ein Mangel an CTSL während der positiv Selektion zu einer schweren Beeinträchtigung des $CD4^+$ T-Zell-Kompartiments, was sowohl die Anzahl der T-Zellen als auch die TCR Diversität betrifft, trotz alledem konnten wir einige TCRs identifizieren, welche unabhängig von der CTSL Expression waren. Darüber hinaus offenbarten polyklonale TCR Stimulationen und LLO Immunisierungen in CTSL-defizienten Mäusen defekte T-Zell-Reaktionen, welche auf eine verminderten Funktionalität der TCR *per se* oder dem Fehlen einiger spezifischer TCR Klone zurückzuführen sind.

Um zu testen, ob ein und der selbe TCR – ausgewählt in der An- und Abwesenheit von CTSL – gleichermaßen funktionell sein kann, re-exprimieren wir derzeit einige mutmaßliche „CTSL-unabhängige" TCRs in retrogenen Mäusen. Diese Experimente werden klären, ob die positiv-selektierenden Peptide, die von CTSL produziert werden, eine direkte Rolle bei der Erzeugung eines funktionellen $CD4^+$ T-Zell-Kompartiments spielen.

Table of contents

1. Introduction

1.1 Overview

1.1.1 Adaptive immunity

The "Big Bang" of immunology dates back to 500 million years ago, when the adaptive branch of the immune system suddenly appeared in vertebrates, in concomitance with the development of the jaw. This new anatomical structure endowed fish, such as sharks, with an extraordinary predatory capacity, but increased also the likelihood that ingested material could provoke intestinal injuries and infections [1]. It is however only in warm-blooded vertebrates, in which pathogens can replicate quickly, that the full potential of adaptive immunity began to be exploited. Indeed, birds and mammals can recognize and fight threats with extreme specificity and efficiency, thanks to the generation of virtually infinite antigen-receptor diversity, as well as of long-lasting memory that protects them from further reinfection with the same microbes.

The effectors of adaptive immunity are known as lymphocytes, which comprise T (from Thymus) and B (from Bursa of Fabricius in birds and Bone marrow in mammals) cells. Lymphocytes clonally express antigen receptors named T Cell Receptors (TCRs) or antibodies, which recognize peptides presented on major histocompatibility complex (MHC) molecules or proteins in their native conformation, respectively. T lymphocytes can be further classified, based on their function and/or expression of CD8 or CD4 TCR co-receptor molecules, into cytotoxic $CD8^+$ T cells, helper $CD4^+$ T cells and regulatory $CD4^+$ T cells. Since the CD8 co-receptor facilitates contacts to MHC class I molecules (MHCI), present on all nucleated cells, cytotoxic T cells are specialized in detecting and eliminating infected or tumor cells from the organism. In a parallel way, CD4 enables interactions to MHC class II molecules (MHCII), which are expressed on antigen-presenting cells (APCs), including B cells. Therefore helper and regulatory T lymphocytes can influence the differentiation and behavior of these cells, thereby amplifying or dampening the immune response, respectively. Of note, both the T and B arms of the adaptive immune system are required for an optimal immune response: on one hand the cytotoxic action of $CD8^+$ T cells allows the elimination of infected or transformed cells, whereas on the other hand

the production of high-affinity antibodies by B cells, with the "help" of $CD4^+$ T cells, assures the direct neutralization of pathogens.

1.1.2 The thymus

Although the notion that the thymus fulfills a unique physiological function is nowadays included in all textbooks, less than sixty years ago the majority of world-renowned scientists could not accept this idea and considered it only a useless vestigial organ. Indeed, in support of the latter theory, thymectomy performed on adult mice and humans failed to cause any sign of pathology. It was not until the early 60s that an "immunological function of the thymus" was postulated, when pioneer work by Jacques Miller revealed that thymectomized newborn mice were severely lymphopenic, could not reject skin grafts from allogeneic donors and had an increased susceptibility to tumors and infections [2-5]. However, when thymectomized newborns received a thymic graft, their immunological competence was restored; furthermore, if the thymus graft came from a different mouse strain, the recipient could accept skin grafts of both donor and recipient – but not of third-party – origin [3]. These and other follow-up experiments suggested that the thymus could be the organ where lymphocytes mature into functional and self-tolerant cells. At that time, the distinction between T and B cells was not yet clear, but the thymus was later identified as the primary lymphoid organ where T lymphocytes develop (reviewed in [6]).

From an evolutionary perspective, the thymus appeared in jawed vertebrates as key tissue of the adaptive immune system and it was originally located bilaterally, next to the gills. In mammals it is a bi-lobed structure situated in the upper thorax, behind the sternum and right above the heart. Histologically, one can distinguish different lobules, each containing an outer, cell-dense cortex and an inner, less compact medulla. This structural bipartition reflects a functional compartmentalization, which will be clarified in section 1.2. The architecture and cellular composition of thymic lobules are illustrated in figure 1: the cortex contains mainly developing T cells, known as thymocytes, and cortical thymic epithelial cells (cTECs), but also some macrophages, which eat up the dying thymocytes, and very few dendritic cells (DCs); the medulla is composed mostly of mature thymocytes, medullary thymic epithelial cells (mTECs) and DCs, but also scattered macrophages and B cells. During embryonic development, the thymus originates from the third pharyngeal pouch endoderm as early as the sixth gestational week in humans

(around embryonic day 11 in mice): it is initially a purely epithelial structure, but it is soon colonized by hematopoietic cells (reviewed in [7]). Indeed, the first phase of differentiation of the thymic epithelium is thymocyte-independent and relies only on the expression of Foxn1 (the mutated gene in *nude* mice); subsequently, the "crosstalk" between thymocytes and thymic epithelial cells is fundamental to ensure proper maturation and organization of the final thymic environment (reviewed in [8]).

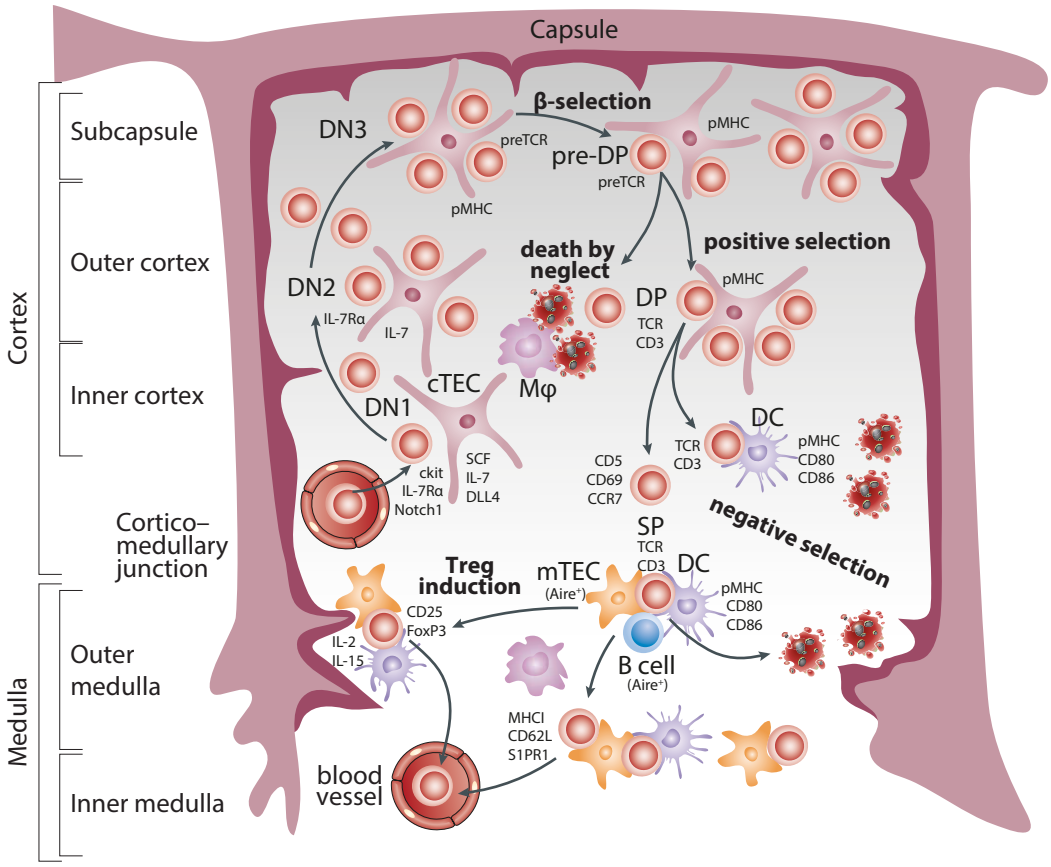

Figure 1: T cell developmental stages map to distinct thymic regions
DN1 (double negative 1, $CD4^-$ $CD8^-$) T cell precursors enter the thymus through venules at the cortico-medullary junction and start migrating outwards in the cortex. DN2 are found in the outer cortex, whereas DN3 and pre-DP (double positive, $CD4^+$ $CD8^+$) thymocytes prevail in the subcapsular region. From this stage on, thymocytes invert their direction of migration and proceed towards the inner cortex, so DP cells are found in the outer and inner cortex. cTECs (cortical thymic epithelial cells) play a crucial role throughout the cortical stages of development, by providing cytokines (e.g. SCF, IL-7), ligands (e.g. DLL4) and pMHC (peptide-Major Histocompatibility Complex) that promote survival, proliferation, T cell lineage commitment and/or maturation of thymocytes. SP (single positive, CD4SP or CD8SP) thymocytes are prominent in the outer medulla, where they encounter a variety of APCs (antigen-presenting cells), such as mTECs (medullary thymic epithelial cells), DCs (dendritic cells) and B cells. Interaction of SP thymocytes with pMHC displayed by any of these cell types induces central tolerance, i.e. either negative selection or diversion into the Treg (T regulatory) compartment. Negative selection can also be induced by DCs residing in the cortico-medullary junction, which interact with DP cells. The final stages of maturation take place in the inner medulla, where thymocytes acquire the expression of MHCI and

molecules necessary for egress (CD62L, S1PR1). Crucial factors involved in every developmental step are depicted in the figure. Macrophages are present both in the cortex and the medulla, in order to remove cellular debris that result from death by neglect or negative selection events. The figure was adapted from [9].

One striking feature of the thymus is that it increases in size in the first years of life, when T cell production is of utmost importance because of lack of a memory compartment, while it starts declining with puberty, until almost the entire parenchyma is replaced by fat and connective tissue in late adulthood. This process is known as thymic involution and is believed to be partially responsible for age-related immunosenescence, although adults are still capable of producing new T cells and do not entirely rely on memory. As an interesting side note, the name "thymus" dates back to the ancient Greek physician and philosopher Galen of Pergamon, who found a resemblance between this organ and the "thyme" plant: oddly enough, the etymology of both terms is connected with the concept of fumes/vapors, as thyme was burnt during religious sacrifices, while the thymus was observed to "evaporate" with age [10].

All in all, the thymus is still an extremely fascinating organ, which shapes the immunocompetence of our T cells in many different – and not yet completely understood – ways. Needless to say, if we had uncovered all its mysteries, I wouldn't have been working on this thesis in the "thymus function" laboratory of Prof. Dr. Ludger Klein.

1.2 αβT cell development

A great advantage brought about by the adaptive immune system is certainly the specificity of pathogen recognition, which is obtained by somatic rearrangements in the genes encoding the antigen receptors. However, for the first time in evolution, this randomly generated diversity of the lymphocyte receptor repertoire put the host at risk of developing autoimmunity, as also self-proteins could be attacked. A primary requisite for a healthy and functional T cell repertoire is therefore its ability to discriminate between "self" and "foreign", hence to mount effective immune responses only against the latter. To ensure this, T cell progenitors undergo in the thymus finely orchestrated selection steps, which aim at maximizing the diversity of the mature repertoire, while minimizing auto-reactivity. T cell development is generally subdivided into three discrete stages, according to the expression of the surface co-receptor molecules CD4 and CD8: an initial

$CD4^-$ $CD8^-$ double negative phase (DN), followed by a $CD4^+$ $CD8^+$ double positive (DP) and finally a $CD4^+$ or $CD8^+$ single positive (SP) one [11] (see figure 2 for more detailed characterization). The most important developmental events taking place in each of these stages are discussed below. Of note, I will focus on the truly adaptive branch of T lymphocytes, i. e. conventional αβT cells, which express TCRs composed of an α and a β chain, unless otherwise specified.

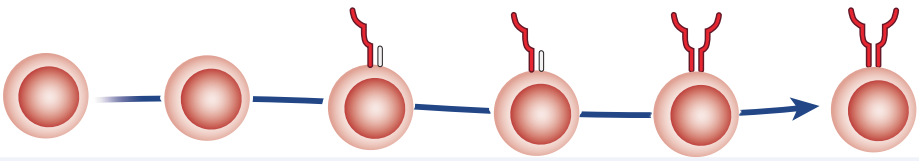

Maturation stage	Early T-cell progenitor/ DN1	Pro-T/ DN2	Early Pre-T/ DN3	Late Pre-T/ DN4/ pre-DP	DP	CD4SP or CD8SP
Location within thymus	cortico-medullary junction	inner cortex	outer cortex/ subcapsule	subcapsule	outer and inner cortex	medulla
Surface markers	ckit+ CD44+ CD25- CD3-	ckit+ CD44+ CD25+ CD3-	ckit- $CD44^{lo}$ CD25+ CD3-	$CD44^{lo}$ CD25- $CD4^{lo}$ $CD8^{lo}$	CD4+ CD8+ $CD3^{lo}$	CD4+ or CD8+ $CD3^{hi}$
TCR genes	Unrecombined (germline) DNA		Recombined TCRβ genes		Recombined TCRβ and TCRα genes	
TCR expression	None		Pre-TCR (TCRβ/pTα)		αβ TCR	
Proliferation	1000-fold		4-fold	250-fold	None	None
Duration	10 days	2 days	2 days	1 day	2 days	7 days
% of total thymocytes	≈0.2%	≈0.2%	≈1.5%	≈1%	≈80%	≈15%

Figure 2: Detailed characterization of T cell developmental stages
The main parameters that characterize the six thymocyte stages, from early T cell progenitor to mature thymocyte, are listed. The figure was adapted from [12]. Estimation of proliferation and duration are based on [13]. DN: double negative; DP: double positive; SP: single positive; TCR: T cell receptor; pTα: pre-TCRα.

1.2.1 DN stages: T cell lineage commitment and β-selection

As shown in figure 1, progenitor cells coming from the bone marrow enter the thymus at the cortico-medullary junction as DN thymocytes, sometimes also referred to as

$CD3^-$ $CD4^-$ $CD8^-$ triple negative (to exclude mature γδT cells and iNKT cells). Their maturation starts in the cortex, thanks to factors – such as SCF (stem cell factor/ckit ligand), IL-7 and DLL4 (Delta-like 4) – provided by cTECs that initially support proliferation, survival and commitment to the T cell lineage [14-16]. Let's not forget, though, that any hematopoietic cell seeding the thymus falls by definition into the DN compartment, but not all of these cells will give rise to conventional αβ T cells. In fact, DN cells are extremely heterogeneous and have been classified into further subsets to better understand their origin and fate. The most traditional classification divides murine DN thymocytes into four chronologically subsequent subsets, known as DN1-4, on the basis of expression of the adhesion molecule CD44 and the receptor CD25 (IL-2Rα) [17]. In this context, CD44 is believed to facilitate interactions with cTECs [18], whereas the function of CD25 remains poorly understood. DN1 thymocytes, i. e. the $CD44^+$ $CD25^-$ and least committed fraction of DN, can be further phenotyped to identify truly lymphoid progenitors, which appear to be $ckit^+$ (CD117) and to bear B, T and NK potential [19]. One of the first events taking place after $ckit^+$ DN1 thymocytes seed the thymus is extensive proliferation, initially in response to SCF [14] and, starting from the late DN1 stage, also to IL-7 [15]. Indeed, the greatest proliferative capacity among thymocytes resides in the $ckit^+$ DN1 fraction [19], which is also one of the longest developmental stages: it is estimated that each progenitor entering the thymus will produce one thousand thymocytes after the first 10 days of serial cell divisions [13]. Another important early event affecting thymic immigrants is the repression of B and NK lineages [20] thanks to the Notch1-DLL4 axis [16], which will signal throughout the entire thymocyte development to ensure T cell lineage specification.

From the cortico-medullary junction, DN thymocytes migrate outwards towards the subcapsular region as they proceed with development, with different stages mapping to specific cortical regions (see figure 1) [21]. DN2 ($CD44^+$ $CD25^+$) thymocytes, also known as pro-T cells, are found in the inner cortex and strictly depend on IL-7 for survival and expansion. At this point the RAG-1 and RAG-2 (recombination activating gene-1 and 2) recombinases start to be expressed and form a heterodimer that targets the TCRβ, TCRδ and/or TCRγ loci, thus producing the first somatic rearrangements among the variable (V), diversity (D) and joining (J) genes of these TCRs [22].

As DN thymocytes move to the outer cortex, they downregulate ckit and CD44 expression, thereby acquiring the phenotype of DN3 ($CD44^-$ $CD25^+$), otherwise known as

early pre-T cells. At this stage, T cell lineage commitment is completed and the αβ/γδ lineage choice is made. Typically 90% of DN3 thymocytes productively rearrange their TCRβ first; this leads to surface expression of the TCRβ chain together with an invariant pre-TCRα (pTα) chain and the CD3 signaling molecules, to form the pre-TCR complex (reviewed in [23]). However, in roughly 10% of the cases both TCRδ and TCRγ loci are rearranged to produce a functional γδTCR that provides stronger signaling than the pre-TCR, thus inducing the commitment to the γδ lineage [24, 25]. Rearrangements on the TCRβ locus are ordered, and require a first D-J_β recombination, followed by a V-DJ_β one: thymocytes that fail to produce an in-frame VDJ_β recombination (and do not divert to the γδ lineage) die by apoptosis; the ones that manage to do so, instead, will express the pre-TCR and be rescued from programmed cell death. This process is known as β-selection and is the first key checkpoint in T cell development. It appears that the pre-TCR can signal both in a ligand-independent manner and upon binding to peptide-MHC (pMHC) (reviewed in [26]), either way promoting survival, TCRβ allelic exclusion and proliferation. This ensures that each thymocyte successfully rearranging a TCRβ chain will terminate VDJ recombination on the second β-allele and expand, so that a single TCRβ will have the chance to pair with different TCRα chains. However, thymocytes expressing β chains predisposed to binding pMHC may be favored in this proliferation phase, so that β-selection would skew the TCRβ repertoire towards mild self-reactivity already before the DP stage.

Relocation to the subcapsular zone takes place at the transition from DN3 to DN4 phase: this area can be visualized as a dense band of proliferating cells [21], as here signaling from the pre-TCR induces respectively a 4-fold and 250-fold expansion of DN3 and DN4 thymocytes [13]. Formally there are no thymocytes that remain DN after the DN3 stage [27], so DN4 have been more appropriately renamed pre-DP cells, as they are in fact $CD4^{lo}$ $CD8^{lo}$. Entry into the pre-DP stage coincides with downregulation of CD25 and initiation of TCRα rearrangements.

1.2.2 DP stage: positive selection, negative selection and CD4/CD8 lineage choice

Expression of detectable levels of both CD4 and CD8 co-receptors marks the beginning of the DP stage, during which thymocytes invert their direction of migration and start moving back into the inner cortex. DP cells are mainly characterized by lack of

proliferative potential, unresponsiveness to cytokines and low surface expression of the TCR. Indeed, random gene recombinations on the TCRα locus that start at the pre-DP phase are completed here; this results in irreversible commitment to the αβ lineage, since the TCRδ genes – which reside within the TCRα locus – are excised when productive VJ_{α} recombinations occur. Unlike VDJ_{β} recombination, though, VJ_{α} recombinations can be generated on both alleles due to lack of allelic exclusion for the TCRα; therefore roughly 8% of mature T cells will express two different TCRα chains on the surface [28]. Further details on the mechanisms that generate αβTCR diversity are shown in figure 3.

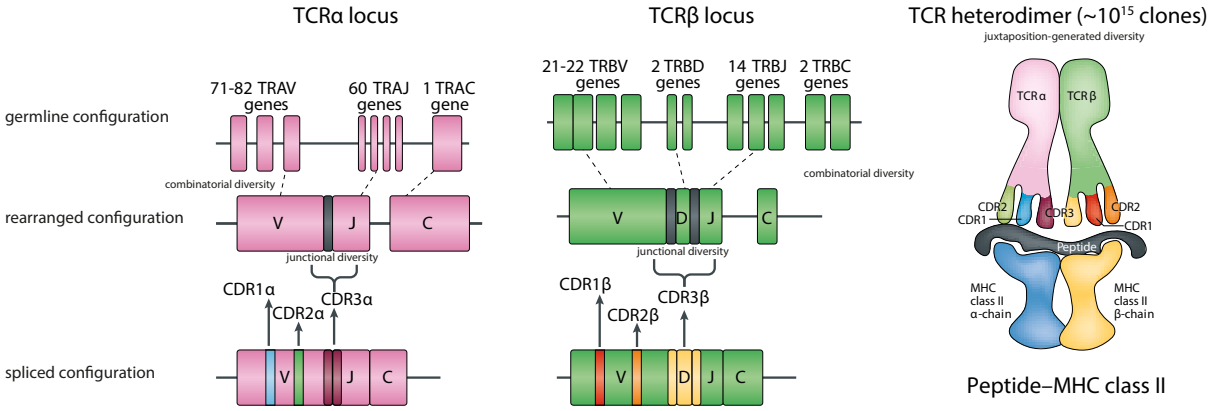

Figure 3: Generation of TCR diversity

Generation of αβTCR diversity in the mouse. In the germline configuration, the TCRα and TCRβ loci contain multiple Variable (V) and Joining (J) genes, while Diversity (D) genes are present only in the TCRβ locus. Thanks to the RAG recombinases, random individual V, (D) and J segments are rearranged together on each locus, conferring a first level of diversity, known as combinatorial diversity. Afterwards, the RAG and TdT enzymes generate the so-called junctional diversity at the junction between V, (D) and J rearranged genes, through insertion and deletion of nucleotides. The three portions of each TCR chain that will contact pMHC are known as CDR1, 2 and 3 (complementarity determining region 1, 2 and 3): CDR1 and 2 are germline encoded, while CDR3 is generated through combinatorial and junctional diversity and is the most variable portion of the TCR. The rearranged DNA is then transcribed into mRNA and spliced: besides the removal of introns, this step connects the constant (C) region to the V(D)J part. Finally, the mRNA is translated into protein and the TCRα and TCRβ chains are paired to form the TCR heterodimer (juxtaposition-generated diversity). Theoretically, up to 10^{15} different TCRs could be generated through the afore-mentioned steps [29]. However, due to thymic positive and negative selection and to spatial constraints, the actual observed diversity in one individual at one given time is closer to 10^{7} TCR clones in both mice and humans [30, 31]. The figure was adapted from [32]. RAG: recombination activating gene; TdT: terminal deoxyribonucleotidyl transferase; TRAV/J/C: TCRα V/J/C gene; TRBV/D/J/C: TCRβ V/J/C gene.

In the light of the random nature of gene rearrangements responsible for generating TCR diversity, it is crucial to ensure that only useful TCR clones are retained in the mature repertoire. For this purpose, the specificity of each newly-expressed TCR is tested through

interactions with pMHC present on cTECs, in a process known as positive selection: during this phase, DP thymocytes undergo apoptosis unless their TCR interacts weakly with cortical pMHC complexes (see figure 4). This checkpoint guarantees the survival of DP cells bearing a functional TCR, i. e. able to recognize peptides mounted on self-MHC, whereas those that do not meet these criteria die by neglect. Interestingly, the burden of this fate choice falls almost entirely on the MHC-bound peptides, as TCRs contact MHC molecules through their CDR1 and 2 portions, which are germline-encoded [33]. In other words, all TCRs are evolutionarily biased towards MHC-reactivity: it is the ability to bind the specific peptides that the host´s MHC haplotype can present that dictates MHC-restriction of the TCR repertoire. Given the importance of peptides displayed by cTECs, I will examine this topic in depth in section 1.3. Certainly, it is also possible that the randomly-generated TCRs recognize non-MHC ligands, but these would not be able to induce a positive selection signal, because most of the required Lck molecules are associated with the CD4 and CD8 co-receptors´ intracellular tails and would be recruited to the TCR only upon binding to MHCII and I, respectively [34].

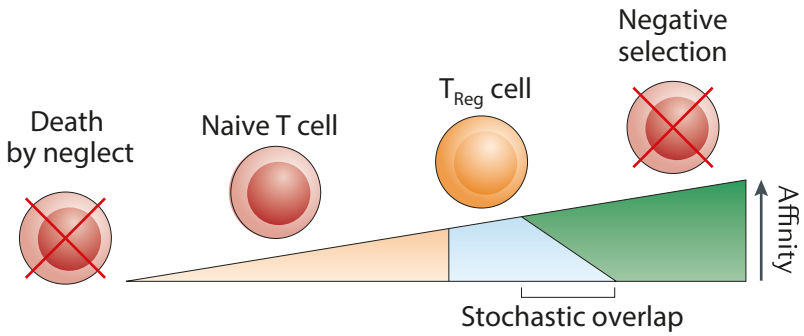

Figure 4: The affinity/avidity model of thymic selection
According to this model, the affinity (and/or avidity) of interaction between the TCR and pMHC determines the thymocyte fate. No interaction results in death by neglect, weak interactions lead to positive selection of conventional naïve T cells, intermediate ones induce Treg diversion and high affinities delete T cells from the repertoire. Based on data obtained from TCR transgenic mice, to a certain range of intermediate-high affinities might correspond dual fates, depending on stochastic factors. The figure was taken from [35].

Although they express lower TCR levels on their surface, DP thymocytes have been shown to be more sensitive than mature T cells to TCR stimulation [36]: this ensures that low-affinity interactions between TCR and self-pMHC induce positive selection in DP thymocytes, and at the same time do not activate peripheral T cells, thus preventing autoimmunity. At the molecular level, such dichotomy is achieved through the expression

of positive regulators of TCR signaling, such as mir181a [37], VGSC [38], Tespa-1 [39] and Themis [40], specifically at the DP stage. At this developmental point, if the interaction with cortical pMHC induces a sufficient stimulus through the TCR, the downstream signaling cascade on the thymocyte side will induce positive selection, which leads not only to survival but also to further differentiation towards the SP stage. These events include the upregulation of TCR and CD3 molecules, as well as of CD5 and CD69, which are commonly used markers for post-selection DP cells [41, 42]. Post-selection thymocytes also gradually re-acquire the expression of the IL-7Rα, which will allow them to survive in the following stages of thymic maturation and, ultimately, in the periphery.

More than 90% of DP thymocytes die in the cortex, because their TCRs fail to recognize with sufficient strength pMHC presented by cTECs [43]. However, another substantial fraction of DP cells die as a consequence of high-affinity TCR:pMHC interactions (see figure 4): this process, known as negative selection or clonal deletion, is responsible for eliminating overtly autoreactive T cells from the mature repertoire. A first wave of negative selection is believed to eliminate DP cells reacting to ubiquitous self-antigens, which are first encountered in the cortex; afterwards, SP thymocytes will be tested for recognition of tissue-restricted antigens (TRAs) in the medulla (see paragraph 1.2.3). While a variety of medullary APCs are specialized in promoting negative selection, in the cortex the only APC type believed to mediate negative selection is represented by the few DCs residing in the proximity of the medulla [44]: cortical DCs and all medullary APCs, unlike cTECs, express co-stimulatory molecules and are therefore more likely to induce firmer TCR ligation.

The question of how an analog signal such as the strength of TCR:pMHC binding can be converted into a digital cell fate decision of life or death has intrigued scientists for decades and has been only partially solved. Discrimination between “weak” and “strong” TCR:pMHC interactions likely depends on the numerous feedback loops controlling the kinetics, duration of activation and subcellular localization of critical TCR downstream signaling molecules, including Lck [45], ZAP-70 [46], calcium [47] and ERK [48, 49]. Ultimately, stable TCR:pMHC interactions able to recruit sufficient amounts of Lck and ZAP-70 kinases to the CD3´s immunotyrosine activation motifs (ITAMs), to briefly activate ERK at the plasma membrane and to trigger persistent calcium mobilization would initiate migratory arrest and clonal deletion. Conversely, TCR:pMHC contacts inducing incomplete

phosphorylation of CD3´s ITAMs, transient calcium influx and sustained ERK activation at the Golgi membrane would lead to positive selection and continued migration.

DP thymocytes that receive appropriate TCR stimulation and undergo positive selection next start a differentiation program, which includes the termination of CD8 transcription and the transition through a $CD4^{+}CD8^{lo}$ intermediate stage [50], regardless of the MHC-restriction specificity of the TCR. At this point, an MHCII-restricted TCR would engage in prolonged signaling and therefore induce expression of ThPOK, i.e. the CD4 lineage-specifying transcription factor. Instead, an MHCI-restricted TCR would generate much shorter signaling, given the decrease in CD8 expression; interestingly, CD8 lineage fate was recently found to be entirely signaled by six cytokines [51], downstream of which the expression of Runx3d – the master regulator of the CD8 lineage – is initiated. Runx3d inhibits ThPOK and causes the so-called co-receptor reversal, by terminating CD4 transcription and inducing CD8´s. Expression of either ThPOK or Runx3d irreversibly determines lineage commitment and marks the entry into the SP stage. As an interesting note, the association of more Lck molecules with the intracellular portion of CD4 as compared to CD8, results in the positive selection of more CD4SP than CD8SP in most mammalian species [52].

1.2.3 SP stage: central tolerance induction and final maturation

SP thymocytes migrate to the thymic medulla thanks to the expression of the chemokine receptor CCR7. Here they encounter a complex mixture of APCs, specialized in the induction of central tolerance: in order of abundance, mTECs, thymic resident DCs, migratory DCs and B cells. With the expression of up to 19000 protein-coding genes, mTECs are the cell type in the body with the highest potential for gene transcription [53]. Indeed, a unique feature of the thymic medullary epithelium is the ectopic expression of otherwise TRAs, which is governed by the Autoimmune Regulator (Aire) [54] and by the FEZ Family Zinc Finger 2 (Fezf2) [55] transcription factors. Aire and Fezf2 control the transcription of nonredundant TRA subsets and their absence results in severe autoimmunity in mice. mTECs are the main cell population expressing TRAs and play an autonomous role in central tolerance [56]. However, DCs can also display antigens acquired from the cell membrane of mTECs – including intact pMHC – to SP thymocytes [57]. In fact, DCs are regarded as the most potent APCs for central tolerance induction, as

they can present both TRAs and blood-borne antigens. Finally, thymic B cells also express Aire, but only a negligible amount of Aire-induced TRAs; therefore, it is likely that Aire fulfills a different role in this cell subset and that they present mainly B cell-specific antigens [58]. To which extent different medullary APCs overlap in their contribution to central tolerance is still to be determined.

Regardless of the APC type involved, central tolerance can be imposed on the developing T cell repertoire through two main mechanisms: negative selection or diversion into the T regulatory (Treg) lineage. Again, it appears that the strength of TCR:pMHC interaction is responsible for dictating the T cell fate. High affinity/avidity TCR:pMHC contacts are believed to induce clonal deletion, whereas intermediate ones result in Treg conversion (see figure 4). Although not explained by the affinity/avidity model, other factors, such as the local concentration of IL-2 and IL-15 in thymic niches, seem to be crucial for Treg induction [59].

Once overtly autoreactive TCR specificities have been purged from the repertoire or converted into Tregs, SP thymocytes must complete their maturation in order to achieve full functional competence. SP thymocytes can be classified into three consecutive stages, known as semi-mature (SM), mature 1 (M1) and mature 2 (M2). Interestingly, TCR stimulation has different outcomes, according to the thymocyte developmental status: during the SM phase ($CD69^+$ $MHCI^-$) it leads to apoptosis or Treg conversion, while it induces proliferative responses from the M1 stage ($CD69^+$ $MHCI^+$) on. Finally, SP thymocytes downregulate CD69 at the M3 stage, they acquire the ability to produce cytokines and they start expressing molecules necessary for egress ($CD62L^+$ $S1PR1^+$) into the blood-stream [60].

1.3 Antigen presentation in the thymus

The idea that apparently similar self-pMHC complexes can drive opposite thymocyte fates is known as the selection paradox. Indeed, the affinity/avidity model alone does not explain why cTECs are the only APCs to induce positive selection and why different APCs reside in specific thymic niches. Part of the solution comes from the observation that cTECs possess specialized antigen-processing machineries, which differ from the classical pathways of MHC loading used by other APC types, and in particular by mTECs and DCs (detailed in figure 5). Thus cTECs can theoretically generate and present

unique peptides, which might be the most suited to positive selection, either in terms of affinity to the TCR or of general biochemical properties. Alternatively, it is possible that a broad TCR repertoire is selected only if different arrays of peptides are presented during positive and negative selection – a hypothesis known as the "peptide switch" model. The two theories are not mutually exclusive, but should rather be combined, according to the most recent findings.

In the following sections, I will summarize the current knowledge on antigen presentation in the thymus, with a particular focus on cTEC-specific pathways.

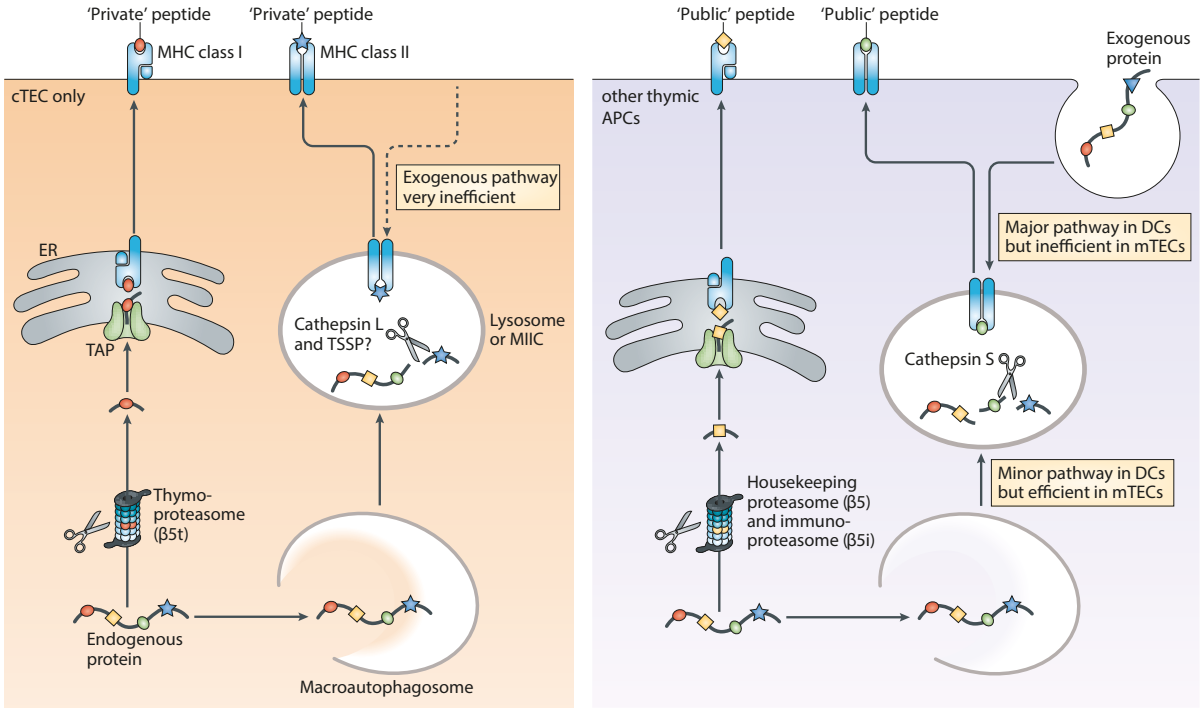

Figure 5: Thymic cortex and medulla utilize different antigen-processing pathways
The left panel shows antigen-processing pathways restricted to cortical thymic epithelial cells (cTECs), which can therefore generate a set of "private" peptides to display on both surface MHCI and MHCII for T cell positive selection. Specialized players in cTECs include the β5t catalytic subunit of the proteasome - giving rise to the thymoproteasome and influencing the MHCI-loading pathway – as well as unconventional lysosomal proteases, such as cathepsin L and thymus-specific serine protease (TSSP), shaping the MHCII-loading axis. The right panel depicts the generation of possible "public" peptides in all the other thymic APCs (antigen-presenting cells), due to the common expression of housekeeping/immunoproteasome and cathepsin S. Another pathway shared between cTECs and mTECs (medullary TECs), but which differs from DCs (dendritic cells), is constitutive macroautophagy, which ensures that mainly endogenous antigens are presented on MHCII. The figure was adapted from [35]. MIIC: MHC class II loading compartment; ER: endoplasmic reticulum; TAP: transporter associated with antigen processing.

1.3.1 Presentation of peptides on MHCI

Peptides presented on MHCI are generated through digestion of cytoplasmic proteins, which are generally produced by the cell itself. For example, TECs use endogenous proteins as source of MHCI-bound peptides to promote positive selection or central tolerance of MHCI-restricted thymocytes. Typically, all nucleated cells in the body express MHCI, so that any alteration in their content can be readily detected by patrolling $CD8^+$ T cells, for instance in case of malignant transformation or viral infection. However most professional APCs, such as DCs, preferentially load MHCI with peptides derived from phagocytosed material, in a process known as cross-presentation, as they are specialized in starting immune responses. Irrespective of the endogenous or exogenous origin of such proteins, the proteasome cleaves them in the cytoplasm and the resulting peptides are transported by the transporter associated with antigen processing (TAP) complex into the endoplasmic reticulum (ER), where they can bind nascent MHCI molecules and from here be finally delivered to the cell membrane for antigen presentation. Carboxy-terminal (C-terminal) cleavage of proteins by the proteasome is particularly crucial to create MHCI-binding peptides, whereas amino-terminal (N-terminal) cleavage can be performed by an aminopeptidase in the ER, known as the endoplasmic reticulum aminopeptidase associated with antigen processing (ERAAP).

The proteasome is a multimolecular complex responsible for the degradation of intracellular proteins, whose composition varies according to the cell type and the cytokine milieu. Three proteasome isoforms exist in jawed vertebrates, differing in their β catalytic subunits: the constitutive proteasome, which integrates the β1, β2 and β5 subunits; the immunoproteasome, incorporating β1i, β2i and β5i, and the thymoproteasome, which uses β1i, β2i and β5t (recently reviewed in [61]). The immunoproteasome is constitutively expressed in mTECs and in all hematopoietic cells, and it is induced in other cell types after exposure to pro-inflammatory cytokines, especially IFN-γ. It is specialized in the production of antigenic peptides, as it preferentially generates C-terminal hydrophobic residues, which fit better in the MHCI groove. The thymoproteasome is instead expressed exclusively by cTECs (figure 5) and has a decreased chymotrypsin-like activity, due to the hydrophilic residues present in the substrate-binding pocket of the β5t subunit [62]. Deletion of the β5t subunit of the thymoproteasome in mice dramatically affects the positive selection of $CD8^+$ T cells,

reducing their cellularity and peripheral immunocompetence [62-65]. Of note, cTECs compensate the loss of β5t with the expression of β5i and β5, so the defective $CD8^+$ T cell compartment selected in $\beta5t^{-/-}$ mice could derive from the use of the same peptides for positive and negative selection, which would lead to excessive deletion. However, when β5i was knocked in in place of β5t in $\beta5i^{-/-}$ mice – in other words when cTECs were the only cell type able to express β5i – the positive selection defect persisted, suggesting that the selection of a functional $CD8^+$ T cell repertoire is granted not only by the expression of distinct proteasomes in cTECs compared to other thymic APCs, but most importantly by the unique biochemical features of the positively-selecting ligands generated by the thymoproteasome itself [64]. More recently, the four immune-related proteasome subunits β1i, β2i, β5i and β5t were knocked out to generate a mouse bearing only the constitutive proteasome: in this model, both positive and negative selection are disrupted, arguing that peptide switching between cTECs and other thymic APCs is nonetheless an important mechanism for the establishment of a diverse TCR repertoire [66].

1.3.2 Presentation of peptides on MHCII

Peptides presented on MHCII are generated through digestion of proteins of various origin in the endo-lysosomal compartment. Only professional APCs express MHCII, and they load it with peptides mostly derived from phagocytosed material. However, TECs cannot efficiently uptake exogenous molecules; on the contrary, they display high levels of constitutive macroautophagy, which ensures the preponderant loading of intracellular peptides on MHCII [67]. Since their synthesis in the ER, immature MHCII dimers are complexed with the invariant chain (Ii) chaperone, which assists them with folding and promotes their trafficking to the Golgi and, later, to the so-called MHCII loading compartment (MIIC). In the MIIC, proteases belonging to the cathepsin family degrade the Ii until only the Class-II associated Ii peptide (CLIP) fragment is left in the MHCII peptide-binding cleft. At the same time, the peptides that will be presented on MHCII are produced in distinct endosome compartments by cleavage of proteins by endo-lysosomal proteases, including cathepsins; peptide-containing endosomes eventually fuse with MIIC, where HLA-DM (H2-M in mice) facilitates the exchange of CLIP with the antigenic

peptides. Vesicles budding from the MIIC finally transport mature pMHCII to the cell membrane for antigen presentation.

With regard to thymic APCs, cTECs uniquely express the lysosomal proteases cathepsin L and thymus-specific serine protease (TSSP), whereas mTECs, DCs, B cells and macrophages express cathepsin S. Both cathepsin L and S are cysteine proteases involved in the degradation of Ii, as well as in the generation of MHCII-bound peptides. Interestingly, the whole family of cathepsins seems to have originated from the same genome duplication that gave rise to MHC, TCR and immunoglobulin loci in jawed vertebrates [68]. Knock-out of cathepsin L in mice causes a severe impairment in the positive selection of MHCII-restricted thymocytes (60-80% reduction) [69], whereas loss of cathepsin S compromises peripheral antigen presentation [70]). Of note, mice deficient in both cathepsin L and Ii show a more marked $CD4^+$ T cell defect compared to single knock-out mice, providing the first *in vivo* evidence for cathepsin L's role in shaping the repertoire of MHCII-associated peptides in cTECs [71]. On the same line, knock-out of TSSP also affects the generation of pMHCII in cTECs, but only impairs positive selection of a few MHCII-restricted TCR specificities, without reducing total $CD4^+$ T cell numbers [72].

In order to directly address the nature of MHCII-bound positively-selecting peptides, one study compared peptides eluted from MHCII molecules of wild-type (WT) cTECs and splenocytes. In spite of pooling up to 375 mice per group, the authors could identify only the 17 most abundant peptides, which turned out to be overlapping between the two tissues, and therefore discarded the "peptide switch" hypothesis [73]. Let's keep in mind, though, that peptides presented by cTECs are extremely diverse – hence rare in the whole pool – and probably fall below the detection limit of even the most sophisticated mass-spectrometry analyses.

The requirement for diverse, low-abundance positively-selecting peptides was clarified some years later, through the generation of mice with a limited array of MHCII-associated peptides. For instance, H2-$M^{-/-}$ mice are not able to efficiently exchange CLIP with other peptides and therefore present mainly MHCII-CLIP on the surface of APCs, including cTECs [74]. These mice select a surprisingly broad repertoire of $CD4^+$ T cells, although the total numbers are reduced by half and some TCR specificities are not selected in bone-marrow (BM) chimeras. Addition of anti-MHCII blocking antibodies to H2-$M^{-/-}$ fetal thymic organ cultures (FTOCs) significantly impairs positive selection only

when targeting all MHCII molecules, and not specifically MHCII-CLIP, suggesting that in this mouse model most CD4SP thymocytes are selected by rare peptides, distinct from CLIP [75]. Another proof that low-abundance peptides can make the difference in positive selection is given by "single-peptide:MHCII" mice [76-78]. Transgenic expression of the human invariant chain (hIi), whose CLIP portion is replaced by a given peptide (on a $Ii^{-/-}$ background), is sufficient to present such peptide on 95% of MHCII molecules, without affecting MHCII processing and expression levels. In this scenario, $CD4^+$ T cells develop in normal numbers. When these mice are further bred to the H2-$M^{-/-}$ background, where the exchange of the CLIP-replacing peptide is inhibited, virtually all MHCII molecules can be indeed occupied by a single peptide, and only then does the selection of $CD4^+$ T cells dramatically decrease (70% reduction). The impaired selection is due to the loss of that 5% of MHCII molecules occupied by diverse peptides, as shown by administration of anti-MHCII blocking antibodies to FTOCs [76]. The same loss of $CD4^+$ T cells is obtained when crossing two or three different "single-peptide" mice, demonstrating that a certain peptide diversity is needed for positive selection of multiple TCR specificities [77, 78]. Overall, recognition of rare and diverse peptides on MHCII is needed to positively select a broad $CD4^+$ T cell repertoire; furthermore this TCR:pMHCII interaction is specific, as individual pMHCII select distinct subsets of $CD4^+$ T cells. Indeed, whenever the diversity of positively-selecting pMHCII was experimentally reduced, the quality of the $CD4^+$ T cell repertoire was affected to some level, even without an evident reduction in cell numbers.

A final aspect that should be considered is the stability of pMHCII complexes on the surface of different thymic APCs, which might affect the quality of signals transmitted to developing thymocytes. cTECs constitutively express CD83, a molecule upregulated on activated DCs and B cells, which inhibits ubiquitin-mediated internalization of pMHCII from the cell membrane. Deletion of CD83 in mice impairs positive selection of MHCII-restricted thymocytes, by accelerating the MHCII turnover in cTECs [79], implying that a long pMHCII half-life in cTECs is needed to induce stable and efficient selection events.

1.4 Aim of the research project

Although fascinating, the process of positive selection is still poorly understood. On one hand, it is virtually impossible to characterize the biochemical properties of antigens presented in the thymic cortex, due to the lack of sensitivity of the current proteomic

approaches. On the other hand, it is much easier to understand why negative selection wipes out dangerous autoreactive T cell specificities, than to envisage the reasons behind the requirement for moderate self-reactivity among all positively-selected T cells. For a long time, positively-selecting self-pMHC:TCR interactions have been explained by the necessity of shaping a repertoire of T cells with the proper MHC restriction, meaning that "useful" T cells should be selected on the basis of their ability to recognize the host's MHC haplotype. However, antigen-specificity, MHC-restriction and even cross-reactivity are inextricably-linked properties of the TCR; therefore not only MHC-binding but all the features which make a TCR functional in the periphery are likely shaped by positive selection, rendering it a research topic of utmost importance for T cell immunologists.

With our project, we aimed at unravelling the importance of cTEC-specific antigen-processing pathways in shaping a functional T cell repertoire. We particularly investigated the impact of a single cortical protease, namely cathepsin L, on the quality of the selected MHCII-restricted T cell compartment. Germline knock-out of cathepsin L in mice was previously shown to drastically reduce the number of $CD4^+$ T cells that mature and exit the thymus [69, 71]; yet, nothing is known about the TCR diversity and functionality of such repertoire. To address this aim, we took advantage of a new mouse model with conditional knock-out of cathepsin L in TECs. We performed both TCR sequencing and functional analyses of $CD4^+$ T cells selected in cathepsin L-deficient or sufficient animals, i.e. under the pressure of non-physiological or physiological selecting ligands, both in the polyclonal background and in a new TCR oligoclonal setting.

2. Materials and methods

2.1 Reagents

2.1.1 Antibodies

The antibodies used for flow-cytometry, cell enrichment or depletion and *in vitro* T cell stimulation are listed below:

Specificity	Clone	Source
Anti-mouse CD16/CD32 (Fc block)	2.4G2	Hybridoma (house)
Anti-mouse CD4 BV510	RM4-5	BioLegend
Anti-mouse CD8a PerCP	53-6.7	BioLegend
Anti-mouse CD3ε Alexa-488	145-2C11	BioLegend
Anti-mouse CD69 PE	H1.2F3	BD Biosciences
Anti-mouse CD5 Alexa-647	53-7.3	BioLegend
Anti-mouse CD62L FITC	MEL-14	BioLegend
Anti-mouse I-A/I-E APC/Cy7	M5/114.15.2	BioLegend
Anti-mouse I-A^b:CLIP FITC	15G4	Santa Cruz Biotechnology
Anti-mouse I-A^b:nonCLIP	BP107	Hybridoma (kindly provided by Dr. Alexander Rudensky, Sloan Kettering Institute, New York)
Anti-mouse CD45.1 BV421	A20	BioLegend
Anti-mouse CD45.2 Alexa-647	104	BioLegend
Anti-mouse CD25 PE/Cy7	PC61	BioLegend
Anti-mouse CD44 Pacific Blue	IM7	BioLegend
Anti-mouse phospho-p44/42 MAPK (ERK1/2) (Thr202/Tyr204) PE	197G2	Cell Signaling
Anti-mouse vα2 (TRAV14) APC/Cy7	B20.1	BioLegend
Anti-mouse vα3.2 (TRAV9) FITC	RR3-16	BD Biosciences
Anti-mouse vβ6 (TRBV19) PE	RR4-7	BioLegend
Anti-human CD2 APC	RPA-2.10	BioLegend
Anti-mouse/human CD11b BV421	M1/70	BioLegend
Anti-mouse CD11c BV421	N418	BioLegend
Anti-mouse/human B220 BV421	RA3-6B2	BioLegend
Anti-mouse F4/80 BV421	BM8	BioLegend
Anti-mouse Ly51 PE	6C3	BioLegend
Anti-mouse CD326 (Ep-CAM) PE/Cy7	G8.8	BioLegend

Anti-mouse CD4 MicroBeads	GK1.5	Miltenyi Biotec
Anti-mouse CD8a MicroBeads	53-6.7	Miltenyi Biotec
Anti-mouse CD45 MicroBeads	30F11.1	Miltenyi Biotec
Anti-APC MicroBeads	Not specified	Miltenyi Biotec
Anti-PE MicroBeads	Not specified	Miltenyi Biotec
Purified anti-mouse CD3ε	145-2C11	BioLegend
Purified anti-mouse CD28	37.51	BioLegend

2.1.2 Genotyping primers

All genotyping primers were purchased from Integrated DNA Technologies (IDT).

Gene	Forward primer (5´-3´)	Reverse primer (5´-3´)	Amplicon size
Ctsl wt/flox	CACACAGAAGACTGTATGGC	TCAAACTCAGAAATCTGCCTG	598 bp (wt); 771 bp (flox)
Ctsl wt/ko	GCTTGCTCTAGAATGAGGAAGAG	CATACCTGGTTCTTCACAGGAG (wt) CGGAGAACCTGCGTGCAATCC (ko)	385 bp (wt); 700 bp (ko)
Foxn1-CRE tg	CATACGATTTAGGTGACACTATAG	AATCTCATTCCGTTACGCAG	300 bp
Plp wt/ko	GAAAGGTTCCATGGTCAAGG	CTGTTTTGCGGCTGACTTTG (wt) CTTGCCGAATATCATGGTGG (ko)	562 bp (wt); 806 bp (ko)
TCRβ-PLP1 tg	CCCAGAGCCAAAGAAAGTC	AGCCTGGTCCCTGAGCCGAA	700 bp
TCRα-PLP1 tg	ACAACAGAGCTGCAGCCTTC	GCAGTGCTAGGAAGGGCGGC	700 bp
TCRα-shorT tg	TCTGCTCCTGGTAGCCATTT	ATAAACCTCGTGTGGCAAGG	770 bp
TCRα wt/ko	TGACTCCCAAATCAATGTGC	GGTGAGATGACCCAAAGCAG (wt) CCTACCCGCTTCCATTGCTCA (ko)	250 bp (wt); 400 bp (ko)
MHCI wt/ko	CTGAGCTCTGTTTTCGTCTG (wt) TCTGGACGAAGAGCATCAGGG (ko)	TATCAGTCTCAGTGGGGGTG	261 bp (wt); 410 (ko)
MHCII wt	AGGAGTACGTGCGCTACGACAG	GCAGAGGTGAGACAGGAGGGAGA	332 bp
MHCII ko	GCAGAGGTGAGACAGGAGGGAGA	CACTGAAGCGGGAAGGGAC	888 bp
C2TAkd tg	TAAATTCTGGCTGGCGTGG	ACCGGACTAGTGGAAAAGCGCCTCC CCTACC	750 bp
DEP-TCR tg	CGAGAGGAAGCATGTCTAAC	ACCGCGGTCATCCAACACAG	650 bp
OTII-TCR tg	GCTGCTGCACAGACCTACT	CAGCTCACCTAACACGAGGA	500 bp
AND-TCR tg	GACTTGGAGATTGCCAACCCATAT CTAAGT	TGAGCCGAAGGTGTAGTCGGAGTTT GCATT	410 bp
AD10-TCR tg	GACTTGGAGATTGCCAACCCATAT CTAAGT	TGAGCCGAAGGTGTAGTCGGAGTTT GCATT	410 bp
Rag1 wt/ko	CCGGACAAGTTTTTCATCGT	GAGGTTCCGCTACGACTCTG (wt) CCGGACAAGTTTTTCATCGT (ko)	474 bp (wt); 530 bp (ko)

2.1.3 Cell lines and bacterial strains

The ecotropic packaging cell line GP+E-86 was previously described [80]. Briefly, GP+E-86 cells were generated from transfection of 3T3 cells with two separate helper virus plasmids, derived from Moloney murine leukemia virus (MMLV): one containing the Gag-Pol genes and the other encoding the Env gene.

The competent *E. Coli* strains SoloPack Gold® and One Shot™ TOP10 were purchased from Stratagene and Invitrogen, respectively.

2.1.4 Cell culture media

Cell culture media were prepared as follows:

Medium	Supplements	Cell type
Iscove´s Modified Dulbecco´s Medium (IMDM, Gibco™) +25 mM Hepes	8% heat-inactivated Fetal Bovine Serum cat#S0115 (Merck Millipore) 4 mM L-Glutamine (Gibco™) 1% Non-Essential Amino Acids (100X, Gibco™) 100 U/ml Penicillin and 100 µg/ml Streptomycin (Gibco™) 1 mM Sodium Pyruvate (Gibco™) 50 µM 2-Mercaptoethanol (Gibco™)	Thymocytes/ primary T cells
Iscove´s Modified Dulbecco´s Medium (IMDM, Gibco™) +25 mM Hepes	20% heat-inactivated Fetal Bovine Serum cat#S0115 (Merck Millipore) 4 mM L-Glutamine (Gibco™) 1% Non-Essential Amino Acids (100X, Gibco™) 100 U/ml Penicillin and 100 µg/ml Streptomycin (Gibco™) 1 mM Sodium Pyruvate (Gibco™) 50 µM 2-Mercaptoethanol (Gibco™) recombinant mouse IL-3 (20 ng/ml Biolegend) recombinant mouse IL-6 (10 ng/ml Biolegend) recombinant mouse SCF (200 ng/ml, Biolegend)	BM cells
Dulbecco´s Modified Eagle Medium (DMEM, Gibco™) + 4.5 g/L D-Glucose	8% heat-inactivated Fetal Bovine Serum cat#S0115 (Merck Millipore) 4 mM L-Glutamine (Gibco™) 1% Non-Essential Amino Acids (100X, Gibco™) 100 U/ml Penicillin and 100 µg/ml Streptomycin (Gibco™) 1 mM Sodium Pyruvate (Gibco™) 50 µM 2-Mercaptoethanol (Gibco™)	GP+E-86
Freezing medium	70% cell medium 20% heat-inactivated Fetal Bovine Serum cat#S0115 (Merck Millipore) 10% DiMethyl SulfOxide (DMSO)	All cells

Lysogeny Broth (LB) medium	5% Trypton 5% NaCl 2.5% Yeast	*E. Coli*
LB-Agar	1.5% Agar 1% Trypton 0.5% Yeast 0.5% NaCl	*E. Coli*

2.1.5 Chemicals

All chemicals were purchased from Merck, Roth or Peqlab, except the ones listed below:

Reagent	Source	Use
Neomycin	Belapharm	Drinking water for lethally irradiated mice
Carboxyfluorescein succinimidyl ester (CFSE)	Thermo Fisher	Labeling of cells before adoptive transfer
Complete Freund Adjuvant (CFA)	Difco	Adjuvant for immunization
5-Fluoro-Uracil (5-FU)	Medac	Chemotherapic; kills proliferating cells before isolation of BM stem cells
Protamine sulfate	Sigma	Transduction with retrovirus
Phorbol Myristate Acetate (PMA)	Sigma	In vitro stimulation of T cells

2.1.6 Enzymes

Enzyme	Source
Proteinase K	Roche
Liberase TM	Roche
DNase	Roche
Taq polymerase	Made in house
Reverse Transcriptase	Bio-Rad
Exonuclease I	Thermo Fisher
Terminal deoxynucleotide Transferase	Promega
Herculase II Fusion DNA Polymerase	Agilent
T4 DNA Ligase	Roche
Restriction enzymes	New England Biolabs

2.1.7 Commercial kits

Kit	Source
Red Blood Cell Lysis 10X	BD
Lineage depletion kit	Miltenyi Biotec
iScript™ Select cDNA Synthesis kit	Bio-Rad
QIAquick Gel Extraction Kit	Qiagen
Zero Blunt® PCR cloning kit	Invitrogen
QIAprep Spin miniprep kit	Qiagen
Arcturus PicoPure™ RNA isolation kit	Applied Biosystems
iScript™ cDNA Synthesis kit	Bio-Rad
Nextera index kit	Illumina
Agencourt AMPure XP PCR Purification Kit	Beckman Coulter
QuikChange Multi Site-Directed Mutagenesis kit	Agilent
QIAGEN plasmid maxi kit	Qiagen

2.1.8 Buffers and solutions

All buffers and solutions were produced in house:

Buffer/solution	Composition
Gitocher buffer (10X)	670 mM Tris (pH 8.8) 166 mM ammonium sulfate 65 mM $MgCl_2$ 0.1% gelatin
Tail digestion buffer	0.6 mg/ml Proteinase K 0.5% Triton-X 1X Gitocher buffer 1% β-mercaptoethanol
PBS (10X, pH 7.2-7.4)	1.5 M NaCl 30 mM KCl 80 mM Na_2HPO_4 20 mM KH_2PO_4
FACS buffer	1X PBS 2% fetal calf serum (FCS) 1 mM EDTA
Tetramer buffer	1X PBS 2% fetal calf serum (FCS) 0.1% sodium azide

PCR buffer (5X)	250 mM KCl 50 mM Tris (pH8.3) 43% glycerol 7.5 mM $MgCl_2$ 2 mM Cresol Red
Tris Acetate EDTA (TAE) buffer (50X)	2 M Tris 17.5% Glacial acetic acid 64 mM EDTA
HEPES-buffered saline (HEBS) (2X, pH 7.05)	50 mM HEPES 1.5 mM Na_2HPO_4

2.1.9 Plasmids

The pinco-33 plasmid, derived from the original PINCO plasmid [81], was kindly provided by Dr. Naoto Kawakami in the BioMedical Center (LMU). As detailed in map 1, it contains the long-terminal repeats (LTRs) of the murine embryonic stem cell virus (MESV), including the packaging signal (ψ) and a truncated gag gene lacking the start codon. Inside the LTRs, a calcium sensitive fluorescent reporter (composed of cyan fluorescent protein, calcium binding domain and yellow fluorescent protein) is cloned. Outside of the LTRs, this plasmid bears a puromycin resistance gene (PuroR) under the PKG promoter, useful for the selection of transfected packaging cells, as well as the Epstein-Barr virus origin of replication (EBV oriP) and the EBNA1 gene, which maintain retroviral vectors episomally within packaging cells. A bacterial origin of replication (ori) and an ampicillin resistance gene (AmpR) for selection of transformed bacteria are also present.

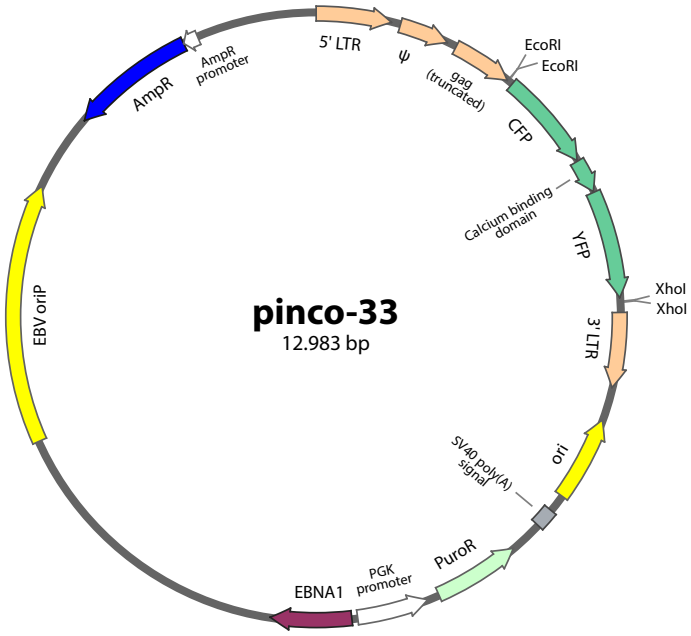

Map 1: pinco-33 retroviral vector
The LTRs (long-terminal repeats), ψ (packaging signal) and truncated gag gene derive from murine embryonic stem cell virus. CFP: cyan fluorescent protein; YFP: yellow fluorescent protein; ori: bacterial origin of replication; SV40: simian-virus 40; poly(A): poly adenylation; PuroR: puromycin resistance; EBV oriP: Epstein-Barr virus origin of replication; AmpR: ampicillin resistance. The map was designed with SnapGene_v4.3.2 software.

2.2 Animals

2.2.1 Mouse strains

Ctsl$^{fl/fl}$ (unpublished) and Ctsl$^{-/-}$ [82] mice were kindly provided by Dr. Thomas Reinheckel (University of Freiburg). Dep [83], C2TAkd [56], TCRα-PLP1 and TCRβ-PLP1 [84] were previously generated by lab members and already described elsewhere. LLO56 and LLO118 [85] were generously offered by Dr. Paul Allen (Washington University School of medicine in St. Louis). AND and AD10 [86] mice were a gift from Dr. Reinhard Obst in the BioMedical Center (LMU). Foxn1-Cre [87], MHCI$^{-/-}$ (B2m$^{-/-}$) [88], MHCII$^{-/-}$ (H2-Ab1$^{-/-}$) [89], Rag1$^{-/-}$ [90], OT-II [91], Plp$^{-/-}$ [92] and TCRα$^{-/-}$ mice [93] were purchased from the Jackson Laboratory. ShorT mice were obtained by crossing TCRα-shorT (unpublished), TCRβ-PLP1, TCRα$^{-/-}$ and Plp$^{-/-}$ animals. TCRα-shorT mice were generated in the lab by Dr. Jelena Nedjic: the transgene, integrated in the Y chromosome, is composed of the pTαcass cassette vector [94], in which TRAV9n-3 and TRAJ34 unrecombined sequences, joined by recombination signal sequences, were cloned.

All mice used were on a C57BL/6N background. Mice were maintained under specific pathogen-free conditions in individually ventilated cages. All phenotypic analyses were performed in mice of 6–10 weeks of age, unless otherwise indicated. Animal studies and procedures were approved by local authorities.

2.2.2 Genotyping

Tail biopsied were collected from 3-week-old mice to extract genomic DNA, with the following digestion mix (50 μl/sample): 5 μl 10X Gitocher buffer, 2.5 μl 10% Triton-X, 0.5 μl β-mercaptoethanol, 3 μl proteinase K, 39 μl H_2O. Digestion was carried out at 55°C for 5 hours, followed by 5 minutes inactivation of proteinase K at 95°C. 1 μl of the obtained lysate was directly PCR-amplified to determine genotypes, with the following PCR mix (30 μl/sample): 6 μl 5X PCR buffer, 3 μl dNTP mix (2.5 mM), 3 μl primer mix (10 μM), 1 μl Taq DNA polymerase (5 U/μl), 16 μl H_2O. Unless otherwise stated, the touch-down (TD) 54 x 30 PCR program was used; for TCRα-PLP1 tg, TCRβ-PLP1 tg and TCRα wt/ko genes, the TD 58 x 30 program was used; for MHCI wt/ko, MHCII ko, Ctsl wt/flox and

TCRα-shorT tg genes specific programs were used. The cycling conditions for all the genotyping PCR programs are listed below.

MHCI program			MHCII ko program			Ctsl wt/flox program			TCRα-shorT program		
94°C	3min		94°C	3min		95°C	30sec		94°C	3min	
94°C	20sec		94°C	30sec		60°C	45sec	x 15	94°C	30sec	
61°C	30sec	x 35	60°C	30sec	x 35	72°C	90sec		54°C	45sec	x 35
72°C	30sec		72°C	30sec		95°C	30sec		72°C	1min	
72°	5min		72°	5min		56°C	30sec	x 21	72°	5min	
4°C	forever		4°C	forever		72°C	90sec		4°C	forever	
						72°	5min				
						4°C	forever				

TD 54 x 30 program			TD 58 x 30 program		
94°C	3min		94°C	3min	
94°C	45sec		94°C	45sec	
60°C	45sec	x 2	64°C	45sec	x 2
72°C	1min		72°C	1min	
94°C	45sec		94°C	45sec	
58°C	45sec	x 2	62°C	45sec	x 2
72°C	1min		72°C	1min	
94°C	45sec		94°C	45sec	
56°C	45sec	x 2	60°C	45sec	x 2
72°C	1min		72°C	1min	
94°C	45sec		94°C	45sec	
54°C	45sec	x 30	58°C	45sec	x 30
72°C	1min		72°C	1min	
72°	5min		72°	5min	
4°C	forever		4°C	forever	

The size of PCR products was determined through agarose gel electrophoresis and subsequent visualization of bands under UV light (312 nm), by comparison to 100 bp DNA ladder markers (GeneDireX). The gels were prepared by dissolving 1.5% agarose in 1x TAE buffer and by adding 0.15 μg/ml of ethidium bromide.

2.3 Flow cytometry

2.3.1 Organ preparation

Thymi, spleens and lymph nodes were smashed with non-coated glass slides in ice-cold FACS buffer to obtain single-cell suspensions of lymphocytes. Red blood cell lysis was always performed on splenocytes, by resuspending them in 1 ml of 1X lysis buffer (BD) and incubating for 2 minutes at room temperature. The reaction was stopped with excess of FACS buffer.

Alternatively, to isolate TECs, thymic lobes were carefully separated and placed in plain RPMI medium. Fat and connective tissue was removed and the thymic capsule was gently disrupted by small superficial cuts. The obtained thymic pieces were pipetted up and down with a cut tip to release thymocytes into the medium. The medium was then removed, the thymic pieces were resuspended in 1 ml of RPMI containing 0.5 U/ml liberase TM and 10 mg/ml DNAse, incubated at 37°C for 15 minutes and pipetted up and down every 5 minutes. The digested material was collected into a tube and the reaction was stopped with an excess of ice-cold FACS buffer. Another 0.5 ml of liberase/DNase solution was added to the remaining undigested fraction, which was again incubated at 37°C for 15 minutes and pipetted up and down every 5 minutes. The second digested fraction was pooled to the first one on ice. $CD45^+$ cells were depleted with anti-CD45 MicroBeads, according to the MACS manufacturing protocol.

2.3.2 Tetramer staining

$LLO_{(190\text{-}201)}$:I-A^b tetramers conjugated to APC or PE were kindly provided by Dr. Marc Jenkins (University of Minnesota). Single-cell thymic, splenic or LN samples were incubated 1 hour at 37°C in tetramer buffer containing 10 nM $LLO_{(190\text{-}201)}$:I-A^b APC and $LLO_{(190\text{-}201)}$:I-A^b PE tetramers. Cells were next washed and enriched with anti-APC and anti-PE MicroBeads, according to the MACS manufacturing protocol. Counting beads (Thermo Fisher) were used to determine the number of tetramer positive cells in the column-bound fraction, using the following formula:

$$\left(\frac{cell\ count}{bead\ count}\right)(bead\ stock\ conc)\left(\frac{bead\ vol}{cell\ vol}\right)(tot\ sample\ vol)(\%\ tetramer\ positive\ cells).$$

2.3.3 Surface and intracellular staining

Cell number was determined with a Casy Counter and 2-5 x 10^6 cells/sample were stained. Surface staining was performed in 100 µl of FACS buffer containing antibodies at 4°C for at least 15 minutes. For intracellular staining of pERK, cells were fixed with 2% PFA for 10 minutes at 37°C, then placed on ice for 1 minute. 3 ml of ice-cold methanol were added and cells were stored at -20°C overnight. The next day, cells were extensively washed with 0.5% BSA (in PBS) and stained with anti-pERK antibody diluted in 0.5% BSA for 1 hour at room temperature.

Cells were acquired with a BD FACSCanto II and data were analyzed with FlowJo_v9.9.4 software.

2.3.4 Sorting

For bulk sort experiments, CD4SP thymocytes or $CD4^+$ LN cells were sorted with a 70 µm nozzle and a purity > 98%. For single-cell TCR sequencing experiments, $CD11b^-$ $CD11c^-$ $F4/80^-$ $B220^-$ $CD3^+$ $CD4^+$ $v2\alpha^+$ $LLO_{190-201}$:I-A^b APC^+ and $LLO_{190-201}$:I-A^b PE^+ cells isolated from draining LNs were single-cell sorted into 96-well plates with a 100 µm nozzle, leaving column 6 and the four wells at the corners empty as negative controls. All sorting experiments were performed with a BD FACSAria™ Fusion sorter, belonging to the Core Facility Flow Cytometry located at the BioMedical Center (LMU).

2.4 In vivo experiments

2.4.1 BM chimeras

Recipient mice were subjected to two rounds of irradiation (5.5 Gy each), separated by at least 2 hours, the day before BM transfer. The next day femurs and tibiae were harvested from donor mice and crashed with a mortar and pestle to release BM cells. After red blood cell lysis, a MACS lineage depletion kit was used to deplete differentiated cells, following the manufacturer's instructions. Cells were extensively washed with PBS and counted, and 10^6 cells/100 µl were injected into the tail vein of each recipient mouse. Neomycin was supplemented in drinking water for the first 4 weeks and mice were sacrificed 6 weeks after reconstitution.

2.4.2 Adoptive transfers

For homeostatic proliferation experiments, recipient mice were subjected to sublethal irradiation (6 Gy) the day before the adoptive transfer. The next day CD4SP $CD25^-$ $CD69^-$ $CD62L^+$ thymocytes were sorted from wt and from $CtsI^{\Delta TEC}$ donor mice, counted and mixed in a 1:1 ratio. The cells were then labeled with 0.5 μM CFSE for 3 minutes at 37°C (2 x 10^6 cells/ml), followed by extensive washing in PBS containing 10% FCS. 7 x 10^5 cells/100 μl were injected into the tail vein of each recipient mouse. Mice were bled regularly until day 30 or sacrificed at day 9 for analysis.

For immunization experiments, CD4SP $CD25^-$ $CD69^-$ $CD62L^+$ thymocytes were sorted from wt and from $CtsI^{\Delta TEC}$ donor mice and 1/10 of the cell pool was stained with $LLO_{(190-201)}$:I-A^b tetramers. The number of tetramer positive cells present in the remaining 9/10 of the pool was inferred from the calculation on the stained fraction. Tetramer-unstained cells of wt and $CtsI^{\Delta TEC}$ origin were then mixed in a way that equal numbers of theoretic tetramer positive cells of each genotype would be present in the mix, and injected into the tail vein of recipient mice.

2.4.3 Intra-footpad immunization

50 μg of $LLO_{(190-201)}$ peptide (NEKYAQAYPNVS, peptides&elephants) were dissolved in PBS and emulsified with an equal volume of CFA by mixing the liquids through two interconnected syringes. 50 μl of the emulsion were injected into the hind footpad of isofluran-anesthetized mice.

2.4.4 Retrogenic mice

BM donor mice received an i.p. injection of 5-FU (0.15 mg/g weight) 4 days before BM harvesting. On day 0, femurs and tibiae were smashed with a mortar and pestle to release BM cells. After red blood cell lysis, a MACS lineage depletion kit was used to deplete differentiated cells, following the manufacturer's instructions. Cells were then counted and plated at 1.5 x 10^6/ml in IMDM 20% FCS, supplemented with IL-3 (20 ng/ml), IL-6 (10 ng/ml) and SCF (200 ng/ml). On day 2, cells were transduced with thawed aliquots of the desired retroviral vector (MOI 0.3) and protamine sulfate (10 μg/ml). After 5-7 hours the medium was carefully removed and replaced with new fresh medium. On day 3, recipient mice were subjected to two rounds of irradiation (5.5 Gy each), separated by at least 2 hours. The next day, BM cells were extensively washed with PBS and counted, and

0.5-1 x 10^6 cells/100μl were injected into the tail vein of each recipient mouse. Neomycin was supplemented in drinking water for the first 4 weeks and mice were sacrificed 7-8 weeks after reconstitution.

2.5 In vitro stimulation assays

For anti-CD3/28 stimulation, plates were coated with anti-CD3 antibodies (10 μg/ml) for 1 hour at 37°C. CD4SP $CD25^-$ $CD69^-$ $CD62L^+$ thymocytes were plated in 8% IMDM and soluble anti-CD28 antibodies (1 μg/ml) were added to the culture. 40 hours later FSC-A, CD25, CD69, CD44 were analyzed by flow-cytometry.

For PMA stimulation, cell were incubated in 100 ng/ml PMA in plain RPMI medium for 5 minutes at 37°C and fixed immediately afterwards.

2.6 TCR sequencing

2.6.1 Single-cell sequencing

After single-cell sorts, 96-well plates were frozen at -80°C. Reverse transcription was directly performed, without prior RNA isolation, using the iScript™ Select cDNA Synthesis kit (Bio-Rad) with the following mix of primers, specific for the TCRα and TCRβ constant regions:

TRAC215:	GGTGAAGCTTGTCTGGTTGCTC	TRBC5:	CCATTCACCCACCAGCTCAGCT
TRAC222:	GATATCTTGGCAGGTGAAGCTTGTC	TRBC6:	CTGACCCCACTGTGGACCTCC
TRAC254:	ACTGGGGTAGGTGGCGTTG	TRBC7:	CTCCTTGTAGGCCTGAGGGTCCG

The reaction volume was set to 4 μl/sample, with the following components: 0.8 μl of 5X iScript buffer, 0.5 μl of 0.83% Triton-X100, 0.4 μl of Enhancer, 0.2 μl of TCRα primers (TRAC215-222-254), 0.2 μl of TCRβ primers (TRBC5-7), 0.2 μl of Reverse Transcriptase, 1.7 μl of H_2O. The retrotranscription reaction was run with the following program: 25°C 5min, 42°C 30min, 85°C 5min, 4°C forever.

Retrotranscription was followed by a digestion step with exonuclease I (Thermo Scientific), in order to remove the single-stranded primers. 0.25 μl of exonuclease I (20 U/ml), 0.5 μl of 10X exonuclease buffer and 0.25 μl of H_2O were added to the 4 μl of iScript product and kept at 37°C for 45min, followed by 85°C for 15min. The exonuclease

digestion product was further subjected to a dGTP tailing step, by addition of 1.6 μl of 5X TdT buffer, 0.65 μl dGTP (25mM), 0.2 μl Terminal deoxyribonucleotidyl Transferase (30 U/ml, Promega) and 0.75 μl of H_2O. The reaction was performed at 37°C for 45min, followed by 75°C for 10min.

After this step, the dGTP tailing product was split into two 96-well plates to continue with separate PCRs for TCRα and TCRβ sequencing. All the PCRs were run with the following cycling conditions: 94°C for 3min; 94°C for 15sec, 60°C for 30sec, 72°C for 45sec (for 24 cycles); 72°C for 5 min; 4°C forever. The primers used for the three PCR steps are listed below:

Name	**Sequence**
Anchor_fw	ACAGCAGGTCAGTCAAGCAGTAGCAGCAGTTCGATAAGCGGCCGCCATGGACCCCCCCCCCC
TRAC6	GTCAAAGTCGGTGAACAGGC
TRBC4	ACGTGGTCAGGGAAGAAGCC
Adaptor 1	ACAGCAGGTCAGTCAAGCAGTA
TRAC13	GAGACCGAGGATCTTTTAACTG
TRBC3	ACGAGGGTAGCCTTTTGTTT
Adaptor 2	AGCAGTAGCAGCAGTTCGATAA
TRAC 2nd nested	CAGGTTCTGGGTTCTGGATG
TRBC2	TGGCTCAAACAAGGAGACCT

The first PCR was performed by adding 15 μl of the following components to each well: 3.8 μl 5X Herculase buffer, 0.76 μl DMSO, 0.16 μl dNTPs (25 mM each), 0.1 μl anchor_fw primer (100 μM), 0.1 μl TRAC6 (for the TCRα plate, 100 μM) or TRBC4 (for the TCRβ plate, 100 μM) primer, 0.25 μl Herculase II Fusion DNA Polymerase (Agilent) and 9.83 μl H_2O.

The second PCR was performed in a final volume of 21 μl/well by pipetting the following components in a new 96-well plate: 1 μl of the previous PCR product, 4 μl 5X Herculase buffer, 0.8 μl DMSO, 0.16 μl dNTPs (25 mM each), 0.1 μl adaptor 1 primer (100 μM), 0.1μl TRAC13 (for the TCRα plate, 100 μM) or TRBC3 (for the TCRβ plate, 100 μM) primer, 0.2 μl Herculase II Fusion DNA Polymerase (Agilent) and 14.64 μl H_2O.

The third and last PCR step was performed in a final volume of 21 μl/well by pipetting the following components in a new 96-well plate: 1 μl of the previous PCR product, 4 μl 5X Herculase buffer, 0.8 μl DMSO, 0.16 μl dNTPs (25mM each), 0.1 μl adaptor

2 primer (100μM), 0.1μl TRAC 2nd nested (for the TCRα plate, 100 μM) or TRBC2 (for the TCRβ plate, 100 μM) primer, 0.2 μl Herculase II Fusion DNA Polymerase (Agilent) and 14.64 μl H_2O.

PCR products obtained after the second nested PCR were loaded on 1.5% TAE-Agarose for gel electrophoresis. Bands between 250 and 500 bp were excised and purified using the QIAquick Gel Extraction Kit (Qiagen). TCRα chains were directly sequenced with the TRAV14-specific primer AAAGGAAGATGGACGATTCAC.

TCRβ chains were cloned into the pCR®-Blunt vector, according to the Zero Blunt® PCR cloning kit instructions. One Shot™ TOP10 bacteria were transformed with the obtained DNA, plated on LB agar containing selective antibiotic and at least 3 colonies were picked from each plate. After purification of the DNA with the QIAprep Spin miniprep kit, TCRβ inserts were sequenced with the universal M13 uni-21 primer, binding on the pCR®-Blunt vector (TGTAAAACGACGGCCAGT). Both TCRα and TCRβ sequences were annotated using IMGT/V-Quest [95].

2.6.2 Deep sequencing

After bulk sort of shorT $CD4^+$ T cells, RNA was extracted with the Arcturus PicoPure RNA isolation kit (Applied Biosystems). For each sample, RNA was eluted in 15 μl of elution buffer and reverse transcription was directly performed, by adding 5 μl of the iScript™ cDNA Synthesis kit (Bio-Rad) reaction mix. The retrotranscription reaction was run with the following program: 25°C 5min, 42°C 30min, 85°C 5min, 4°C forever. 10 μl of cDNA were then PCR-amplified with the following specific primers binding TRAV9-n3 and TRAC regions and containing Illumina sequencing overhang adapters for downstream PCRs:
TRA9n-3 forward:
GTCTCGTGGGCTCGGAGATGTGTATAAGAGACAGTATCCAGGAGACCCAGTGGT
TRAC reverse:
TCGTCGGCAGCGTCAGATGTGTATAAGAGACAG TGGTACACAGCAGGTTCTGG.
The PCR reaction mix was prepared in 20 μl/sample with the following components: 2 μl 10X PCR buffer (with $MgCl_2$), 2 μl dNTPs (2.5 mM), 2 μl primer mix (10 μM), 1 μl Taq polymerase, 3 μl H_2O, 10 μl cDNA. PCR cycling conditions were the following: 95°C 3min; 95°C 30sec, 63°C 30sec, 72°C 30sec (5 cycles); 95°C 30sec, 72°C 35sec (20-25 cycles); 72°C

4min, forever. PCR products were loaded on 1% TAE-Agarose for gel electrophoresis. Bands of around 350 bp were excised and purified using the QIAquick Gel Extraction Kit (Qiagen). DNA was eluted from the spin column in 25 µl TE-buffer.

For paired-end Illumina sequencing, additional adapters – including a flow cell binding-site for sequencing on the Illumina MiSeq System and indices for demultiplexing – were introduced to the TCR amplicons. The PCR reaction was performed in a total volume of 50 µl, with the following components: 1X Advantage 2 PCR Buffer (Clontech), 1 µM of Index 1 and Index 2 (Nextera Index Kit, Illumina), 1X dNTP Mix (10 mM each, Clontech), 30–40 ng DNA template and 1X Advantage 2 Polymerase Mix (Clontech). PCR products were purified using the Agencourt AMPure XP PCR Purification Kit (Beckman Coulter) according to the manufacturer's recommendation. For library preparation, all samples were pooled in equal amounts and the pool was set to 4 nM. Further preparation and loading of the library to the MiSeq System was done according to the "denature and dilution guide" provided by Illumina.

The obtained fastq sequences were annotated using IMGT/HighV-Quest [95]. Illumina sequencing and bioinformatic downstream analysis were conducted by Dr. Sarina Ravens (postdoctoral fellow in Immo Prinz´s lab, Hannover Medical School), using in-house bash and R scripts (version 3.2.2). In brief, only productive amino acid sequences were taken into consideration. Next, reads with unambiguous V-gene segment annotation were accepted for further analysis. Clonotypes were identified based on identical CDR3 region sequences. To normalize between samples all results are represented as percentages of all productive reads per sample (clonotype frequencies). Calculation of Morisita-Horn similarity indices was performed according to the tcR package [96]. The Shannon diversity index (H) and Shannon evenness (E) were calculated with the following formulas:

$$H = -\sum_{i=1}^{R} pi * \ln(pi)$$

$$E = \frac{H}{lnR}$$

where R = richness, i.e. total number of clonotypes (found in more than 1 read), and pi = frequency of the i^{th} clonotype.

2.7 Generation of retroviral vectors

2.7.1 Cloning

All cloning steps were designed with the ApE (A plasmid Editor)_v2.0.45 software. The TCRαPLP1-T2A-hCD2 (in pEGFP-N1 vector) was used as a template to obtain all other shorT TCRs, by site-directed mutagenesis using the QuikChange Multi Site-Directed Mutagenesis kit (Agilent) and the following mutagenic primers (introducing a new restriction site):

shorTCRα#1_SacI_fw	CTGTATACTTCTGTGCTGTGAGCTCCAATACCAACAAAGTCGTCTTTGG
shorTCRα#1_rev	CCAAAGACGACTTTGTTGGTATTGGAGCTCACAGCACAGAAGTATACAG
shorTCRα#2_MseI_fw	GGCTGTATACTTCTGTGCTGTGACCTTAAGCAATACCAACAAAGTCGTCTTTGGAAC
shorTCRα#2_rev	GTTCCAAAGACGACTTTGTTGGTATTGCTTAAGGTCACAGCACAGAAGTATACAGCC
shorTCRα#3_NruI_fw	CTGTATACTTCTGTGCTGTGAGCATCGCGAATACCAACAAAGTCGTCTTTGGAAC
shorTCRα#3_rev	GTTCCAAAGACGACTTTGTTGGTATTCGCGATGCTCACAGCACAGAAGTATACAG
shorTCRα#4_SpeI_fw	GCTGTATACTTCTGTGCTGTGACTAGTAATACCAACAAAGTCGTCTTTGGAAC
shorTCRα#4_rev	GTTCCAAAGACGACTTTGTTGGTATTACTAGTCACAGCACAGAAGTATACAGC
shorTCRα#5_ScaI_fw	GACTGGGCTGTATACTTCTGTGCAGTACTCTCTTCCAATACCAACAAAGTCGTC
shorTCRα#5_rev	GACGACTTTGTTGGTATTGGAAGAGAGTACTGCACAGAAGTATACAGCCCAGTC
shorTCRα#6_BglII_fw	GGCTGTATACTTCTGTGCTGTGAGATCTTCCAATACCAACAAAGTCGTCTTTG
shorTCRα#6_rev	CAAAGACGACTTTGTTGGTATTGGAAGATCTCACAGCACAGAAGTATACAGCC
shorTCRα#7_XhoI_fw	GCTGTATACTTCTGTGCTGTCTCGAGTTCCAATACCAACAAAGTCGTCTTTG
shorTCRα#7_rev	CAAAGACGACTTTGTTGGTATTGGAACTCGAGACAGCACAGAAGTATACAGC

The mutagenesis products were first verified by digestion with the respective restriction enzyme (SacI, MseI, NruI, SpeI, ScaI, BglII or XhoI, New England BioLabs), followed by TAE-Agarose electrophoresis, and ultimately by sequencing. The target nucleotide and amino acid CDR3α sequences are reported in the following page:

TCRα-PLP1	A gct	V gtg	S agc	P cct	F ttc	S tct	S tcc	N aat	T acc	N aac	K aaa	V gtc	V gtc
shorTCRα#1	A gct	V gtG	S AGC				S TCc	N aat	T acc	N aac	K aaa	V gtc	V gtc
shorTCRα#2	A gct	V gtg	**T** acc	**L** TTA			S Agc	N aat	T acc	N aac	K aaa	V gtc	V gtc
shorTCRα#3	A gct	V gtg	S agc	**I** aTC	**A** GCG			N Aat	T acc	N aac	K aaa	V gtc	V gtc
shorTCRα#4	A gct	V gtg	**T** ACT				S AGT	N aat	T acc	N aac	K aaa	V gtc	V gtc
shorTCRα#5	A gcA	V GTA	**L** CTc			S tct	S tcc	N aat	T acc	N aac	K aaa	V gtc	V gtc
shorTCRα#6	A gct	V gtg	**R** AGA			S TCT	S tcc	N aat	T acc	N aac	K aaa	V gtc	V gtc
shorTCRα#7	A gct	V gtC	S TCG			S AGt	S tcc	N aat	T acc	N aac	K aaa	V gtc	V gtc

Capital letters within nucleotide sequences indicate the inserted restriction sites; letters in bold refer to amino acids that differ from the template CDR3 region of the TCRαPLP1.

Next, TCRαPLP1-T2A-hCD2 and all mutants were PCR-amplified, using the following primers introducing EcoRI and XhoI restriction sites:

EcoRI/va3.2_fw: AAGAATTCGACCACCATGCTCCTGGC

XhoI/hCD2_rev: GAGCTCGAGGTCATTTCTCCGACTCCTCTGT.

The pinco-33 plasmid (see section 2.1.9) and the inserts were digested with EcoRI and XhoI restriction enzymes and ligated with T4 DNA ligase at 18°C overnight with a 1:3 vector to insert ratio. SoloPack Gold® (Stratagene) bacteria were transformed with the ligation products, plated on LB Agar containing ampicillin and the DNA was purified with the QIAGEN plasmid maxi kit. As a result of the described cloning procedure, the calcium-sensitive reporter present in the pinco-33 was eventually substituted by our TCRα of interest, followed by the T2A viral self-cleaving peptide [97] and a hCD2 reporter. The obtained retroviral vector is depicted in the following page:

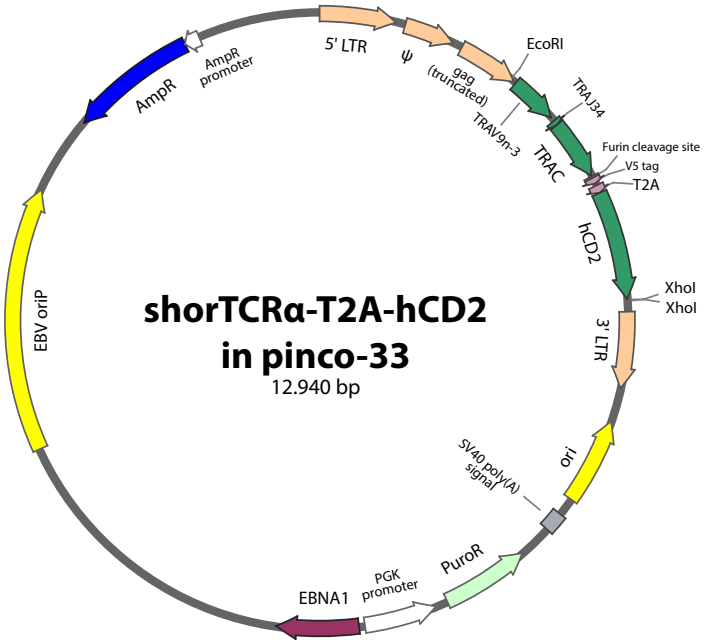

Map 2: shorTCRα-T2A-hCD2 in pinco-33 retroviral vector
The LTRs (long-terminal repeats), ψ (packaging signal) and truncated gag gene derive from murine embryonic stem cell virus. TRAV: TCRα Variable gene; TRAJ: TCRα Joining gene; TRAC: TCRα Constant gene; hCD2: human CD2; ori: bacterial origin of replication; SV40: simian-virus 40; poly(A): poly adenylation; PuroR: puromycin resistance; EBV oriP: Epstein-Barr virus origin of replication; AmpR: ampicillin resistance. The map was designed with SnapGene_v4.3.2 software.

2.7.2 Generation of stable packaging cells

3.5 x 10^5 GP+E-86 cells were seeded in 10 ml of 8% DMEM the day before transfection (in a 100 x 20 mm round cell-culture dish). On day 0, 450 µl of H_2O containing 25 µg of DNA (TCRα-T2A-hCD2 in pinco33) were mixed with 50 µl of 2.5mM $CaCl_2$ and incubated 7 minutes at 37°C. The DNA/$CaCl_2$ mix was added dropwise to 500 µl of 2X HEBS buffer (pH 7.11) while vortexing. The obtained mix was incubated at room temperature for 30 minutes. An opalescent precipitate usually formed within 10-20 minutes. The DNA/$CaPO_4$ precipitate was finally added dropwise to the cells. After 4-16 hours, the medium containing DNA/$CaPO_4$ precipitate was replaced with fresh medium. Stably transfected GP+E-86 cells were selected in puromycin-containing medium (2.5 µg/ml, Roth) starting from day 1.

2.7.3 Virus production

The supernatant of 80-90% confluent, stably transfected GP+E-86 cells was collected for two consecutive days, filtered through a 0.45 µm syringe-filter and ultracentrifuged at maximum speed for 4 hours at 4°C. The pellet was carefully resuspended in a few milliliters of fresh medium and 1ml aliquots were stored at -80°C.

2.8 Statistical analysis

Statistical analysis was performed with Prism 7 software. Statistical significance was calculated with Student´s t-test, one-way ANOVA or two-way ANOVA, as specified in the figure legends. P-values are indicated as ns (not significant, ≥0.05), * (<0.05), ** (<0.01), *** (<0.001) and **** (<0.0001).

3. Results

3.1 Impaired positive selection of MHCII-restricted thymocytes in Ctsl$^{\Delta TEC}$ mice

3.1.1 Ctsl$^{\Delta TEC}$ mice are CD4^{+} T cell lymphopenic

In order to exclusively alter MHCII-associated peptides involved in positive selection, we bred a recently engineered cathepsin L floxed mouse (kindly provided by Dr. Thomas Reinheckel) to a Foxn1-driven Cre transgenic mouse, and obtained what we hereafter refer to as Ctsl$^{\Delta TEC}$ mouse. In this mouse model, cathepsin L (Ctsl: gene, CTSL: protein) is ablated in all TECs and keratinocytes, but since cTECs are the only epithelial cell type to express CTSL for the generation of MHCII-associated peptides, we can envision such model as a cTEC-specific Ctsl knock-out. As shown in figure 6, the main phenotype of Ctsl$^{\Delta TEC}$ mice is a severe reduction in CD4SP thymocytes and CD4^{+} peripheral T cells, both in lymph nodes and spleen, reminiscent of the previously reported CD4^{+} T cell lymphopenia in the full Ctsl$^{-/-}$ mouse [69]. Also in our conditional knock-out, the defect is restricted to the CD4 compartment, while the CD8 compartment develops normally (fig. 6B). As a consequence of the reduction in CD4SP thymocytes, a relative increase in the fraction of DP thymocytes can be observed (fig. 6B).

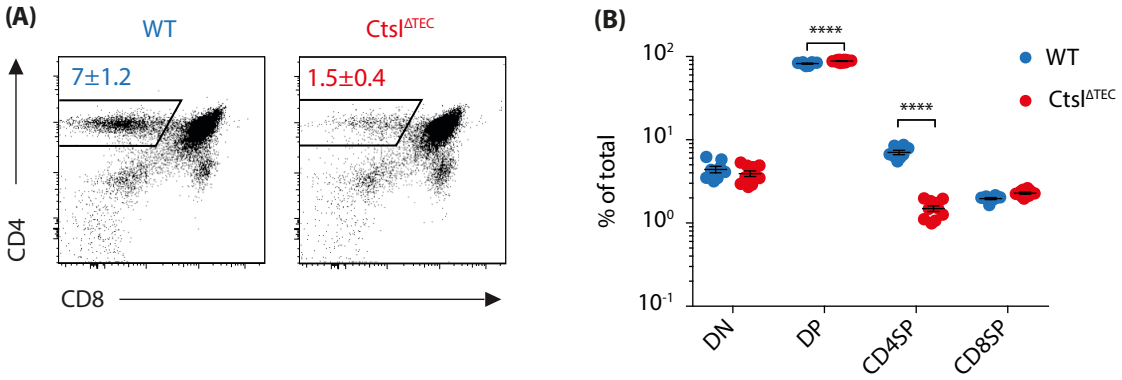

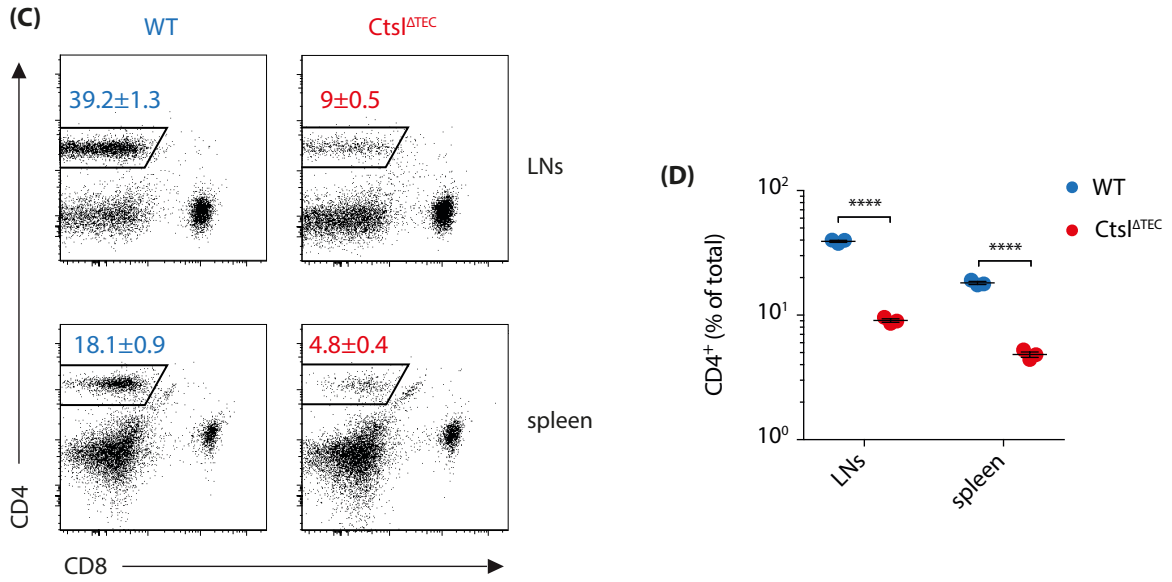

Figure 6: Reduced CD4SP thymocytes and peripheral CD4⁺ T cells in Ctsl$^{\Delta TEC}$ mice (this and previous page)
Thymic (A) and peripheral (C) CD4/CD8 flow-cytometry profiles in Ctsl$^{\Delta TEC}$ and littermate control mice, with gates showing average percentages of CD4SP ± SD. Proportions of DN, DP and SP thymocytes (B), as well as of LN and splenic CD4⁺ T cells (D) from individual mice (mean ± SEM). Results are representative of at least 3 independent experiments with 3-9 mice per group. Statistical significance was calculated with two-way RM ANOVA, applying the Sidak´s multiple comparisons post-test.

3.1.2 MHCII-restricted DP and SP thymocytes selected in the absence of CTSL have a defect in maturation

We next reasoned that, if the decrease of CD4SP thymocytes is due to impaired positive selection, a defect in maturation should be already visible at the stage of cortical DP thymocytes. However, by gating on total DP thymocytes selected in the presence or absence of CTSL, we couldn´t detect any difference (data not shown). We then decided to cross Ctsl$^{\Delta TEC}$ animals to an MHCI$^{-/-}$ background, to make sure that the contribution of MHCI-restricted TCRs didn´t affect our analysis. Indeed, when we analyzed purely MHCII-restricted DP thymocytes, we found that in the absence of CTSL a smaller fraction of them differentiates into TCRβ^{hi}CD69^{hi}(CD3^{hi}) (fig. 7A) and, within this mature fraction, CD5 levels are decreased (fig. 7B). As the expression of CD5 on thymocytes is assumed to mirror the intensity of TCR-pMHC interactions [41], our data suggest that the positive selecting ligands induce a weaker TCR signaling in the absence of CTSL.

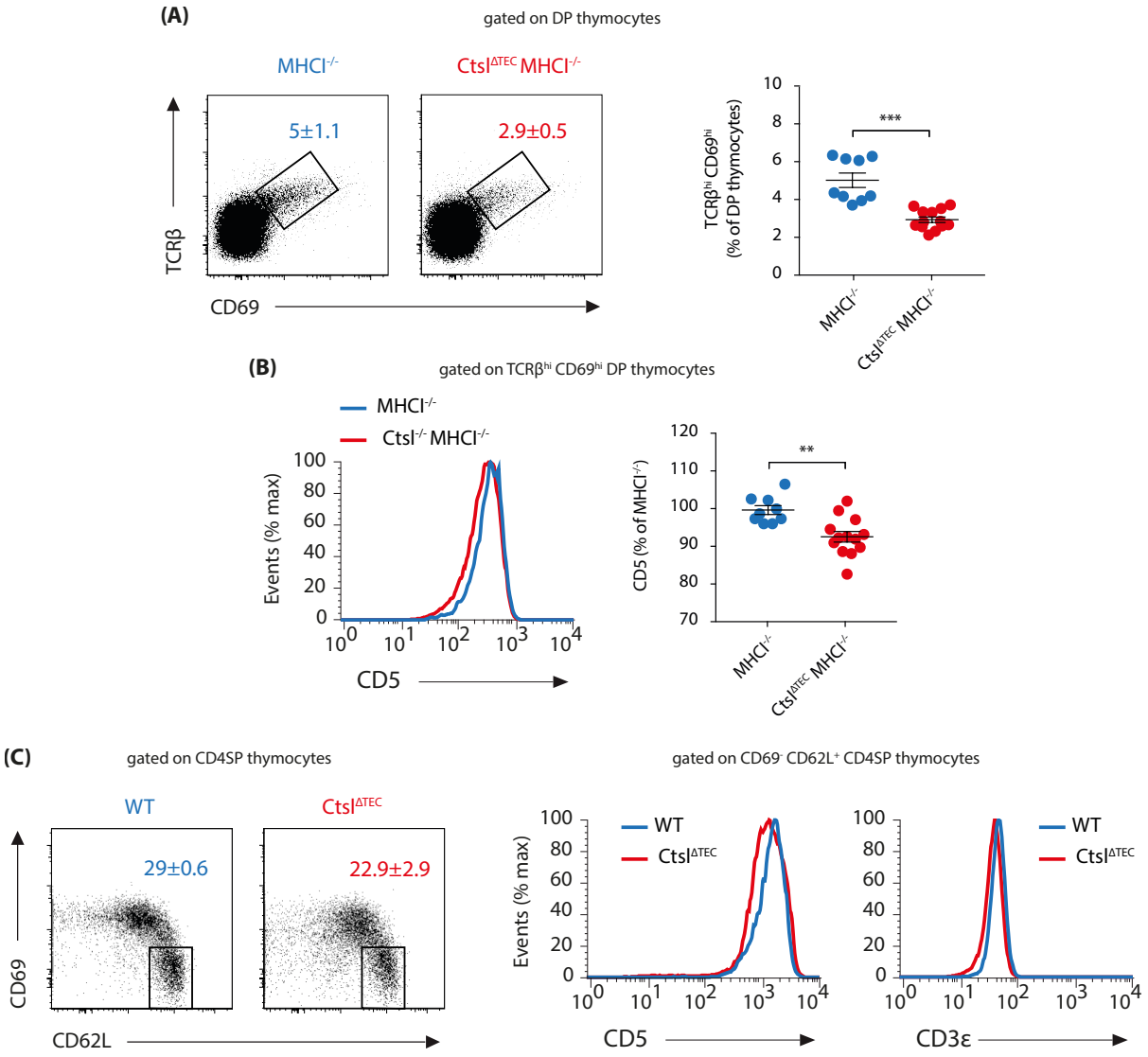

Figure 7: Defective maturation of DP and CD4SP thymocytes in CtsI$^{\Delta TEC}$ mice

(A) The left panel shows representative plots with percentages (± SD) of TCRβ^{hi}CD69^{hi} cells within DP thymocytes in MHCI$^{-/-}$ and CtsI$^{\Delta TEC}$ MHCI$^{-/-}$ mice. On the right, the same values are plotted for individual mice (mean ± SEM). Statistical significance was calculated with unpaired two-tailed Student´s t-test, applying the Welch´s correction for unequal variances. (B) The histogram on the left overlays CD5 levels on TCRβ^{hi}CD69^{hi} DP thymocytes of MHCI$^{-/-}$ and CtsI$^{\Delta TEC}$ MHCI$^{-/-}$ mice; the right graph reports individual MFI values of CD5 on TCRβ^{hi}CD69^{hi} DP thymocytes (mean ± SEM). Statistical significance was calculated with unpaired two-tailed Student´s t-test. (C) CD69/CD62L expression on CD4SP thymocytes in CtsI$^{\Delta TEC}$ and littermate control mice, with gates showing the average percentage of CD69^{-}CD62L^{+} ± SD. On the right, representative overlays of CD5 and CD3ε expression, gated on the latter fraction (n=9/group). Results are pooled from 2 independent experiments.

A similar maturation defect extends also to post-selection CD4SP thymocytes, with regards to both the percentage of fully mature $CD69^{-}CD62L^{+}$ cells and their CD5 and CD3 expression (fig. 7C), pointing altogether at a reduced TCR signaling strength resulting from the interaction with cortical and medullary pMHCII.

3.1.3 Reduced selection of CD4SP thymocytes in CTSL-deficient mice is not a consequence of excessive deletion

It is conceivable that the pMHCII presented by CTSL-deficient cTECs lead to the positive selection of an altered T cell repertoire, which may be subjected to excessive clonal deletion by other thymic APCs. To formally exclude this possibility, we performed two sets of experiments that allowed us to dissect the contribution of bone marrow (BM)-derived APCs and mTECs to the overall $CD4^{+}$ T cell lymphopenia. In the first set of experiments, depicted in figure 8A, we established BM chimeras by reconstituting lethally irradiated CTSL-sufficient and -deficient animals with $MHCII^{+/+}$ or $MHCII^{-/-}$ BM. As expected, WT mice receiving $MHCII^{-/-}$ BM show an increased percentage of CD4SP thymocytes compared to those receiving $MHCII^{+/+}$ BM, reflecting the contribution of BM-derived APCs to negative selection of MHCII-restricted thymocytes. By contrast, the low percentage of CD4SP cells in CTSL-deficient animals is not affected by reconstitution with either $MHCII^{+/+}$ or $MHCII^{-/-}$ BM.

We then addressed the role of mTECs. Based on the notion that TCR-pMHC cognate interactions are crucial for mTEC development [98], we decided to test our question in the C2TA knock-down (C2TAkd) mouse, where MHCII expression is diminished to approximately 10% of WT, without affecting mTEC maturation [56]. Figure 8B shows an increased percentage of CD4SP thymocytes in C2TAkd compared to WT mice, which illustrates the contribution of mTECs to negative selection. However, such contribution does not seem to have a major influence in the absence of CTSL, as crossing $Ctsl^{-/-}$ to C2TAkd animals does not rescue the percentage of CD4SP. Altogether, the data presented in figure 8 suggest that reduced $CD4^{+}$ T cell numbers in $Ctsl^{-/-}$ are not caused by excessive clonal deletion.

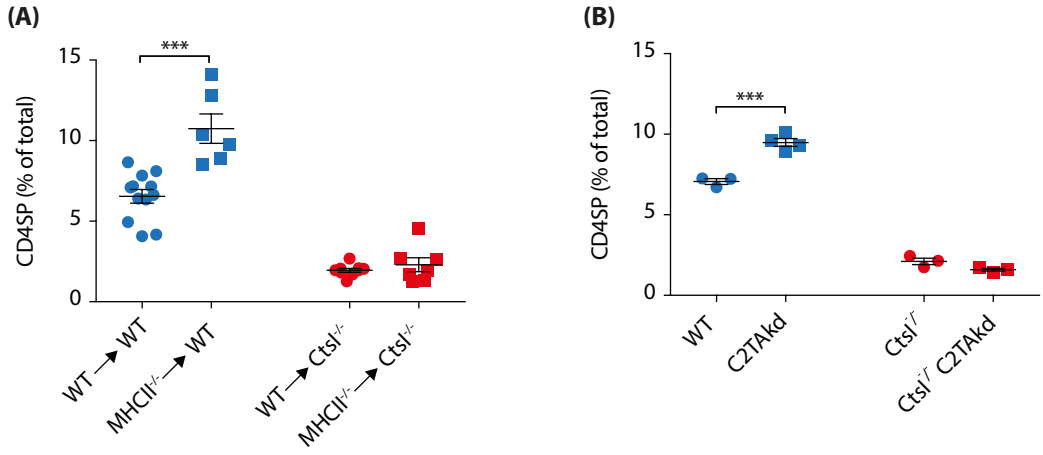

Figure 8: Inhibition of negative selection does not rescue CD4 lymphopenia in Ctsl$^{-/-}$ mice
(A) Ctsl$^{-/-}$ and littermate control mice were lethally irradiated and reconstituted with BM coming from MHCII$^{+/+}$ and MHCII$^{-/-}$ donors. The graph displays percentages of CD4SP thymocytes (mean ± SEM), as detected by flow-cytometry 6 weeks after reconstitution. Results are pooled from 3 independent experiments. (B) The plot shows percentages of CD4SP thymocytes (mean ± SEM) in Ctsl$^{-/-}$ and littermate control mice, either on a pure or on a C2TAkd background. Results are representative of 2 independent experiments. C2TAkd: C2TA knock-down. Statistical significance was calculated with unpaired two-tailed Student´s t-test.

3.1.4 Impaired positive selection of MHCII-restricted TCR^{tg} T cells in Ctsl$^{\Delta TEC}$ mice

To directly test whether Ctsl$^{\Delta TEC}$ mice have a defect in positive selection, we investigated the fate of thymocytes bearing MHCII-restricted monoclonal TCRs specific for foreign antigens; in this scenario, negative selection cannot take place, because the cognate antigen is not expressed in the thymus. As depicted in figure 9, we tested the selection of seven different TCRs in either Ctsl$^{\Delta TEC}$ or littermate control mice, by performing BM chimeras with the following Rag1$^{-/-}$ TCR transgenic (TCR^{tg}) donors: Dep-TCR^{tg} specific for human C reactive protein (hCRP) [83], OTII-TCR^{tg} specific for chicken ovalbumin (OVA) [91], AND-TCR^{tg} and AD10-TCR^{tg} specific for moth and pigeon cytochrome C (MCC, PCC) [86], LLO56-TCR^{tg} and LLO118-TCR^{tg} specific for listeriolysin O (LLO) from *Listeria monocytogenes* [85] and PLP1-TCR^{tg} specific for proteolipid protein (PLP) [84]. Since the latter TCR is specific for a self-antigen, we used recipients lacking the endogenous target protein (Plp$^{-/-}$) to detect only the impact of positive selection. Six weeks after reconstitution, none of the seven TCRs tested was selected in Ctsl$^{\Delta TEC}$ mice, revealing a major defect in positive selection of MHCII-restricted T cells.

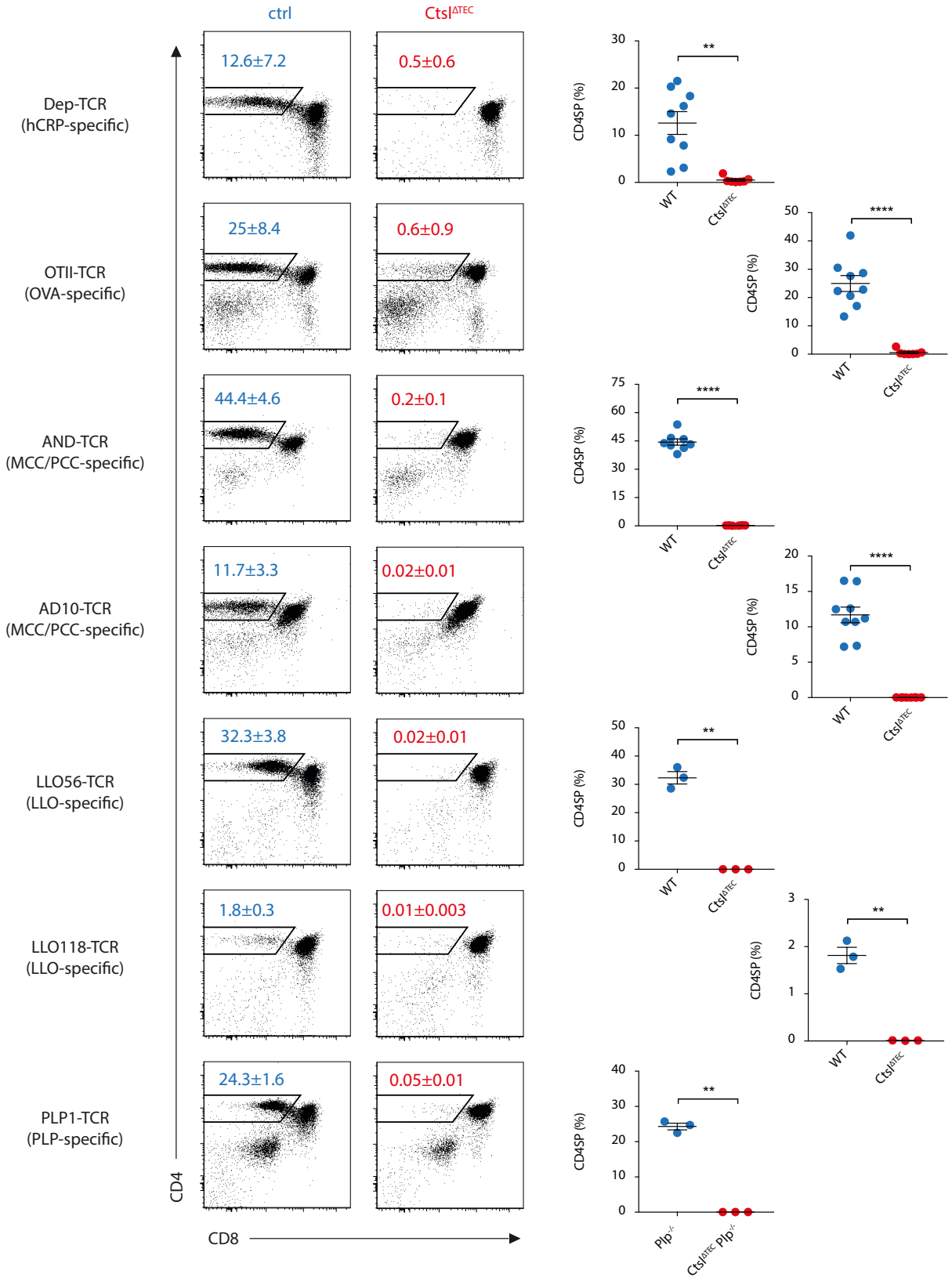
ctrl
Ctsl^ΔTEC
Dep-TCR
(hCRP-specific)
12.6±7.2
0.5±0.6
OTII-TCR
(OVA-specific)
25±8.4
0.6±0.9
AND-TCR
(MCC/PCC-specific)
44.4±4.6
0.2±0.1
AD10-TCR
(MCC/PCC-specific)
11.7±3.3
0.02±0.01
LLO56-TCR
(LLO-specific)
32.3±3.8
0.02±0.01
LLO118-TCR
(LLO-specific)
1.8±0.3
0.01±0.003
PLP1-TCR
(PLP-specific)
24.3±1.6
0.05±0.01
CD4
CD8
CD45P (%)
WT
Ctsl^ΔTEC
Plp^-/-
Ctsl^ΔTEC Plp^-/-
**
****

Figure 9: Impaired selection of multiple CD4^{+} TCR^{tg} T cells in Ctsl$^{\Delta TEC}$ mice (previous page) Ctsl$^{\Delta TEC}$ and littermate control mice were lethally irradiated and reconstituted with BM coming from seven different MHCII-restricted TCR^{tg} Rag1$^{-/-}$ donors: specifically, from top to bottom, Dep, OTII, AND, AD10, LLO56, LLO118 and PLP1 TCR^{tg} donors were used. Flow-cytometry plots on the left and graphs on the right display percentages of CD4SP thymocytes 6 weeks after reconstitution. Results are representative of 2 independent experiments for each TCR. Recipients of the TCR-PLP1 were bred on the Plp$^{-/-}$ background. Statistical significance was calculated with unpaired two-tailed Student´s t-test.

3.1.5 A higher fraction of MHCII on CTSL-deficient cTECs is occupied by Ii-degradation products

CTSL has been described both to generate MHCII-associated peptides and to cleave the invariant chain (Ii). Therefore, we reasoned that the defect in positive selection of Ctsl$^{\Delta TEC}$ mice could be due not only to the presentation of an altered set of MHCII-associated peptides but also to an aberrant MHCII maturation *per se* in cTECs lacking CTSL. To test the latter hypothesis, we stained cTECs of 3-week old WT and Ctsl$^{\Delta TEC}$ mice with antibodies recognizing different conformations of MHCII, and we found that the total surface levels of MHCII are independent of CTSL expression (fig. 10A). However, in CTSL-deficient cTECs a higher fraction of surface MHCII is occupied by fragments of Ii, such as the small leupeptin-induced peptide (SLIP) and/or the class-II associated invariant chain peptide (CLIP), and a lower fraction by peptides different from CLIP, as evinced from the respective staining with 15G4 and BP107 antibody clones (fig. 10B and C).

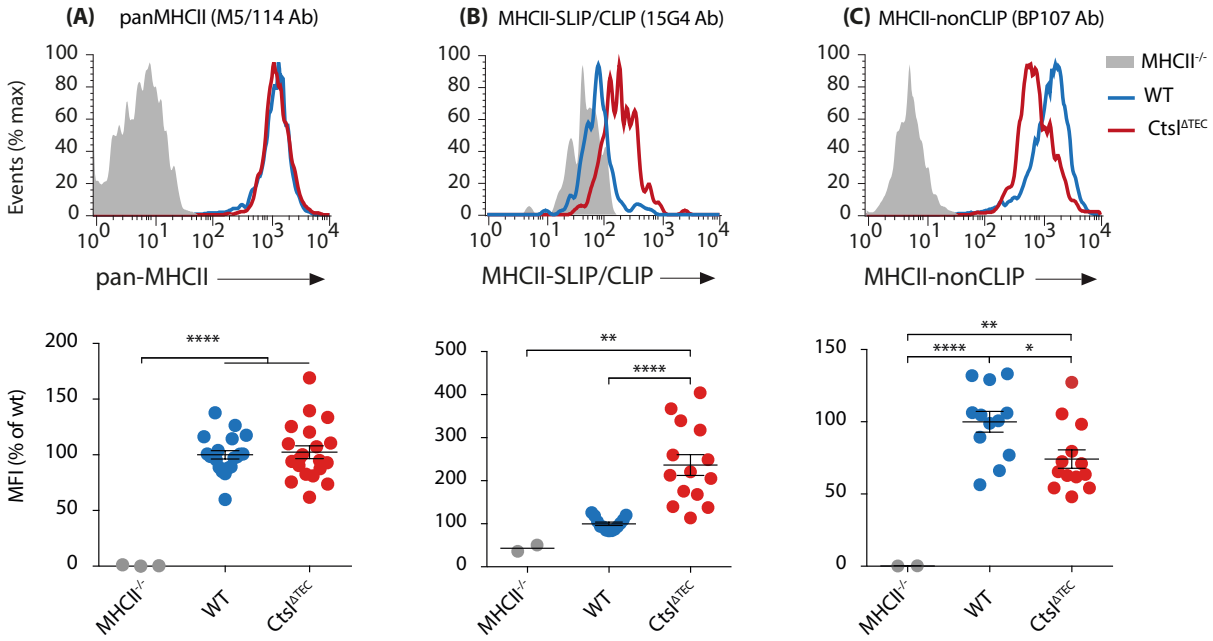

Figure 10: Increased MHCII-SLIP/CLIP on the surface of Ctsl$^{\Delta TEC}$ cTECs (previous page)
TECs were isolated from thymi of 3-week-old Ctsl$^{\Delta TEC}$, littermate controls and MHCII$^{-/-}$ mice and stained with antibodies specific for different conformations of MHCII. All plots show results gated on cTECs (CD45^{-} EpCAM^{+} Ly51^{+}). In the upper row, surface expression of total MHCII (A), MHCII-SLIP/CLIP (B) and MHCII-nonCLIP (C) is overlaid among the three different genotypes. In the lower row, graphs illustrate normalized MFI of the respective MHCII conformation for individual mice (mean ± SEM). Results are pooled from 3 independent experiments. Statistical significance was calculated with one-way ANOVA, applying the Sidak´s multiple comparisons post-test.

This confirms former data obtained on the full Ctsl$^{-/-}$ mouse [69] and suggests that MHCII maturation in cTECs of Ctsl$^{\Delta TEC}$ mice leads to the accumulation of surface MHCII-SLIP/CLIP.

3.2 Hypo-responsiveness of CTSL-independent CD4SP thymocytes

3.2.1 CD4SP thymocytes selected in Ctsl$^{\Delta TEC}$ mice undergo less homeostatic proliferation in lymphopenic hosts

Mice lacking the thymoproteasome catalytic subunit β5t have a defect in positive selection of MHCI-restricted thymocytes and reduced numbers of CD8^{+} T cells in peripheral lymphoid organs [62, 64]. Interestingly, cTECs in β5t$^{-/-}$ mice express the proteasome subunits β5 and β5i, which are believed to generate more stable positive-selecting pMHCI molecules compared to the β5t subunit; in accordance to this hypothesis, CD8SP thymocytes in β5t$^{-/-}$ mice show increased Nur77 and CD5 levels, and proliferate more upon adoptive transfer into lymphopenic recipients, suggesting a higher degree of self-reactivity [64].

With this in mind, we adoptively transferred congenically-marked CFSE-labeled WT and Ctsl$^{\Delta TEC}$ CD4SP thymocytes in a 1:1 ratio into sublethally irradiated hosts (fig. 11A), which resulted in significantly higher proliferation of WT over Ctsl$^{\Delta TEC}$ cells after 9 days. The decreased rate of homeostatic proliferation of Ctsl$^{\Delta TEC}$ CD4SP thymocytes became even more evident at 30 days post transfer, with WT cells outcompeting them 8:1 (fig. 11B). Altogether, cTECs lacking CTSL provide weaker positive-selecting signals to developing thymocytes, thus generating a CD4^{+} T cell repertoire defective in proliferation to peripheral self-pMHCII.

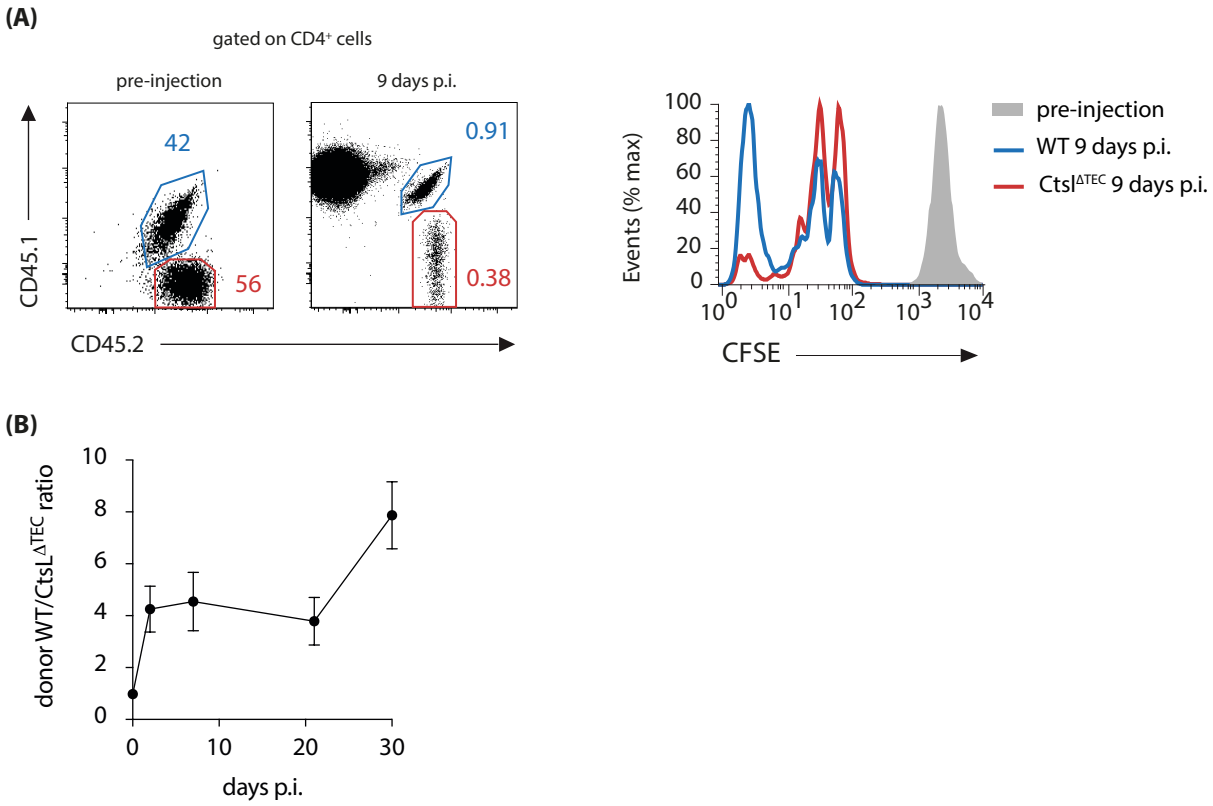

Figure 11: Ctsl$^{\Delta TEC}$ CD4SP thymocytes proliferate less upon adoptive transfer into irradiated hosts

WT CD45.1 recipients were sublethally irradiated (6Gy); on the next day, they received an intravenous injection of FACS-sorted CFSE-labeled CD4SP (CD62L^{+} CD69^{-} CD25^{-}) thymocytes coming from Ctsl$^{\Delta TEC}$ (CD45.2) and WT (CD45.1/.2) mice in a 1:1 ratio. (A) The left panel shows the CD45.1/CD45.2 distribution within CD4^{+} T cells in the injected mix and in LNs of recipient mice (n=2) 9 days post injection (p.i.). On the right, a representative histogram overlays CFSE dilution curves of donor cells pre-injection (grey solid) and after 9 days (WT in blue, Ctsl$^{\Delta TEC}$ in red). (B) The ratio of WT to Ctsl$^{\Delta TEC}$ transferred cells is monitored in the blood of recipient mice for up to 30 days p.i. (n=3).

3.2.2 CD4SP thymocytes selected in Ctsl$^{\Delta TEC}$ mice respond weakly to polyclonal stimulation

In order to test the functionality of CTSL-independent CD4SP thymocytes upon TCR stimulation, we FACS-sorted mature CD69^{-} CD62L^{+} CD4SP cells from WT and Ctsl$^{\Delta TEC}$ thymi and cultured them *in vitro* for 40 hours in the presence of αCD3/CD28 antibodies. As shown in figure 12A, cells derived from Ctsl$^{\Delta TEC}$ mice acquired a less activated phenotype than WT cells, as attested by decreased size (measured by forward scatter area, FSC-A) and levels of CD25, CD69 and CD44. Although this defective response might be partially explained by the lower CD3 basal levels on Ctsl$^{\Delta TEC}$ CD4SP cells (fig. 7C), direct *ex vivo*

activation of the same cells with a TCR-bypassing stimulus resulted in decreased phosphorylation of ERK1 and 2 (fig. 12B), suggesting an intrinsically lower TCR sensitivity of CD4SP thymocytes selected by CTSL-deficient cTECs.

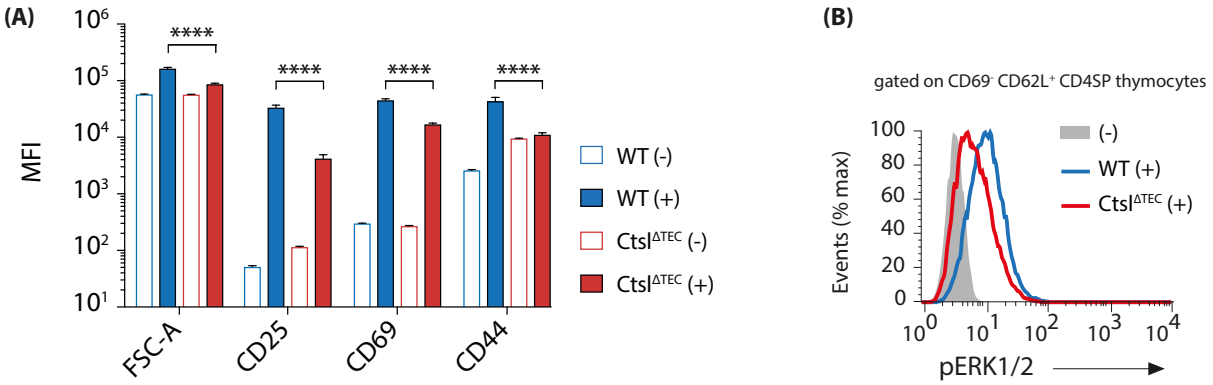

Figure 12: CtsI$^{\Delta TEC}$ CD4SP thymocytes respond less to *in vitro* polyclonal stimulation
(A) Equal numbers of CD4SP (CD62L$^+$ CD69$^-$ CD25$^-$) thymocytes were sorted from WT and CtsI$^{\Delta TEC}$ mice and stimulated for 40 hours in separate wells with anti-CD3/CD28 antibodies (+) or left unstimulated as controls (-). The MFI of forward scatter area (FSC-A), CD25, CD69 and CD44 is reported for all the conditions. Statistical significance was calculated with one-way ANOVA, applying the Sidak´s multiple comparisons post-test. (B) Equal numbers of CD4SP (CD62L$^+$ CD69$^-$ CD25$^-$) thymocytes were sorted from WT and CtsI$^{\Delta TEC}$ mice and stimulated for 5 minutes with PMA (+) or left unstimulated as controls (-). Levels of intracellular phosphorylated ERK1/2 were detected by flow-cytometry.

3.3 Influence of CTSL on the selection of an antigen-specific CD4$^+$ T cell repertoire

3.3.1 LLO-specific CD4$^+$ T cells are selected regardless of CTSL expression

The CD4$^+$ T cell repertoire selected in CtsI$^{\Delta TEC}$ mice is not only reduced in size but also qualitatively different, both in terms of missing TCR specificities (fig. 9) and reduced proliferation to self-antigens (fig. 11) and αCD3/CD28 stimulation (fig. 12A). Since none of the seven TCRs we tested in BM chimeras is selected in the absence of CTSL, we tried to further characterize the CTSL-independent CD4$^+$ T cell repertoire through a different method, namely the MHCII-tetramer technology [99]. Surprisingly, by using an I-A^b tetramer carrying the 190-201 residues of the listeriolysin O (LLO) peptide derived from *Listeria monocytogenes* [100], we were able to identify comparable numbers of LLO-specific CD4$^+$ T cells in the thymus and periphery of WT and CtsI$^{\Delta TEC}$ mice (fig. 13), in spite

of total CD4 counts being much lower in the absence of CTSL. This means that roughly 100-200 LLO-specific CD4SP thymocytes and 400 LLO-specific CD4$^+$ peripheral T cells are found in a naïve mouse, regardless of CTSL expression; of note, the number of antigen-specific peripheral T cells in Ctsl$^{\Delta TEC}$ mice is more variable, possibly due to oligoclonal expansions favored by the lymphopenic environment.

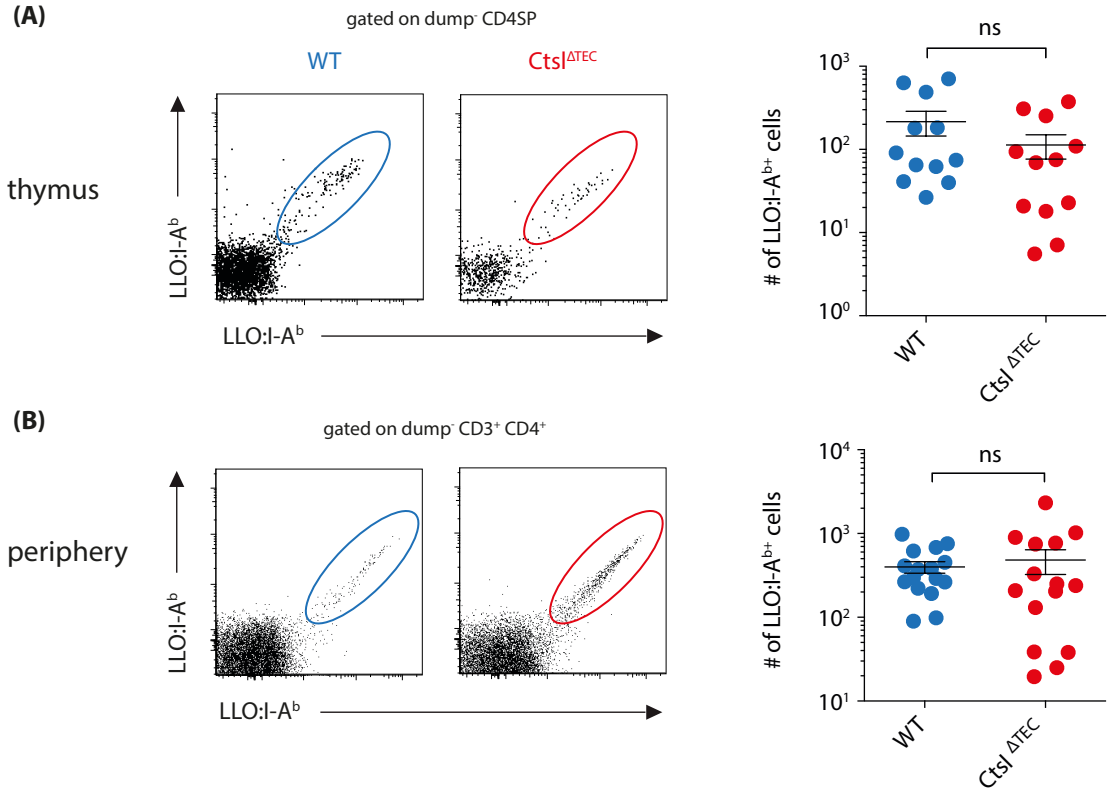

Figure 13: Equivalent numbers of LLO:I-A^{b+} CD4$^+$ T cells in Ctsl$^{\Delta TEC}$ and WT mice
Cells obtained from thymi (A) and peripheral lymphoid organs (B) of WT and Ctsl$^{\Delta TEC}$ mice were stained with the LLO$_{(190-201)}$:I-A^b tetramer labeled in two different colors: only the double positive cells were counted as tetramer positive. Representative plots on the left show the gating strategy for the counts presented on the right (mean ± SEM). Results are pooled from 4 independent experiments. Statistical significance was calculated with unpaired two-tailed Student´s t-test.

3.3.2 Defective response to LLO-immunization in Ctsl$^{\Delta TEC}$ mice

The fact that an equivalent number of LLO-specific CD4$^+$ T cells are selected in the presence or absence of CTSL does not mean that we are dealing with the very same cells; in fact we only know that these cells are binding the LLO:I-A^b tetramer. Therefore we tried to get some insights into the properties of LLO:I-A^{b+} cells by monitoring the response of WT and Ctsl$^{\Delta TEC}$ mice to an intra-footpad immunization with LLO$_{(190-201)}$ immunodominant

epitope in CFA. As shown in figure 14A, one week after the challenge LLO-specific CD4$^+$ T cells had undergone a 20-fold expansion in the draining LNs of WT mice compared to non-immunized controls, whereas only a 2-fold increase could be registered in Ctsl$^{\Delta TEC}$ mice. To exclude that the lymphopenic environment in the periphery of Ctsl$^{\Delta TEC}$ mice could influence their response to LLO-immunization, we next performed an adoptive transfer experiment, in which WT recipients were co-injected with CD62L$^+$ mature CD4SP thymocytes sorted from WT and Ctsl$^{\Delta TEC}$ donors, each containing the same amount of LLO:I-A^{b+} cells (≈60, see input in fig. 14B). Recipient mice were immunized 12 hours later with LLO peptide in CFA and analyzed after one week. Results depicted in figure 14B show that donor Ctsl$^{\Delta TEC}$ CD4$^+$ T cells do not take part in the response to LLO-immunization, as the only tetramer-positive cells detectable in the draining LNs are of WT origin (both donor and recipient).

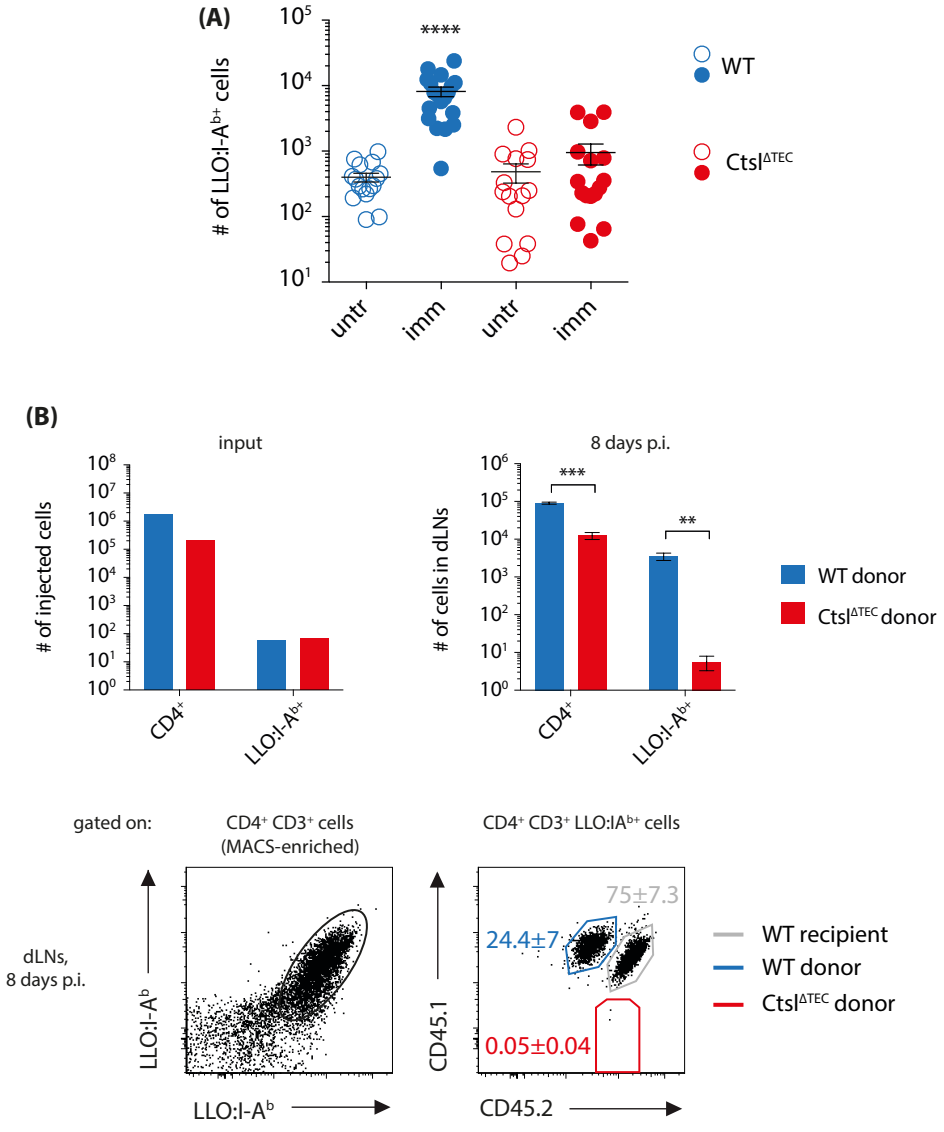

Figure 14: Ctsl$^{\Delta TEC}$ CD4^{+} T cells respond poorly to LLO immunization, even upon adoptive transfer into WT hosts (previous page)
(A) WT and Ctsl$^{\Delta TEC}$ mice were immunized intra-footpad with LLO$_{(190-201)}$ peptide in CFA (imm) or left untreated (untr) as controls. One week later, CD4^{+} LLO:I-A^{b+} cells were counted in the peripheral lymphoid organs; at this time point, CD4^{+} LLO:I-A^{b+} cells in immunized mice were almost exclusively confined to draining LNs (dLNs). Results are pooled from 4 independent experiments. (B) CD4SP (CD62L^{+} CD69^{-} CD25^{-}) thymocytes were FACS-sorted from WT (CD45.1) and Ctsl$^{\Delta TEC}$ (CD45.2) donors and co-injected into WT CD45.1/.2 recipients (n=3). The upper left panel shows the composition of the injected cells, with a 1:1 ratio between WT and Ctsl$^{\Delta TEC}$ LLO:I-A^{b+} cells (≈ 60 cells each). 12 hours after the adoptive transfer, recipient mice were immunized intra-footpad with LLO$_{(190-201)}$ peptide in CFA; draining LNs were analyzed one week later. The upper right graph displays the number of CD4^{+} cells and LLO:I-A^{b+} cells of WT donor (blue) and Ctsl$^{\Delta TEC}$ donor (red) origin, which were found in the dLNs one week after immunization. In the lower row, representative plots show the gating strategy for LLO:I-A^{b} double positive cells in the dLNs, as well as the origin of such cells based on the congenic markers CD45.1 and CD45.2 (mean percentage of single or double positives ± SD). Statistical significance was calculated with one-way ANOVA, applying the Sidak´s multiple comparisons post-test (A) and unpaired two-tailed Student´s t-test (B).

Altogether, data obtained from immunization experiments argue in favor of a cell-intrinsic functional defect of Ctsl$^{\Delta TEC}$ LLO-specific CD4^{+} T cells.

3.3.3. Comparison of LLO-specific CD4^{+} TCR repertoires in WT and Ctsl$^{\Delta TEC}$ mice

The defective response of CD4^{+} T cells to LLO-immunization in Ctsl$^{\Delta TEC}$ mice might be due to alterations in TCR repertoire diversity or TCR signaling or both. Starting from the notion that at least one CD4^{+} T cell clone, the so-called LLO118 TCR – which is stainable with the LLO$_{(190-201)}$:I-A^{b} tetramer and is known to participate in the primary response to *Listeria* infection [85] – is selected in WT but not Ctsl$^{\Delta TEC}$ mice (fig. 9), we hypothesized that LLO-specific CD4^{+} TCR repertoires of WT and Ctsl$^{\Delta TEC}$ mice might be different. In order to address this, we performed single-cell TCRα and TCRβ sequencing of CD4^{+} T cells responding to LLO-immunization in the two genetic backgrounds. However, given the wide diversity of the polyclonal TCR repertoire, we decided to focus only on the TCRs whose α chain contains the TRAV14 gene segment, detectable by an anti-vα2 antibody. We chose to sequence the vα2^{+} clones because the LLO18 TCR is vα2^{+} and, most importantly, because many CD4^{+} T cells responding to LLO-immunization express this TCRα chain in WT mice (fig. 15A). As already seen in steady state and immunized conditions for the entire LLO-specific repertoire, also the number of vα2^{+} LLO-specific

T cells in the draining LNs of immunized Ctsl$^{\Delta TEC}$ mice is rather variable, ranging from 10 to 3000 cells per mouse, which likely reflects an oligoclonality of the repertoire.

Figure 15B shows that vα2^{+} LLO:I-Ab^{+} CD4^{+} T cells sorted from the draining LNs of immunized WT and Ctsl$^{\Delta TEC}$ mice are composed of mostly non-overlapping TCR clones. Indeed, only one TCR clone – out of the 65 clonotypes sequenced – is shared between the two groups (depicted as a red slice in the pie charts). Although many more TCRs need to be analyzed before drawing conclusions, at a first glance the WT LLO-specific repertoire seems to be more diverse than the Ctsl$^{\Delta TEC}$ one, with almost every cell expressing a different TCR.

Results summarized in figure 15 confirm our initial hypothesis that the impaired response of Ctsl$^{\Delta TEC}$ mice to LLO-immunization is due, at least in part, to a different CD4^{+} TCR repertoire.

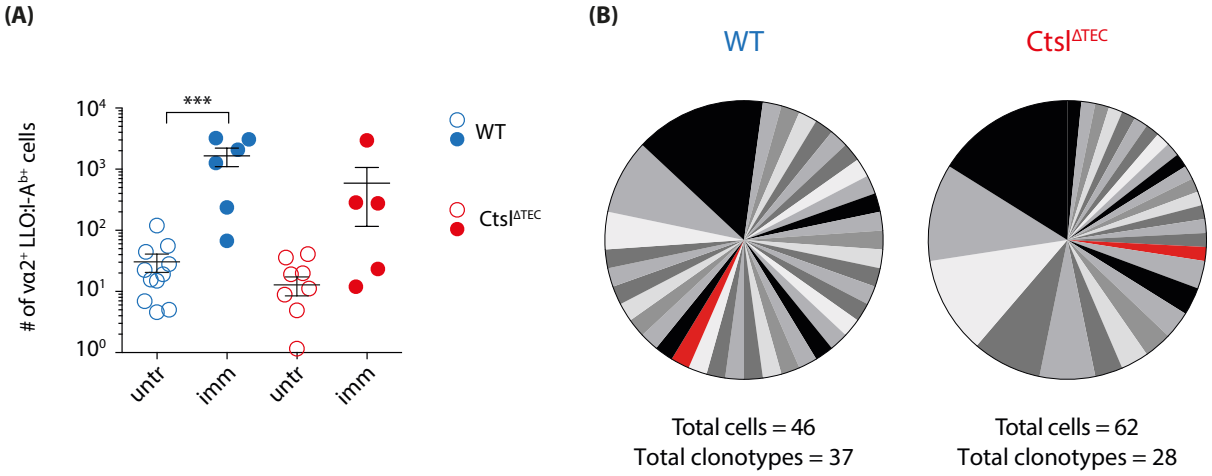

Figure 15: vα2^{+} LLO-specific T cells responding to immunization in Ctsl$^{\Delta TEC}$ and WT mice
WT and Ctsl$^{\Delta TEC}$ mice were immunized intra-footpad with LLO$_{(190-201)}$ peptide in CFA (imm) or left untreated (untr) as controls. One week later, antigen-specific CD4^{+} cells in immunized mice were almost exclusively confined to draining LNs (dLNs). (A) At this time point, CD4^{+} LLO:I-A^{b+} vα2^{+} cells were counted in the peripheral lymphoid organs of immunized and untreated mice. Results are pooled from 2 independent experiments. Statistical significance was calculated with one-way ANOVA, applying the Sidak´s multiple comparisons post-test. (B) CD4^{+} LLO:I-A^{b+} vα2^{+} cells sorted from the dLNs of immunized TCRα$^{+/-}$ (WT, n=2) and Ctsl$^{\Delta TEC}$ TCRα$^{+/-}$ (Ctsl$^{\Delta TEC}$, n=12) mice were subjected to single-cell TCR sequencing. In the pie charts every slice represents a unique TCR clone and the number of total sequences is indicated. The only TCR found in both groups is highlighted in red.

3.4 Influence of CTSL on the selection of an oligoclonal CD4$^+$ T cell repertoire

3.4.1 Generation of the shorT mouse

Historically, thymic selection has been extensively studied exploiting TCR transgenic mice, which are nowadays known to carry along several caveats, mainly due to the development of a non-physiological monoclonal T cell repertoire and to the premature expression of the TCRα chain. In spite of these limitations, as it is extremely difficult to cope with the wide diversity of TCRs present in the polyclonal system (fig. 3), TCR transgenic mice still represent a valuable tool. A good compromise between the polyclonal and the monoclonal systems was achieved by two independent groups in 2001 and 2006: they generated TCR-oligoclonal mice through conventional transgenesis, by keeping the TCRβ chain constant, so that the burden of developing a selectable TCR falls entirely on a pre-selected TCRα locus [101, 102]. More precisely, the TCR gene segments chosen for the purpose derive from classical TCRs (respectively OT-I and Ep) specific for foreign antigens. Due to the expression of a transgenic rearranged TCRβ, the endogenous β locus is subjected to allelic exclusion and this ensures the development of T cells with a single TCRβ chain, whereas crossing the animals to a TCRα$^{-/-}$ strain guarantees the development of T cells bearing a single TCRα chain; finally, premature expression of the TCRα at the DN stage is prevented by the fact that it needs to undergo rearrangements in order to be functional.

Along a similar line, our laboratory generated a mouse where limited TCR diversity is obtained by fixing the β chain, while allowing only a single defined TCRα Variable (V) and two Joining (J) segments to recombine and give rise to a functional TCR (see fig. 16). Unlike the previous TCR-oligoclonal models, the particular Vα (Vα3.2) and Jα (Jα34) genes – as well as TCRβ chain – chosen for this strategy have been identified as part of the TCR-PLP1 [84], which recognizes the self-protein PLP; the only exception is made for the Jα2 segment, which is part of the TCRα cassette vector [103]. Of note, we performed all the experiments on a Plp$^{-/-}$ background, to minimize negative selection events and maximize the TCR repertoire diversity. Our new mouse model, which we named the "shorT mouse", can generate roughly 10^4 different TCR clones, 99% of which use the Jα34 segment.

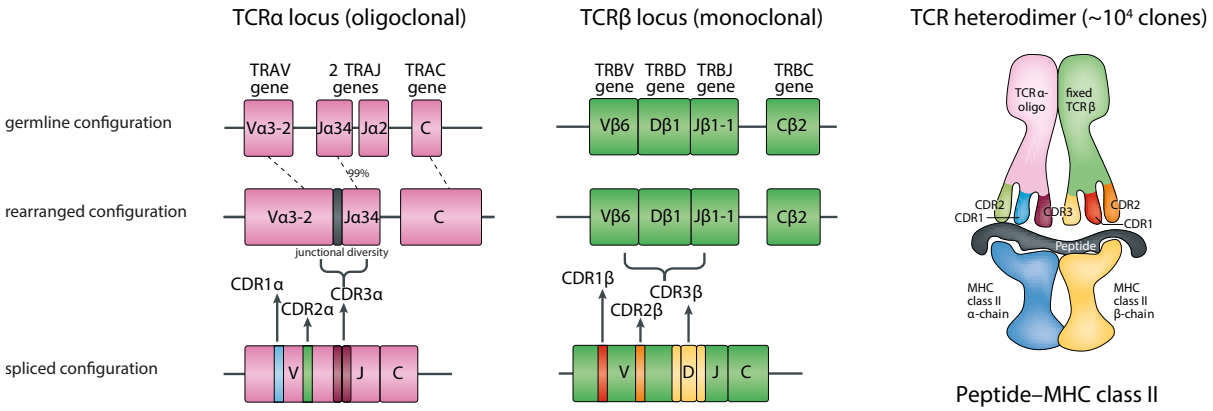

Figure 16: Generation of TCR diversity in the shorT mouse
In the germline configuration, the TCRα locus contains a single V gene (Vα3.2) and 2 J genes (Jα34 and Jα2), which can be rearranged by RAG recombinases due to the presence of recombination signal sequences. Combinatorial diversity is almost absent, as in 99% of cases the Jα34 is chosen. Since the TCRβ is completely fixed, the entire diversity comes from junctional diversity at the complementarity-determining region 3 α (CDR3α) region. With the name "shorT mouse" we refer to a mouse model bearing the described oligoclonal TCRα, a monoclonal TCRβ (TCRβ-PLP1, [84]), an endogenous TCRα$^{-/-}$ locus [93] and Plp$^{-/-}$ [92] locus. The observed TCR diversity in such mouse is ≈10^4. The figure was adapted from [32].

3.4.2 Impaired positive selection of the CD4$^+$ shorT repertoire in Ctsl$^{\Delta TEC}$ mice

Bulk CD4$^+$ T cell selection in the shorT mouse can be easily analyzed by flow-cytometry with fluorescently conjugated anti-vα3.2 and -vβ6 antibodies. As depicted in figure 17A, the TCRα constraints in the shorT mice decrease the percentage of CD3$^+$ CD4SP thymocytes, compared to control mice expressing only the fixed TCRβ chain; when crossed to Ctsl$^{\Delta TEC}$, shorT mice generate even less CD3$^+$ CD4$^+$ T cells, both in the thymus and in the LNs (fig. 17B), mirroring the defect in positive selection seen in the polyclonal setting (fig. 6). Likewise, CD5 levels on CD3$^+$ CD4SP thymocytes are decreased in Ctsl$^{\Delta TEC}$ shorT mice in comparison to TCRβ-PLP1^{tg} or WT shorT mice (fig. 17C), hinting at weaker pMHCII interactions during the selection of this TCR-oligoclonal repertoire in the absence of CTSL.

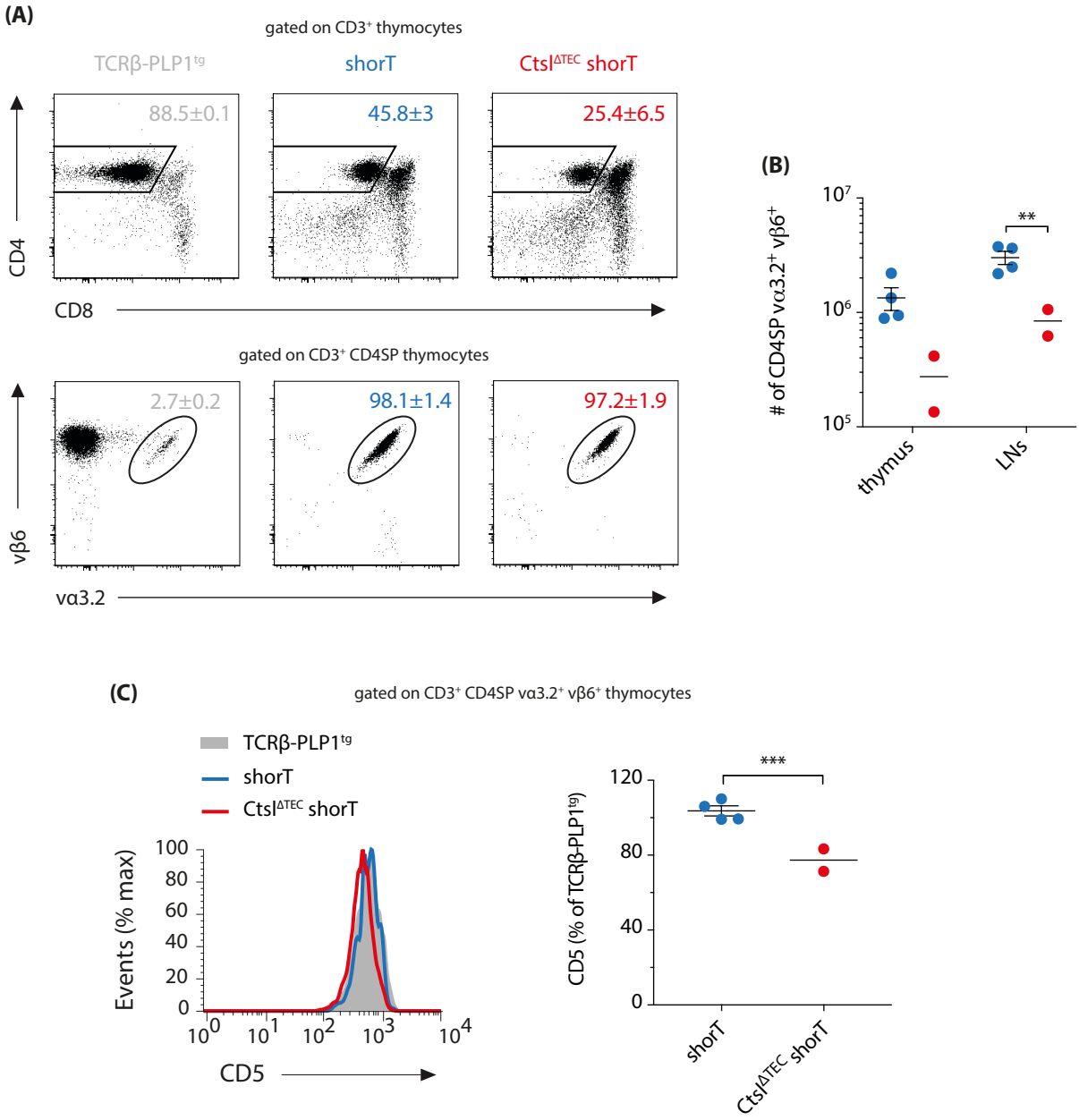

Figure 17: Impaired positive selection of CD4⁺ T cells in CtsI$^{\Delta TEC}$ shorT mice

(A) Representative plots of thymi in WT (blue, n=4) and CtsI$^{\Delta TEC}$ (red, n=2) shorT mice, as well as in mice expressing only the fixed PLP1-TCRβ (grey, n=2). The first row shows the percentage of CD4SP within CD3⁺ thymocytes (mean ± SD); the percentage of vα3.2⁺ vβ6⁺ cells, gated on the latter cell population, is displayed in the second row (mean ± SD). (B) The number of CD3⁺ CD4SP vα3.2⁺ vβ6⁺ cells in the thymus and LNs of individual WT and CtsI$^{\Delta TEC}$ shorT mice is plotted (mean ± SEM). (C) On the left, representative histogram overlay of CD5 surface levels on CD3⁺ CD4SP vα3.2⁺ vβ6⁺ thymocytes in WT (blue, n=4) and CtsI$^{\Delta TEC}$ (red, n=2) shorT mice, as well as in mice expressing only the fixed PLP1-TCRβ (grey, n=2). The right panel shows the individual values of CD5 MFI on the same cells in shorT mice normalized to the level found in PLP1-TCRβ^{tg} mice (mean ± SEM). Statistical significance was calculated with two-way RM ANOVA, applying the Sidak´s multiple comparisons post-test (B) and unpaired two-tailed Student´s t-test (C).

3.4.3 Impact of CTSL on the TCR repertoire diversity of CD4$^+$ shorT cells

As already mentioned, a comprehensive characterization of TCRs selected in the presence or absence of CTSL is technically impossible in a polyclonal scenario, even when focusing on a subset of T cells sharing the same antigen specificity (e.g. vα2$^+$ LLO:I-Ab$^+$ T cells, see fig. 15B). Indeed, the main advantage of dealing with a restricted TCR repertoire – like the one in the shorT mouse – is the possibility to capture the whole TCR diversity by means of TCRα deep sequencing. Due to the difficulty of crossing shorT mice (TCRα-shorT^{tg}, TCRβ-PLP1^{tg}, TCRα$^{-/-}$, PLP$^{-/-}$) to Ctsl$^{\Delta TEC}$ mice (Ctsl$^{fl/fl}$, Foxn1-CRE^{tg}), we conducted all deep sequencing experiments on BM chimeras generated with shorT BM donors and either WT or Ctsl$^{\Delta TEC}$ recipients.

Figure 18A shows the CD4$^+$ TCRα diversity of WT compared to Ctsl$^{\Delta TEC}$ shorT mice, calculated with the Shannon index (H). This index takes into account both the number (richness) and the distribution (evenness) of clonotypes, and represents the uncertainty with which one can predict the identity of a TCR clone: H equals 0 when there is only one clonotype, so the prediction is certain, while it increases with richness and evenness – hence unpredictability – of clones. TCR diversity is higher in WT than in Ctsl$^{\Delta TEC}$ shorT mice, and this difference tends to increase in the periphery. In order to determine if this disparity is due mainly to the richness or evenness of the TCR clones, we also calculated the Shannon index evenness (E), which measures how equally distributed the clones are (from 0 to 1). As depicted in figure 18B, TCR clones are more unevenly distributed in the thymus and especially in the LNs of Ctsl$^{\Delta TEC}$ shorT mice, reminiscent of the peripheral oligoclonality seen within the Ctsl$^{\Delta TEC}$ LLO-specific CD4$^+$ T cell compartment. As for the richness of the repertoires, figure 18C shows no clear difference in the number of clonotypes between WT and Ctsl$^{\Delta TEC}$ shorT mice. Therefore, reduced evenness accounts for the lower TCR diversity observed in Ctsl$^{\Delta TEC}$ mice.

We next addressed the TCR repertoire similarity by calculating the Morisita-Horn index (MHI), which compares the number and frequency of TCR clones between two given samples and assumes values comprised between 0 (no overlap) and 1 (complete overlap). We calculated the MHI for couples of samples belonging either to different genotype groups (inter-genotype similarity, fig. 18D) or to the same genotype group (intra-genotype similarity, fig. 18E). Quite unexpectedly, according to the inter-genotype MHI, the shorT TCR repertoires selected in the presence or absence of CTSL are largely

overlapping (fig. 18D). With regard to the intra-genotype MHI (fig. 18E), the thymic TCR repertoire similarity amongst WT shorT mice is extremely high, almost close to 1; the Ctsl$^{\Delta TEC}$ group also shows a very high MHI in the thymus, although lower than the WT counterpart. In the LNs, both WT and Ctsl$^{\Delta TEC}$ repertoires become clearly less stereotypic from mouse to mouse, with a more pronounced drop within the Ctsl$^{\Delta TEC}$ group: again this might be due to the fact that certain TCR clones expand in the periphery.

Overall, the CD4^{+} shorT repertoire selected in the absence of CTSL shows lower TCR diversity (fig. 18A), yet high similarity to the repertoire selected by WT cTECs (fig. 18D). In general, the distribution of TCR clones tends to be more uneven in the periphery than in the thymus, especially in Ctsl$^{\Delta TEC}$ but also in WT controls (fig.18B), and this is in line with the similarity of TCR repertoires within the same genotype being lower in the periphery as compared to the thymus (fig. 18E).

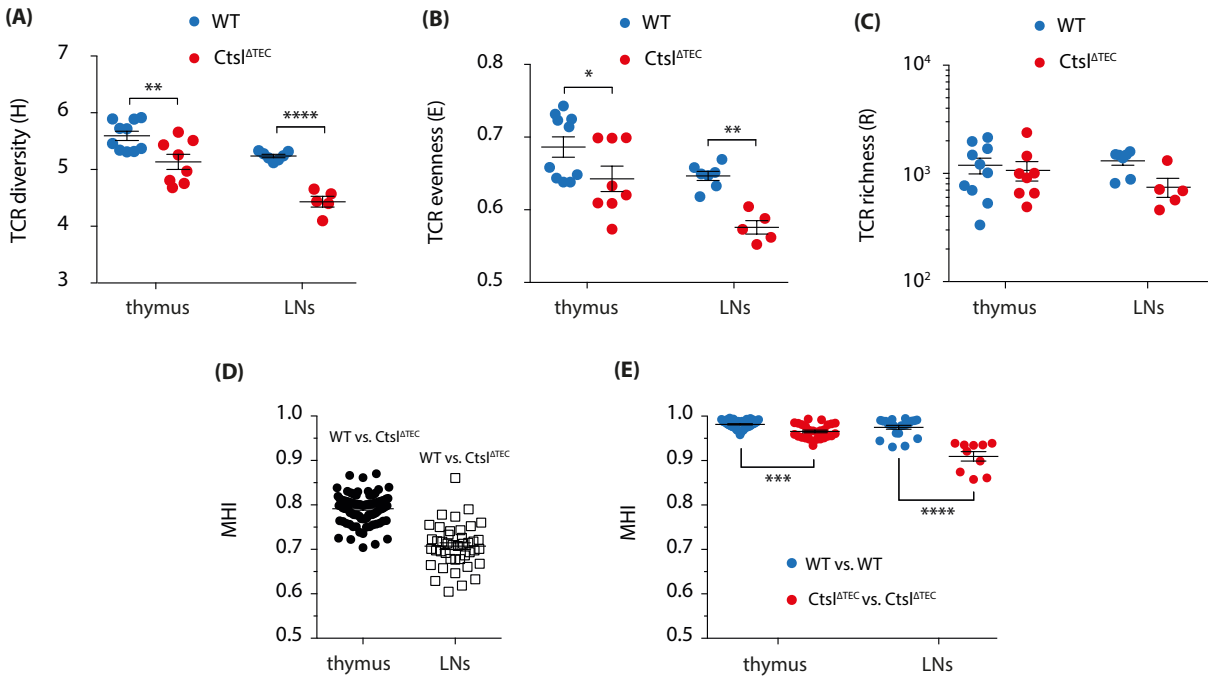

Figure 18: TCR diversity of CD4^{+} shorT cells selected on a WT or Ctsl$^{\Delta TEC}$ background
WT and Ctsl$^{\Delta TEC}$ mice were lethally irradiated and reconstituted with BM coming from shorT donors. 6 weeks after reconstitution, CD4SP vα3.2^{+} vβ6^{+} cells were FACS-sorted from thymi and LNs of recipient mice and subjected to TCRα deep sequencing. Shannon diversity index (A) and Shannon evenness (B) were calculated for individual mice, according to the formulas provided in the materials and methods. The TCR richness (C) was considered as the number of clonotypes found in each mouse, excluding those found in only 1 read. Inter-genotype (D) and intra-genotype (E) Morisita-Horn indexes were also calculated, through pair-wise comparison of mice belonging to different genotypes or to the same genotype, respectively. Results are pooled from 3 independent experiments (n=5-10/group). Statistical significance was calculated with two-way ANOVA, applying the Sidak´s multiple comparisons post-test (A, B, C, E).

3.4.4 Identification of CTSL-dependent and -independent TCRs in the shorT repertoire

Since the WT and Ctsl$^{\Delta TEC}$ shorT CD4^{+} TCR repertoires are very similar to each other, but the latter is less diverse, we hypothesized that some TCRs are strictly dependent on CTSL for selection, while others can be selected in its absence. We therefore sought to identify the most prominent CTSL-dependent and -independent TCRs in the shorT repertoire, with the idea of further characterizing them individually in retrogenic mice and validate our hypothesis. For this purpose, we took into account only the clonotypes present with at least 0.5% frequency in either of the two genotypes: as predicted by the high MHI (fig. 18D), most TCR clones show comparable frequencies within the WT and Ctsl$^{\Delta TEC}$ repertoires and fall along the diagonal, however some are largely missing from Ctsl$^{\Delta TEC}$ mice (fig. 19A). Among these CTSL-dependent TCRs we picked #5, #6 and #7 for further characterization, as they showed an equivalent profile in the thymus and LNs; with regards to CTSL-independent TCRs, which appear to be the vast majority of frequent clonotypes, we selected #1, #2, #3 and #4 for subsequent analyses, as they also maintained an analogous frequency in the periphery (fig. 19A and data not shown). Of note, the most represented TCR in both repertoires is clone #1, accounting for more than 10% of total TCR sequences; TCRs #2, #3 and #4 are overrepresented, whereas TCRs #5, #6 and #7 are underrepresented, in Ctsl$^{\Delta TEC}$ mice (fig. 19B).

When we performed the same analysis on the pre-selection repertoire, differences in clonotype frequency between WT and Ctsl$^{\Delta TEC}$ mice were completely lost (fig. 19C and D), confirming that the observed phenotype is acquired during positive selection.

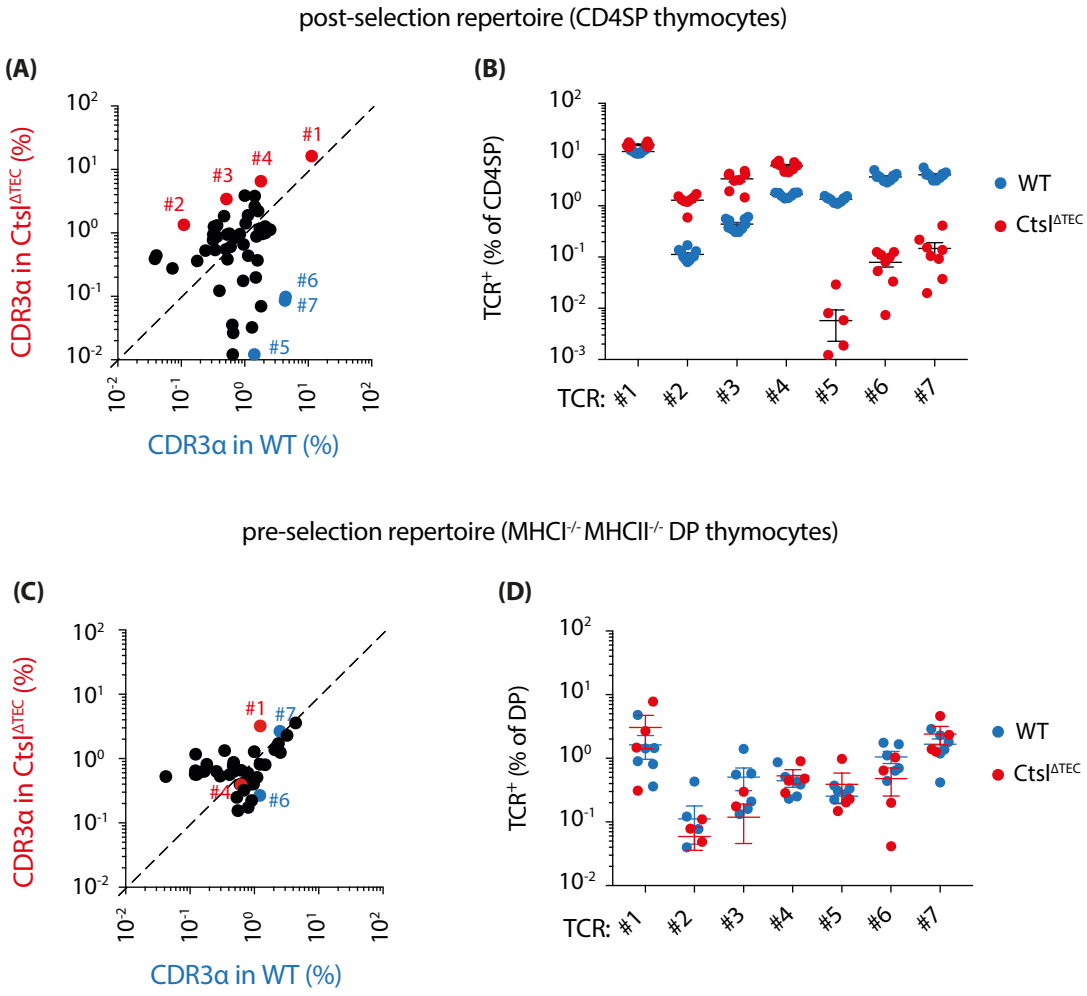

Figure 19: The most frequent CTSL"-dependent" and "-independent" shorT TCRs are identifiable after positive selection

(A, B) WT and Ctsl$^{\Delta TEC}$ mice were lethally irradiated and reconstituted with BM coming from shorT donors. 6 weeks after reconstitution, CD4SP vα3.2^{+} vβ6^{+} thymocytes were FACS-sorted from recipient mice and subjected to TCRα deep sequencing. Only CDR3α sequences present with at least 0.5% frequency in one of the two genotypes were analyzed. (A) The mean frequency with which such CDR3α sequences were found in WT and Ctsl$^{\Delta TEC}$ recipients is plotted (n=3/group). CTSL"-dependent" TCRs are highlighted in blue (#5-7), whereas CTSL"-independent" TCRs in red (#1-4). (B) Individual frequencies of TCRs #1-7 are detailed for WT (n=10) and Ctsl$^{\Delta TEC}$ (n=8) mice. Results are pooled from 3 independent experiments. (C, D) MHCI$^{-/-}$MHCII$^{-/-}$ (WT) and MHCI$^{-/-}$MHCII$^{-/-}$ Ctsl$^{\Delta TEC}$ (Ctsl$^{\Delta TEC}$) mice were lethally irradiated and reconstituted with BM coming from congenic (CD45.1) shorT donors. 6 weeks after reconstitution, vα3.2^{+} vβ6^{+} CD45.1^{+} DP thymocytes were FACS-sorted from recipient mice and subjected to TCRα deep sequencing. Only CDR3α sequences present with at least 0.5% frequency in one of the two genotypes were analyzed. (C) The mean frequency with which such CDR3α sequences were found in WT and Ctsl$^{\Delta TEC}$ recipients is plotted (n=4-6/group). CTSL"-dependent" TCRs are highlighted in blue (#5-7), whereas Ctsl"-independent" TCRs in red (#1-4). (D) Individual frequencies of TCRs #1-7 are detailed for WT (n=6) and Ctsl$^{\Delta TEC}$ (n=4) mice. Results are pooled from 2 independent experiments.

3.4.5 Validation of CTSL-dependent and -independent TCRs in retrogenic mice

In order to functionally validate CTSL-dependent and -independent TCRs, we cloned the TCRα sequences #1-7 into retroviral vectors containing a viral self-cleaving peptide [97] and hCD2 reporter, and transduced with each of these viruses BM progenitor cells harvested from TCRβ-PLP1^{tg} Rag1$^{-/-}$ donor mice. We then reconstituted lethally irradiated, CTSL-sufficient or deficient TCRα$^{-/-}$ recipients, to generate retrogenic mice as formerly described by Vignali´s group [104]. The reason why we chose T cell deficient recipients was to avoid competition by endogenous T cells: indeed, previous BM chimeras experiments with shorT donors and polyclonal recipients revealed that in the periphery endogenous T cells had a great advantage over shorT cells (data not shown).

For most of the TCRs, generation of retrogenic mice is still ongoing. Figure 20 shows preliminary results of retrogenic mice expressing the CTSL-independent TCR#2, eight weeks after reconstitution: just like in the shorT background, this TCR clone is preferentially selected in the absence of CTSL in the monoclonal setting. Specifically, CD4SP thymocytes are found almost exclusively in Ctsl$^{\Delta TEC}$ recipients (fig. 20A and C), whereas LN CD4^{+} T cells are clearly detectable in both groups and reach a cell number of 10^6 in Ctsl$^{\Delta TEC}$ mice, versus 10^5 in WT mice (fig. 20B and C). In conclusion, we could successfully re-express TCR#2 *in vivo* and validate the finding that CTSL is not needed for its selection.

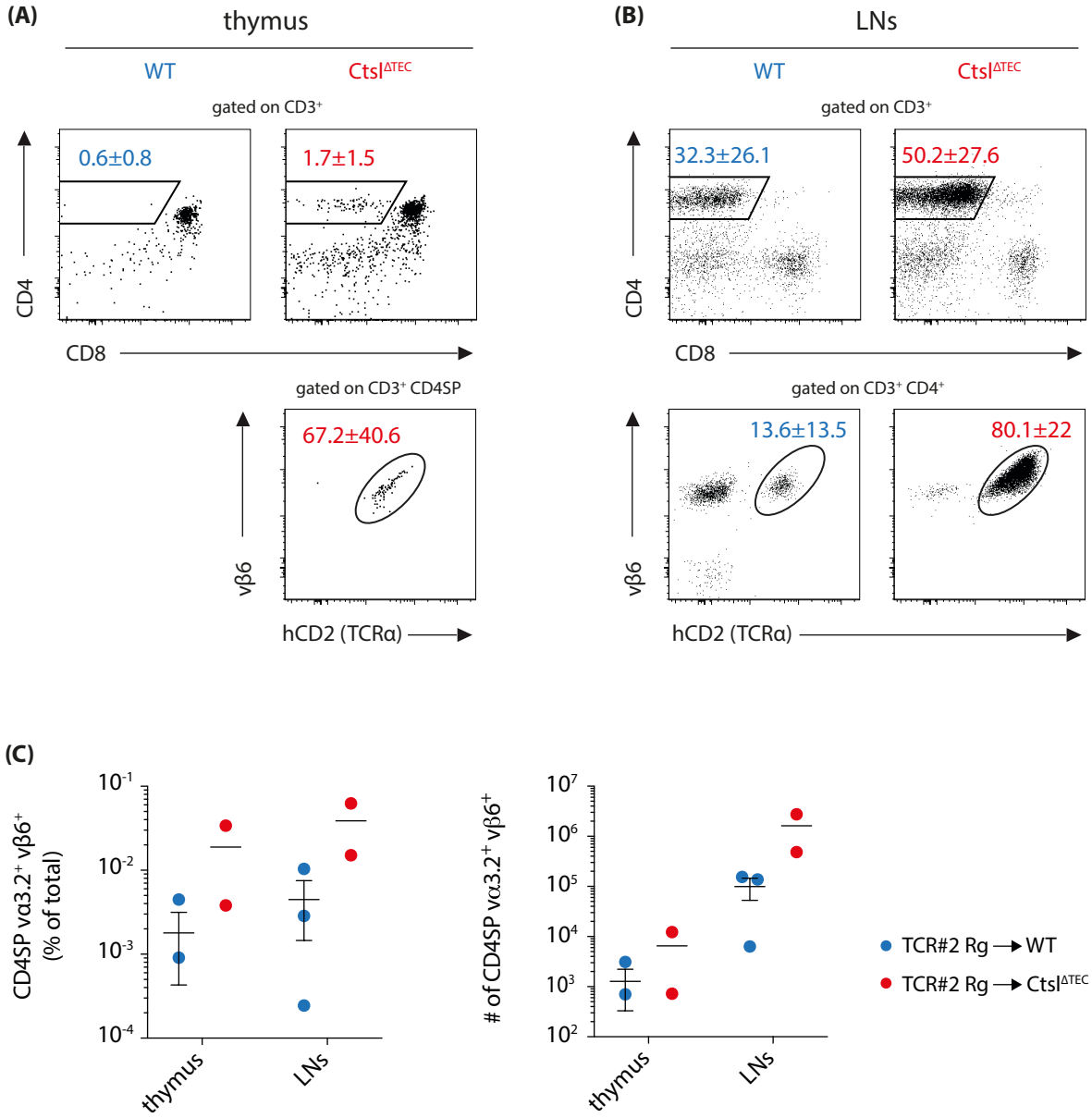

Figure 20: TCR#2 is preferentially selected in the absence of CTSL

BM progenitor cells coming from PLP1-TCRβ^{tg} Rag1$^{-/-}$ donors were transduced with a retroviral vector expressing the TCRα#2 cDNA and a hCD2 reporter. These retrogenic (Rg) BM cells were used to reconstitute TCRα$^{-/-}$ (WT, n=3) and TCRα$^{-/-}$ Ctsl$^{\Delta TEC}$ (Ctsl$^{\Delta TEC}$, n=2) recipient mice; lymphoid organs were analyzed 8 weeks later. Representative flow-cytometry plots show the percentage of CD4SP within CD3$^+$ thymocytes (A) or CD3$^+$ LN cells (B); the percentage of hCD2$^+$ vβ6$^+$ cells, gated on the latter cell populations, is displayed in the second row (mean ± SD). The thymus of WT mice showed barely any CD3$^+$ CD4SP cells, so the fraction of hCD2$^+$ vβ6$^+$ cells is not displayed. (C) The percentage and number of CD3$^+$ CD4SP vα3.2$^+$ vβ6$^+$ cells in the thymus and LNs of individual WT and Ctsl$^{\Delta TEC}$ retrogenic mice is plotted (mean ± SEM). One of the WT points is not visible because equal to zero. Statistical significance was calculated with two-way RM ANOVA, applying the Sidak´s multiple comparisons post-test.

4. Discussion

4.1 Comparison between Ctsl$^{-/-}$ and Ctsl$^{\Delta TEC}$ mouse models

The Ctsl germline knock-out (Ctsl$^{-/-}$) was first described in 1998 [69] and reported to suffer from severe CD4^{+} T cell lymphopenia. It became soon clear that such deficiency was attributable to the lack of CTSL in the radio-resistant thymic stroma and, more precisely, both impaired positive selection and excessive negative selection of MHCII-restricted thymocytes were held responsible for the lymphopenic phenotype [71]. Ctsl$^{-/-}$ mice also exhibit a profound hair loss [82, 105], due to the lack of CTSL in some cells of the inner root sheet of the hair follicle. In our experience, they neither live as long, nor breed as well as WT mice, as CTSL is needed in many tissues such as skin, bones [106], heart [107-109], brain (reviewed in [110]) and adipose tissue [111]. In contrast, when we crossed mice bearing Ctsl floxed alleles (Ctsl$^{fl/fl}$, unpublished) to Foxn1-Cre transgenic ones, we generated healthy Ctsl conditional knock-out mice (Ctsl$^{\Delta TEC}$), which are almost phenotypically indistinguishable from littermate controls. The only visible defect they show is mild alopecia, probably due to the absence of CTSL in keratinocytes. More details are reported in Table 1.

Our initial experiments on Ctsl$^{\Delta TEC}$ mice confirmed that the absence of CTSL in TECs is necessary and sufficient to decrease the percentage and number of CD4SP thymocytes and CD4^{+} peripheral T cells (fig. 6). Behind this CD4^{+} T cell reduction could be either a defect in positive selection or an excess of negative selection, specifically targeting MHCII-restricted thymocytes. Although we cannot exclude that excessive clonal deletion is induced by cTECs themselves in CTSL-deficient mice, the reduced CD5 levels on DP and CD4SP thymocytes (fig. 7) would argue for suboptimal, rather than exaggerated, TCR:pMHCII interactions. Furthermore, when we ruled out the contribution of BM-derived APCs and mTECs to negative selection, we didn't observe any rescue of the CD4SP compartment (fig. 8). Of note, this finding is in disagreement with what shown by Honey and colleagues [71], and advocates that negative selection by BM-derived thymic APCs does not account for the CD4^{+} T cell lymphopenia in CTSL-deficient mice. To directly address the efficiency of positive selection, we generated BM chimeras and tested the

selection of seven different MHCII-restricted TCRs specific for foreign antigens. None of the TCR^{tg} BM donors gave rise to CD4SP cells in $Ctsl^{\Delta TEC}$ recipients (fig. 9), in line with previous data reporting impaired selection of the BDC2.5 [112] and the TCli $CD4^+$ TCR^{tg} BM, but not of the OT-I $CD8^+$ TCR^{tg} BM in $Ctsl^{-/-}$ recipients [71]. The fact that $CD8^+$ T cells are normally selected in the absence of CTSL further suggests that the general ability of cTECs to mediate positive selection is not impaired.

	$Ctsl^{-/-}$ [69]	**$Ctsl^{\Delta TEC}$** (unpublished)
phenotype	- Extensive alopecia [82, 105] - Cardiomyopathy [107-109] - Alterations in skin and bones [106], adipogenesis and glucose tolerance [111] - Defective secretion of neurotransmitters/hormones (reviewed in [110]) - Female infertility - $CD4^+$ T cell lymphopenia	- Mild alopecia - $CD4^+$ T cell lymphopenia
T cell selection	- 80% reduction in positive selection of MHCII-restricted T cells [69] - Deficiency of $v\alpha14^+$ NKT cells [113] - Excessive negative selection of MHCII-restricted T cells [71]; disproved by our data	80% reduction in positive selection of MHCII-restricted T cells
Not selected $CD4^+$ TCRs	- TCli [71], BDC2.5 [112] - Dep, OT-II, AND, AD10, LLO56, LLO118, PLP1	Dep, OT-II, AND, AD10, LLO56, LLO118, PLP1
MHCII on cTECs	- Normal surface MHCII [69] - Higher MHCII-SLIP/CLIP [69] - Lower MHCII-non CLIP [69]	- Normal surface MHCII - Higher MHCII-SLIP/CLIP - Lower MHCII-non CLIP

Table 1: Comparison between $Ctsl^{-/-}$ and $Ctsl^{\Delta TEC}$ mice
The major characteristics of the germline ($Ctsl^{-/-}$) and the conditional ($Ctsl^{\Delta TEC}$) Ctsl knock-outs are listed in the table. The main differences between the two models derive from the ubiquity of CTSL. Indeed $Ctsl^{-/-}$ mice suffer from multi-organ dysfunction, whereas $Ctsl^{\Delta TEC}$ mice are healthy and retain only the defect in positive selection of MHCII-restricted αβT cells.

Besides suffering from $CD4^+$ T cell lymphopenia, $Ctsl^{-/-}$ mice were reported to lack $v\alpha14^+$ NKT cells, as a result of deficiency of CTSL in DP thymocytes [113]. In contrast, in $Ctsl^{\Delta TEC}$ mice, DP thymocytes can present CTSL-dependent ligands on the non-classical

MHCI-like molecule CD1d and promote the selection of vα14^{+} NKT cells. Therefore, we can affirm that conditional knock-out of Ctsl in Foxn1-expressing cells leads mainly to a defect in positive selection of MHCII-restricted conventional αβT cells, whereas other immune and non-immune cell subsets remain – to our knowledge – unaffected (see Table 1 for summary).

4.2 Positively-selecting peptides in the absence of CTSL

How does the loss of CTSL in cTECs induce the substantial defect in positive selection, which characterizes both Ctsl germline and conditional knock-out models? The fact that the selection of certain CD4^{+} TCR transgenic thymocytes is completely blocked in CTSL-deficient mice, while the selection of polyclonal CD4^{+} T cells is only reduced, led us and others to exclude a role for CTSL in regulating molecules required for general CD4^{+} T cell selection. Based on previous work by Honey and coworkers [71], we decided to focus on CTSL's impact on the regulation of MHCII-antigen presentation. CTSL is a lysosomal cysteine protease, which was described to degrade several targets, including the invariant chain (Ii) during MHCII maturation in cTECs [69]. Consistent with reports in the Ctsl$^{-/-}$ model, we could show that overall MHCII levels on the surface of cTECs are unchanged in Ctsl$^{\Delta TEC}$ mice. However, the peptide repertoire displayed on MHCII for positive selection is altered, as a higher fraction is occupied by the Ii degradation products SLIP and/or CLIP, recognized by the 15G4 antibody (fig. 10). This accumulation of immature MHCII on CTSL-deficient cTECs can be explained by incomplete Ii degradation and/or by CLIP having a higher affinity for MHCII than peptides generated in the absence of CTSL. In either case, the severe defect in CD4^{+} T cell selection in Ctsl$^{\Delta TEC}$ mice cannot be explained by the increased fraction of MHCII-SLIP/CLIP on cTECs, as Ctsl$^{-/-}$ animals of a different MHCII haplotype, which is independent of CTSL for Ii degradation, show the same severe CD4 reduction [71]. For this reason, we are rather inclined to believe that the phenotype of Ctsl$^{\Delta TEC}$ mice is attributable to CTSL´s role in the generation of positively-selecting peptides.

Unfortunately, the nature of such peptides cannot be directly investigated with proteomic techniques and we have only indirect evidence supporting our hypothesis. We are also not able to estimate which fraction of MHCII is occupied by SLIP/CLIP on the surface of Ctsl$^{\Delta TEC}$ cTECs, as flow-cytometry staining with anti-MHCII antibodies is not

quantitative. Nevertheless, by staining with the BP107 antibody, we could show that Ctsl$^{\Delta TEC}$ cTECs display a certain amount of peptides different from CLIP, which are likely responsible for the positive selection of the few CD4SP thymocytes found in these mice. The BP107 clone is conformation-sensitive and was initially raised as a broadly alloreactive antibody [114]; later on, it proved unable to stain MHCII molecules in H2-M$^{-/-}$ mice [115] and has been widely used to stain I-A^{b}-nonCLIP complexes ever since. In hindsight, the broad alloreactivity of BP107 can be easily reconciled with its inability to recognize MHCII-CLIP, the rationale being the extreme conservation of CLIP across species. However, caution should be taken in drawing conclusions from the BP107 staining, as its exact target(s) remain(s) unknown.

Another open question remains, as to whether other proteases can compensate for the loss of CTSL in CTSL-deficient mice. This is an extremely technically-demanding question to solve, as many proteases, including cathepsins, are translated into inactive pro-proteases and only active-site labeling can be used to stain their active forms. Active-site labeling would stain only proteases sharing the same catalytic site, so in our case cysteine cathepsins. We could of course use different probes to detect other families of proteases, but, with this technique, we would anyhow not be able to detect unknown proteases or proteases against which specific probes do not exist. So far we could not sort enough cTECs to perform this experiment and we can only rely on the finding that cathepsin S is not upregulated in cTECs of Ctsl$^{-/-}$ mice (data not shown in [69]). In our eyes, it is equally unlikely that cathepsin S compensates for CTSL loss in Ctsl$^{\Delta TEC}$ mice, because in that scenario also the Ii would be degraded.

How are the "non CLIP" peptides presented by Ctsl$^{\Delta TEC}$ cTECs generated, then? Two possible answers are presented in figure 21. According to the hypothesis A, positively-selecting peptides presented by Ctsl$^{\Delta TEC}$ cTECs might be a fraction of those presented by WT cTECs, e. g. the ones generated by the thymus-specific serine protease (TSSP), which is the only other protease that has been implicated in positive selection of MHCII-restricted thymocytes [72, 116, 117]. Alternatively, hypothesis B proposes a smaller overlap between WT and Ctsl$^{\Delta TEC}$ positively-selecting peptides, as new peptides might gain access to MHCII in the absence of CTSL. These peptides could either be newly generated by compensatory proteases or simply be present also in WT mice but gain access to MHCII only in the

absence of CTSL, because of their lower affinity for MHCII. We even cannot exclude that MHCII-SLIP/CLIP itself acts as a positive selecting signal.

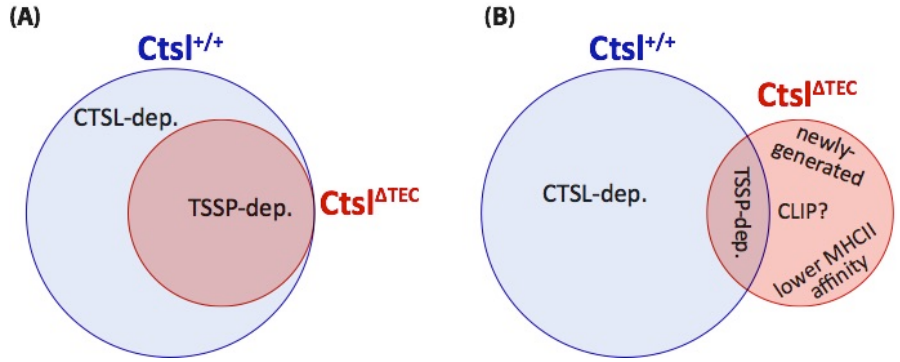

Figure 21: Theoretical overlap of positively-selecting peptides between WT and Ctsl$^{\Delta TEC}$ mice
We propose two hypotheses to describe the relationship between WT and Ctsl$^{\Delta TEC}$ positively-selecting peptides. According to (A), Ctsl$^{\Delta TEC}$ peptides would be a subset of WT peptides and would include, for example, peptides generated by the thymus-specific serine protease (TSSP). According to (B), WT and Ctsl$^{\Delta TEC}$ would be two distinct but intersecting sets. In this case, the non-overlapping CTSL-independent peptides could include the following, non mutually-exclusive options:
1) peptides generated as a consequence of compensatory upregulation of new proteases;
2) peptides that gain access to MHCII only in the absence of CTSL, because they have lower affinity to MHCII compared to CTSL-dependent peptides;
3) CLIP itself, which is clearly presented only by Ctsl$^{\Delta TEC}$ cTECs, but might not be involved in positive selection.

4.3 TCR diversity of CD4$^+$ T cells selected by Ctsl$^{\Delta TEC}$ mice

If a correlation exists between the diversity of positively-selecting peptides and the diversity of the selected TCR repertoire, as evidenced by "single-peptide:MHCII" mice [76-78], then the reduction in positively-selecting peptides seen in Ctsl$^{\Delta TEC}$ mice must be mirrored by a decrease in TCR specificities. We postulate two scenarios for the MHCII-restricted TCR repertoire selected in the absence of CTSL. In one case, depicted in figure 22A, Ctsl$^{\Delta TEC}$ TCRs might be a subset of WT TCRs. In the other case, shown by figure 22B, Ctsl$^{\Delta TEC}$ TCRs might be only partially overlapping with WT TCRs. In both cases we assume that the TCR diversity of Ctsl$^{\Delta TEC}$ mice is reduced compared to WT mice. We have several pieces of evidence supporting this theory: first of all, the fact that none of the seven MHCII-restricted TCRs we tested could be selected in Ctsl$^{\Delta TEC}$ mice (fig. 9) tells us that some WT TCRs are missing from the Ctsl$^{\Delta TEC}$ repertoire. Next, when we analyzed the number of LLO-specific cells in steady state and upon immunization, we were struck by the heterogeneity of Ctsl$^{\Delta TEC}$ samples (fig. 13 and 14A), which we attributed to an

oligoclonality of the TCR repertoire. TCR sequencing data eventually confirmed our suspicions, demonstrating that the Ctsl$^{\Delta TEC}$ vα2^{+} LLO-specific repertoire is less diverse than the WT one (fig. 15B). Although we need to sequence many more cells, these preliminary results show already a tiny overlap between Ctsl$^{\Delta TEC}$ and WT repertoires, therefore excluding the possibility that the two sets differ completely from one another. Whether model A or B describes this dataset better, we still cannot say.

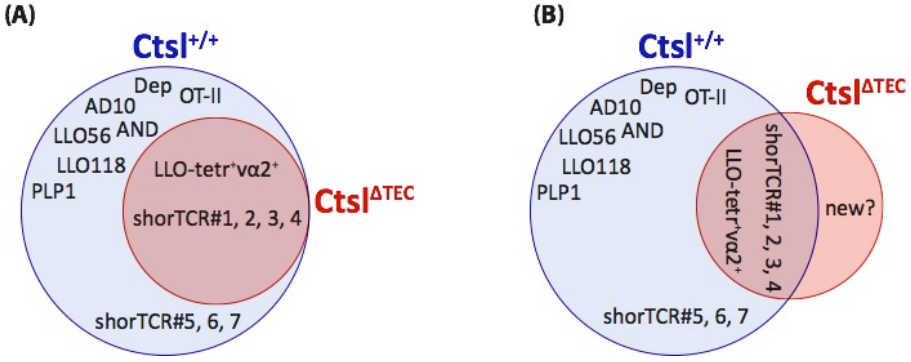

Figure 22: Theoretical overlap of CD4^{+} TCR repertoires between WT and Ctsl$^{\Delta TEC}$ mice
We propose two hypotheses to describe the relationship between WT and Ctsl$^{\Delta TEC}$ positively-selected MHCII-restricted TCRs. According to (A), Ctsl$^{\Delta TEC}$ TCRs are a subset of WT TCRs. According to (B), WT and Ctsl$^{\Delta TEC}$ are two distinct but intersecting sets. In both cases, overlapping TCRs include the vα2^{+} LLO:I-A^{b+} clone found with single-cell sequencing (red slice in fig. 15B) and the four CTSL-independent TCRs found in the shorT mouse (TCR#1, 2, 3, 4 highlighted in red in fig. 19A). TCRs found only in CTSL-sufficient mice contain the seven TCRs tested in BM chimera experiments (fig. 9) and the three CTSL-dependent TCRs detected in the shorT mouse (TCR#5, 6, 7 highlighted in blue in fig. 19A).

We soon realized that sequencing LLO-specific TCRs in the polyclonal setting is quite a challenge, although we focused only on the vα2^{+} subset. Furthermore, with this method, we cannot get an insight on the complexity of the entire repertoire. For these reasons, we decided to conduct our next TCR sequencing experiments on the shorT mouse model, where the TCR repertoire is restricted to a maximum of 10000 clones and we could capture the whole TCR diversity by deep sequencing. Also on this TCR-oligoclonal background, results indicated that the Ctsl$^{\Delta TEC}$ CD4^{+} TCR repertoire is less diverse than the WT counterpart, as shown by the lower Shannon diversity index (fig. 18A). Along these lines, the lower Shannon evenness (fig. 18B) and intra-genotype Morisita-Horn Index (MHI, fig. 18E) proved that oligoclonal expansions are common in the periphery of Ctsl$^{\Delta TEC}$ shorT mice. At this point, we could test if model A (fig. 22A) or B (fig. 22B) fitted the data better. To do so, we compared the similarity of the whole TCR

repertoires with each other and obtained an unexpectedly high overlap, according to the inter-genotype MHI (fig. 18D). The few non-overlapping clones turned out to be TCRs present in the WT but absent from the $Ctsl^{\Delta TEC}$ repertoire, and not vice versa. We named these TCRs "CTSL-dependent" and "CTSL-independent", respectively, and selected the main representatives for each category for further functional studies: TCR#5, 6 and 7 as "CTSL-dependent" and TCR#1, 2, 3 and 4 as "CTSL-independent" (fig. 19). Altogether, data obtained from the shorT background favor hypothesis A (fig. 22A). However, given the limited TCR diversity in this model, we think that data from the polyclonal background should be used to complement our finding.

4.4 TCR functionality of $CD4^+$ T cells selected by $Ctsl^{\Delta TEC}$ mice

Given the similarity between figures 21 and 22, it is very tempting to assume that positively-selecting peptides shape the selected TCRs in a 1:1 fashion. However, the peptides displayed by cTECs are clearly outnumbered by the potential diversity of the nascent TCR repertoire, so more TCRs have to contact a given peptide. At the same time, due to the extensive migration of thymocytes through the cortex, a single TCR clone might interact with numerous pMHC and the selection process might result from the sum of multiple signals. Due to this complexity, it is reasonable to think that a certain strength of TCR:pMHC interaction during positive selection does not simply rescue DP thymocytes from programmed cell-death, but also imprints a qualitative mark on the selected cells, which might ultimately determine their functionality as peripheral T cells. This idea is supported by the interesting case of the LLO56 and LLO118 TCRs, two TCRs that recognize the $LLO_{(190\text{-}205)}$ antigen with equal affinity and yet react to it in completely different ways [118]. The explanation for these different behaviors seems to lie in their respective thymic positively-selecting ligands: indeed, the strength of thymic TCR:pMHCII interactions, reflected by CD5 expression levels, is higher for the LLO56-TCR compared to the LLO118-TCR. This positively correlates with the phosphorylation of TCRζ and ERK, IL-2 secretion, calcium flux and the amount of activation-induced cell death upon antigenic stimulation. The result is that LLO118-TCR^+ cells are better responders during primary *Listeria* infections, as they undergo less apoptosis than LLO56-TCR^+ cells [85]. In a different study, the authors found a direct relationship between the degree of TCR self-reactivity (mirrored by CD5 expression) and the strength of binding to the agonist pMHCII [119], concluding

that positive selection favors the emergence of CD5^{high} T cells to ensure efficient recognition of pathogens. Although slightly contradictory, these examples argue that positive selection contributes to shaping the functionality of the mature T cell pool, through a process known as developmental TCR tuning (reviewed in [120]). As depicted in figure 23A, the positively-selecting signal(s) provided by cTECs might allow a developmental adaptation of the TCR signaling cascade, with high affinity interactions leading to higher expression of CD5, and presumably of other TCR-associated molecules.

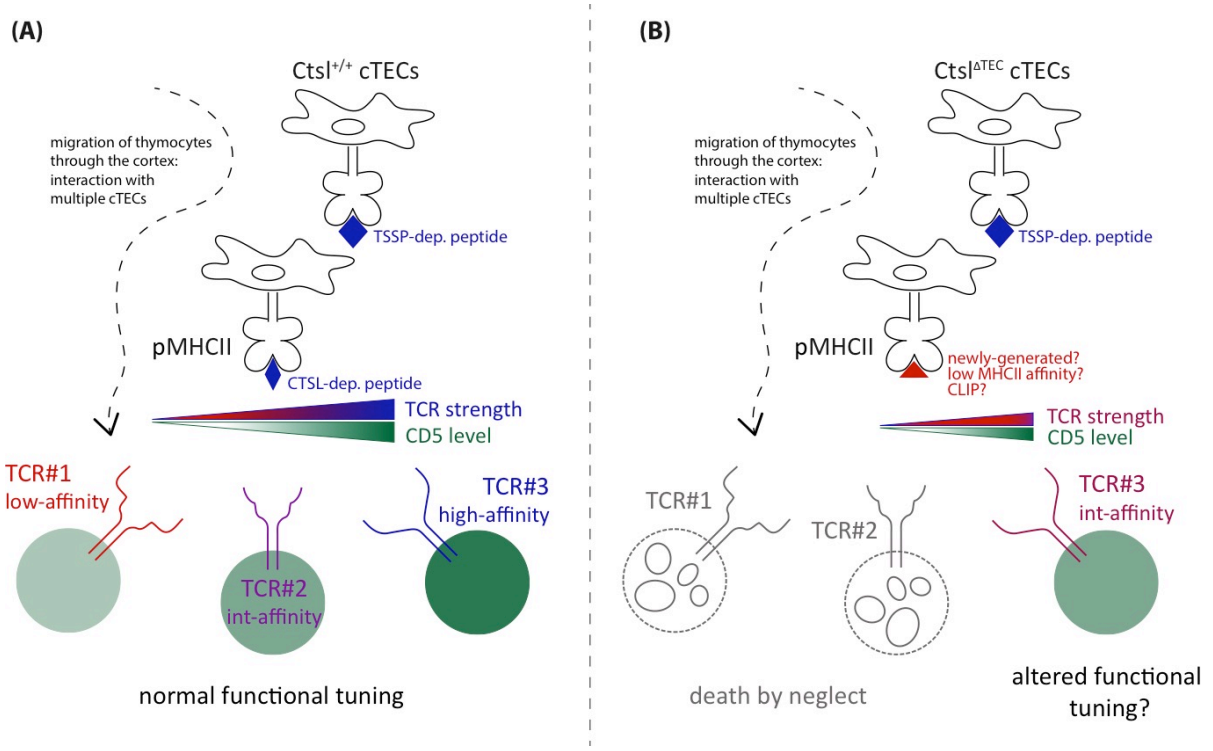

Figure 23: Developmental functional tuning of TCRs selected in WT and Ctsl$^{\Delta TEC}$ thymi
During their migration through the cortex, DP thymocytes encounter multiple peptides presented on cTECs. If the sum of these signals is comprised within the affinity range of positive selection, the thymocytes are rescued from cell death, undergo developmental TCR tuning and further maturation. On the left (A), WT cTECs induce positive selection of thymocytes across a wide range of TCR:pMHCII interaction affinities, thanks to the presentation of mainly CTSL-generated peptides. The strength of TCR signaling is used as a sensor to tune the expression levels of CD5, a transmembrane molecule that in turn act as a negative regulator of TCR activation. Thymocytes bearing moderately self-reactive TCRs will therefore express high CD5 levels. On the right (B), CTSL-deficient cTECs induce positive selection of thymocytes across a limited range of TCR:pMHCII interaction affinities, due to the lack of CTSL-generated peptides. On average, TCRs interact poorly with CTSL-independent peptides and, as a consequence of loss of binding, many thymocytes die by neglect (e.g. TCR#1 and 2). Given the decreased strength of TCR:pMHCII interactions, the average CD5 expression on Ctsl$^{\Delta TEC}$ thymocytes is lower than on WT cells. We hypothesize that some WT TCRs might be selected also in the Ctsl$^{\Delta TEC}$ background, but with altered affinities. This could lead to an altered functional tuning, i.e. to the very same T cell clone (such as the one expressing TCR#3) leaving the thymus with different CD5 expression levels in the two scenarios. TSSP: thymus-specific serine protease; dep: dependent; int: intermediate.

As for the significance of CD5, this marker can be used as readout of the intensity of recent TCR signaling events, not only in the thymus, but also in the periphery. Indeed, CD5 is upregulated upon TCR engagement in a negative feedback mechanism [41], which presumably dampens TCR signaling to restrain damage to the host. Self-pMHC recognition during development and homeostasis, as well as high-affinity cognate-pMHC interactions during infections might all contribute to tuning the CD5 levels that we measure at a given time. The case of Ctsl$^{\Delta TEC}$ mice is a peculiar one, as CD4^{+} T cells undergo enhanced homeostatic proliferation in their periphery due to the lymphopenic environment, as evidenced by the prevalent CD44^{high} phenotype of LN and splenic cells (data not shown). This chronic TCR engagement in the periphery of Ctsl$^{\Delta TEC}$ mice might be the reason why, although CD4SP thymocytes express suboptimal levels of CD5, CD3 and TCR, after thymic egress they catch up with WT T cells. In order to discard confounding effects due to lymphopenia-induced proliferation in the periphery of Ctsl$^{\Delta TEC}$ mice, we decided to perform all our functional experiments on CD4SP thymocytes.

We reasoned that, if positive selection directly shapes the functionality of mature T cells, Ctsl$^{\Delta TEC}$ mice should display impaired CD4^{+} T cell responses. First of all, we tested the self-reactivity of Ctsl$^{\Delta TEC}$ CD4SP thymocytes by co-transferring them together with WT thymocytes into sublethally irradiated WT recipients. 9 days after transfer, the thymocytes of Ctsl$^{\Delta TEC}$ origin had undergone less homeostatic proliferation than those of WT origin (fig. 11), implying that CD4^{+} T cells selected in the absence of CTSL are less self-reactive, as suggested by their lower CD5 expression (fig. 7C). To proceed with our functional characterization, we stimulated freshly isolated Ctsl$^{\Delta TEC}$ or WT CD4SP thymocytes *in vitro* with polyclonal stimuli such as anti-CD3/CD28 antibodies or PMA, which resulted in reduced activation of Ctsl$^{\Delta TEC}$ cells (fig. 12). Of note, anti-CD3/CD28 antibodies might not be the best stimulation strategy, because CD4SP cells selected by Ctsl$^{\Delta TEC}$ mice express reduced basal levels of CD3 and TCR (fig. 7C and data not shown). Thus a proximal TCR-bypassing stimulus such as PMA [121] might better serve the purpose, as its action should be independent of the surface levels of TCR and TCR-associated molecules. As a last piece of data, we co-transferred Ctsl$^{\Delta TEC}$ and WT CD4SP thymocytes into WT recipients and immunized them with LLO$_{(190\text{-}201)}$ peptide in CFA, which resulted in the expansion of LLO-specific cells only of WT (both donor and recipient) origin (fig. 14B).

Based on all these data, Ctsl$^{\Delta TEC}$ mice seem to select hypo-responsive CD4^{+} T cells. However, we cannot know if the impaired responsiveness we observed is due to the lack of specific TCR clones. The only way to uncouple TCR specificity from TCR functionality would be to compare CD4^{+} T cells expressing the very same TCR, selected either in the presence or absence of CTSL. Indeed, as outlined in figure 23B, we believe that CTSL-independent positively-selecting peptides might cause, on one hand, extensive death by neglect due to loss of binding between TCR and pMHCII. On the other hand, they might select by chance some TCRs found also in the WT repertoire, but with an altered affinity; this would lead to an altered developmental TCR tuning, which could result in a different functional outcome upon TCR stimulation in the periphery. In other words, truly "CTSL-independent" TCRs might not even exist. Re-expression of individual putative "CTSL-independent" TCRs in WT and Ctsl$^{\Delta TEC}$ retrogenic mice will help us test our hypothesis.

4.5 Lessons from the thymoproteasome

The purpose of positive selection seems to be the generation of the fittest T cell repertoire, both in terms of quantity (i.e. cell number) and of quality (i.e. TCR diversity and TCR tuning). Perturbation of the physiological positively-selecting peptides produced either by CTSL (pMHCII) or by the thymoproteasome (pMHCI) leads to the emergence of a severely impaired CD4^{+} or CD8^{+} T cell compartment, respectively. Indeed, many similarities exist between Ctsl$^{\Delta TEC}$ and β5t$^{-/-}$ mice, as summarized in table 2. The main differences between the two models derive from the multimolecular nature of the thymoproteasome. In β5t$^{-/-}$ mice, the β5i subunit of the immunoproteasome, as well as the β5 subunit of the constitutive proteasome, compensate for the loss of β5t in cTECs [64], thus generating more stable pMHCI and selecting more self-reactive CD8SP thymocytes (expressing more CD5) [64]. On the contrary, we have no evidence that other proteases compensate for the loss of CTSL in Ctsl$^{\Delta TEC}$ mice, which select less self-reactive CD4SP thymocytes (expressing less CD5). This might be part of the reason why we struggled to find a TCR that could be selected by Ctsl$^{\Delta TEC}$ mice, whereas many classical TCR^{tg} CD8^{+} T cells, such as OT-I cells, were readily selected by β5t$^{-/-}$ mice [63, 65]. When Rag$^{-/-}$ OT-I TCR^{tg} naïve T cells were analyzed in β5t$^{-/-}$ compared to WT mice, though, many functional differences were observed [65]. Indeed, cells selected in the absence of the thymoproteasome respond less to stimulation with anti-CD3/CD28 or cognate antigen *in vitro*, in terms of phosphorylation of TCRζ and

ERK, upregulation of CD69 and CD25, calcium flux and increase in cell size. Furthermore, they acquire a memory-like CD44^{high} phenotype in steady state and fail to differentiate into long-lived memory cells, upon infection with a *Listeria monocytogenes* strain expressing the OVA cognate peptide (LM-OVA). Differently from what observed for polyclonal CD8$^+$ T cells, the levels of CD5 on OT-I CD8SP thymocytes are decreased in β5t$^{-/-}$ mice, thus providing an explanation for the hyporesponsive phenotype. This is the first direct proof that positively-selecting peptides can influence the functionality of mature T cells.

	β5t$^{-/-}$ [62, 64]	**Ctsl$^{\Delta TEC}$** (unpublished)
phenotype	CD8$^+$ T cell lymphopenia	- Mild alopecia - CD4$^+$ T cell lymphopenia
T cell selection	80% reduction in positive selection of MHCI-restricted T cells (less CD69$^+$ TCRβ$^+$ DP cells) [64]	80% reduction in positive selection of MHCII-restricted T cells (less CD69$^+$ TCRβ$^+$ DP cells)
Not selected TCRs	HY [63]	Dep, OT-II, AND, AD10, LLO56, LLO118, PLP1
Selected TCRs	- OT-I, 2C in equal or higher amount [63] - P14, F5 in lower amount [63, 65]	- shorTCR#1, 2, 3, 4 - 1 LLO-specific vα2$^+$ clone
MHC on cTECs	- Reduced surface MHCI [64] - Different peptides presented on MHCI (stained with 25-D1.16) [63]	- Normal surface MHCII - Higher MHCII-SLIP/CLIP - Lower MHCII-non CLIP
Self-reactivity	Higher than WT in polyclonal (CD5, Nur77, CFSE^{lo}) [64]; lower than WT in monoclonal (OT-I, P14, F5) [65]	Lower than WT (CD5, CFSE^{lo})
Peripheral memory-like cells	Increased (CD44^{hi}, CD122$^+$) [64]	Increased (CD44^{hi})

Table 2: Comparison between β5t$^{-/-}$ and Ctsl$^{\Delta TEC}$ mice
The major characteristics of the thymoproteasome (β5t$^{-/-}$) and the conditional Ctsl (Ctsl$^{\Delta TEC}$) knock-out mouse models are listed in the table.

Genetic variants of the thymoproteasome-specific catalytic subunit β5t have been reported in humans. When some of these variants affecting the processing of β5t were knocked in the mouse genome, they led to decreased $CD8^+$ T cell production, especially in mice bearing the G49S homozygous mutation [122, 123]. A GWAS study on autoimmune diseases found an association between the homozygous G49S variant in the Japanese population and a higher risk for Sjögren's syndrome [123], underlining a possibly crucial function of the thymoproteasome in humans.

Unlike the thymoproteasome, CTSL is not expressed exclusively in cTECs. Two homologs of murine CTSL exist in humans: cathepsin L and cathepsin L2, otherwise known as cathepsin V (CTSV). The expression of human cathepsin L is quite ubiquitous, while CTSV is particularly abundant in cTECs, cornea, epidermis and testis [124]. The fact that CTSV is involved in Ii degradation [125] and that its expression in $Ctsl^{-/-}$ mice rescues $CD4^+$ T cell numbers and the epidermal phenotype [126, 127] suggests that CTSV might be the equivalent of CTSL in human positive selection. Regarding possible genetic variants of Ctsv affecting the $CD4^+$ T cell compartment, associations have been found between polymorphisms in the Ctsv gene and the incidence of type 1 diabetes and early-onset myasthenia gravis [128, 129]. However, the link between mutations in the thymoproteasome or Ctsv human genes and the development of autoimmunity has not been further investigated.

In conclusion, positive selection is crucial to generate an optimal amount of T cells expressing broadly-reactive and functional TCRs. A unique antigen-processing machinery, consisting of the thymoproteasome for MHCI and CTSL (or human CTSV) for MHCII, is expressed by cTECs to ensure the generation of peptides in the ideal range of TCR affinity to induce positive selection. This was so far proven in mice, but future TCR repertoire analysis of individuals bearing homozygous polymorphisms in β5t or Ctsv might help unravel the translational significance of murine findings.

5. References

1. Matsunaga, T. and A. Rahman, What brought the adaptive immune system to vertebrates?--The jaw hypothesis and the seahorse. Immunol Rev, 1998. **166**: p. 177-86.
2. Miller, J.F., Immunological function of the thymus. Lancet, 1961. **2**(7205): p. 748-9.
3. Miller, J.F.A.P., Effect of neonatal thymectomy on the immunological responsiveness of the mouse. Proceedings of the Royal Society of London. Series B. Biological Sciences, 1962. **156**(964): p. 415-428.
4. McIntire, K.R., S. Sell, and J.F. Miller, Pathogenesis of the Post-Neonatal Thymectomy Wasting Syndrome. Nature, 1964. **204**: p. 151-5.
5. Miller, J.F., Influence of Thymectomy on Tumor Induction by Polyoma Virus in C57bl Mice. Proc Soc Exp Biol Med, 1964. **116**: p. 323-7.
6. Roitt, I.M., et al., The cellular basis of immunological responses. A synthesis of some current views. Lancet, 1969. **2**(7616): p. 367-71.
7. Blackburn, C.C. and N.R. Manley, Developing a new paradigm for thymus organogenesis. Nat Rev Immunol, 2004. **4**(4): p. 278-89.
8. Lopes, N., et al., Thymic Crosstalk Coordinates Medulla Organization and T-Cell Tolerance Induction. Front Immunol, 2015. **6**: p. 365.
9. Klein, L., et al., Antigen presentation in the thymus for positive selection and central tolerance induction. Nat Rev Immunol, 2009. **9**(12): p. 833-44.
10. Laios, K., The thymus gland in ancient Greek medicine. Hormones (Athens), 2018. **17**(2): p. 285-286.
11. Fowlkes, B.J., et al., Early T lymphocytes. Differentiation in vivo of adult intrathymic precursor cells. J Exp Med, 1985. **162**(3): p. 802-22.
12. Abbas, A.K.L., A. H.; Pillai, S., Cellular and molecular immunology, 9th edition. 2018: Elsevier.
13. Shortman, K., et al., The generation and fate of thymocytes. Semin Immunol, 1990. **2**(1): p. 3-12.
14. Rodewald, H.R., et al., Intrathymically expressed c-kit ligand (stem cell factor) is a major factor driving expansion of very immature thymocytes in vivo. Immunity, 1995. **3**(3): p. 313-9.

15. von Freeden-Jeffry, U., et al., The earliest T lineage-committed cells depend on IL-7 for Bcl-2 expression and normal cell cycle progression. Immunity, 1997. **7**(1): p. 147-54.
16. Hozumi, K., et al., Delta-like 4 is indispensable in thymic environment specific for T cell development. J Exp Med, 2008. **205**(11): p. 2507-13.
17. Godfrey, D.I., et al., A developmental pathway involving four phenotypically and functionally distinct subsets of CD3-CD4-CD8- triple-negative adult mouse thymocytes defined by CD44 and CD25 expression. J Immunol, 1993. **150**(10): p. 4244-52.
18. Schwarzler, C., S. Oliferenko, and U. Gunthert, Variant isoforms of CD44 are required in early thymocyte development. Eur J Immunol, 2001. **31**(10): p. 2997-3005.
19. Porritt, H.E., et al., Heterogeneity among DN1 prothymocytes reveals multiple progenitors with different capacities to generate T cell and non-T cell lineages. Immunity, 2004. **20**(6): p. 735-45.
20. Schmitt, T.M., et al., Maintenance of T cell specification and differentiation requires recurrent notch receptor-ligand interactions. J Exp Med, 2004. **200**(4): p. 469-79.
21. Lind, E.F., et al., Mapping precursor movement through the postnatal thymus reveals specific microenvironments supporting defined stages of early lymphoid development. J Exp Med, 2001. **194**(2): p. 127-34.
22. Burtrum, D.B., et al., TCR gene recombination and alpha beta-gamma delta lineage divergence: productive TCR-beta rearrangement is neither exclusive nor preclusive of gamma delta cell development. J Immunol, 1996. **157**(10): p. 4293-6.
23. von Boehmer, H., Unique features of the pre-T-cell receptor alpha-chain: not just a surrogate. Nat Rev Immunol, 2005. **5**(7): p. 571-7.
24. Hayes, S.M., L. Li, and P.E. Love, TCR signal strength influences alphabeta/gammadelta lineage fate. Immunity, 2005. **22**(5): p. 583-93.
25. Haks, M.C., et al., Attenuation of gammadeltaTCR signaling efficiently diverts thymocytes to the alphabeta lineage. Immunity, 2005. **22**(5): p. 595-606.
26. Yang, X. and R.A. Mariuzza, Pre-T-cell receptor binds MHC: Implications for thymocyte signaling and selection. Proc Natl Acad Sci U S A, 2015. **112**(27): p. 8166-7.
27. Petrie, H.T., et al., Development of immature thymocytes: initiation of CD3, CD4, and CD8 acquisition parallels down-regulation of the interleukin 2 receptor alpha chain. Eur J Immunol, 1990. **20**(12): p. 2813-5.

28. Corthay, A., K.S. Nandakumar, and R. Holmdahl, Evaluation of the percentage of peripheral T cells with two different T cell receptor alpha-chains and of their potential role in autoimmunity. J Autoimmun, 2001. **16**(4): p. 423-9.

29. Davis, M.M., et al., Ligand recognition by alpha beta T cell receptors. Annu Rev Immunol, 1998. **16**: p. 523-44.

30. Casrouge, A., et al., Size estimate of the alpha beta TCR repertoire of naive mouse splenocytes. J Immunol, 2000. **164**(11): p. 5782-7.

31. Arstila, T.P., et al., A direct estimate of the human alphabeta T cell receptor diversity. Science, 1999. **286**(5441): p. 958-61.

32. La Gruta, N.L., et al., Understanding the drivers of MHC restriction of T cell receptors. Nat Rev Immunol, 2018. **18**(7): p. 467-478.

33. Zerrahn, J., W. Held, and D.H. Raulet, The MHC reactivity of the T cell repertoire prior to positive and negative selection. Cell, 1997. **88**(5): p. 627-36.

34. Van Laethem, F., et al., Deletion of CD4 and CD8 coreceptors permits generation of alphabetaT cells that recognize antigens independently of the MHC. Immunity, 2007. **27**(5): p. 735-50.

35. Klein, L., et al., Positive and negative selection of the T cell repertoire: what thymocytes see (and don't see). Nat Rev Immunol, 2014. **14**(6): p. 377-91.

36. Davey, G.M., et al., Preselection thymocytes are more sensitive to T cell receptor stimulation than mature T cells. J Exp Med, 1998. **188**(10): p. 1867-74.

37. Li, Q.J., et al., miR-181a is an intrinsic modulator of T cell sensitivity and selection. Cell, 2007. **129**(1): p. 147-61.

38. Lo, W.L., D.L. Donermeyer, and P.M. Allen, A voltage-gated sodium channel is essential for the positive selection of CD4(+) T cells. Nat Immunol, 2012. **13**(9): p. 880-7.

39. Wang, D., et al., Tespa1 is involved in late thymocyte development through the regulation of TCR-mediated signaling. Nat Immunol, 2012. **13**(6): p. 560-8.

40. Choi, S., et al., THEMIS enhances TCR signaling and enables positive selection by selective inhibition of the phosphatase SHP-1. Nat Immunol, 2017. **18**(4): p. 433-441.

41. Azzam, H.S., et al., CD5 expression is developmentally regulated by T cell receptor (TCR) signals and TCR avidity. J Exp Med, 1998. **188**(12): p. 2301-11.

42. Yamashita, I., et al., CD69 cell surface expression identifies developing thymocytes which audition for T cell antigen receptor-mediated positive selection. Int Immunol, 1993. **5**(9): p. 1139-50.
43. Surh, C.D. and J. Sprent, T-cell apoptosis detected in situ during positive and negative selection in the thymus. Nature, 1994. **372**(6501): p. 100-3.
44. McCaughtry, T.M., et al., Clonal deletion of thymocytes can occur in the cortex with no involvement of the medulla. J Exp Med, 2008. **205**(11): p. 2575-84.
45. Mallaun, M., et al., The T cell receptor's alpha-chain connecting peptide motif promotes close approximation of the CD8 coreceptor allowing efficient signal initiation. J Immunol, 2008. **180**(12): p. 8211-21.
46. Mallaun, M., G. Zenke, and E. Palmer, A discrete affinity-driven elevation of ZAP-70 kinase activity initiates negative selection. J Recept Signal Transduct Res, 2010. **30**(6): p. 430-43.
47. Melichar, H.J., et al., Distinct temporal patterns of T cell receptor signaling during positive versus negative selection in situ. Sci Signal, 2013. **6**(297): p. ra92.
48. Daniels, M.A., et al., Thymic selection threshold defined by compartmentalization of Ras/MAPK signalling. Nature, 2006. **444**(7120): p. 724-9.
49. McNeil, L.K., T.K. Starr, and K.A. Hogquist, A requirement for sustained ERK signaling during thymocyte positive selection in vivo. Proc Natl Acad Sci U S A, 2005. **102**(38): p. 13574-9.
50. Brugnera, E., et al., Coreceptor reversal in the thymus: signaled CD4+8+ thymocytes initially terminate CD8 transcription even when differentiating into CD8+ T cells. Immunity, 2000. **13**(1): p. 59-71.
51. Etzensperger, R., et al., Identification of lineage-specifying cytokines that signal all CD8(+)-cytotoxic-lineage-fate 'decisions' in the thymus. Nat Immunol, 2017. **18**(11): p. 1218-1227.
52. Bosselut, R., et al., Strength of signaling by CD4 and CD8 coreceptor tails determines the number but not the lineage direction of positively selected thymocytes. Immunity, 2001. **14**(4): p. 483-94.
53. Sansom, S.N., et al., Population and single-cell genomics reveal the Aire dependency, relief from Polycomb silencing, and distribution of self-antigen expression in thymic epithelia. Genome Res, 2014. **24**(12): p. 1918-31.

54. Anderson, M.S., et al., Projection of an immunological self shadow within the thymus by the aire protein. Science, 2002. **298**(5597): p. 1395-401.

55. Takaba, H., et al., Fezf2 Orchestrates a Thymic Program of Self-Antigen Expression for Immune Tolerance. Cell, 2015. **163**(4): p. 975-87.

56. Hinterberger, M., et al., Autonomous role of medullary thymic epithelial cells in central CD4(+) T cell tolerance. Nat Immunol, 2010. **11**(6): p. 512-9.

57. Perry, J.S.A., et al., Transfer of Cell-Surface Antigens by Scavenger Receptor CD36 Promotes Thymic Regulatory T Cell Receptor Repertoire Development and Allo-tolerance. Immunity, 2018. **48**(6): p. 1271.

58. Yamano, T., et al., Thymic B Cells Are Licensed to Present Self Antigens for Central T Cell Tolerance Induction. Immunity, 2015. **42**(6): p. 1048-61.

59. Lio, C.W. and C.S. Hsieh, A two-step process for thymic regulatory T cell development. Immunity, 2008. **28**(1): p. 100-11.

60. Xing, Y., et al., Late stages of T cell maturation in the thymus involve NF-kappaB and tonic type I interferon signaling. Nat Immunol, 2016. **17**(5): p. 565-73.

61. Murata, S., et al., The immunoproteasome and thymoproteasome: functions, evolution and human disease. Nat Immunol, 2018. **19**(9): p. 923-931.

62. Murata, S., et al., Regulation of CD8+ T cell development by thymus-specific proteasomes. Science, 2007. **316**(5829): p. 1349-53.

63. Nitta, T., et al., Thymoproteasome shapes immunocompetent repertoire of CD8+ T cells. Immunity, 2010. **32**(1): p. 29-40.

64. Xing, Y., S.C. Jameson, and K.A. Hogquist, Thymoproteasome subunit-beta5T generates peptide-MHC complexes specialized for positive selection. Proc Natl Acad Sci U S A, 2013. **110**(17): p. 6979-84.

65. Takada, K., et al., TCR affinity for thymoproteasome-dependent positively selecting peptides conditions antigen responsiveness in CD8(+) T cells. Nat Immunol, 2015. **16**(10): p. 1069-76.

66. Kincaid, E.Z., et al., Specialized proteasome subunits have an essential role in the thymic selection of CD8(+) T cells. Nat Immunol, 2016. **17**(8): p. 938-45.

67. Nedjic, J., et al., Autophagy in thymic epithelium shapes the T-cell repertoire and is essential for tolerance. Nature, 2008. **455**(7211): p. 396-400.

68. Flajnik, M.F. and M. Kasahara, Origin and evolution of the adaptive immune system: genetic events and selective pressures. Nat Rev Genet, 2010. **11**(1): p. 47-59.
69. Nakagawa, T., et al., Cathepsin L: critical role in Ii degradation and CD4 T cell selection in the thymus. Science, 1998. **280**(5362): p. 450-3.
70. Nakagawa, T.Y., et al., Impaired invariant chain degradation and antigen presentation and diminished collagen-induced arthritis in cathepsin S null mice. Immunity, 1999. **10**(2): p. 207-17.
71. Honey, K., et al., Cathepsin L regulates CD4+ T cell selection independently of its effect on invariant chain: a role in the generation of positively selecting peptide ligands. J Exp Med, 2002. **195**(10): p. 1349-58.
72. Gommeaux, J., et al., Thymus-specific serine protease regulates positive selection of a subset of CD4+ thymocytes. Eur J Immunol, 2009. **39**(4): p. 956-64.
73. Marrack, P., et al., Comparison of peptides bound to spleen and thymus class II. J Exp Med, 1993. **178**(6): p. 2173-83.
74. Miyazaki, T., et al., Mice lacking H2-M complexes, enigmatic elements of the MHC class II peptide-loading pathway. Cell, 1996. **84**(4): p. 531-41.
75. Grubin, C.E., et al., Deficient positive selection of CD4 T cells in mice displaying altered repertoires of MHC class II-bound self-peptides. Immunity, 1997. **7**(2): p. 197-208.
76. Barton, G.M. and A.Y. Rudensky, Requirement for diverse, low-abundance peptides in positive selection of T cells. Science, 1999. **283**(5398): p. 67-70.
77. Barton, G.M., et al., Positive selection of self-MHC-reactive T cells by individual peptide-MHC class II complexes. Proc Natl Acad Sci U S A, 2002. **99**(10): p. 6937-42.
78. Wong, P., et al., Dynamic tuning of T cell reactivity by self-peptide-major histocompatibility complex ligands. J Exp Med, 2001. **193**(10): p. 1179-87.
79. von Rohrscheidt, J., et al., Thymic CD4 T cell selection requires attenuation of March8-mediated MHCII turnover in cortical epithelial cells through CD83. J Exp Med, 2016. **213**(9): p. 1685-94.
80. Markowitz, D., et al., Retroviral gene transfer using safe and efficient packaging cell lines. Ann N Y Acad Sci, 1990. **612**: p. 407-14.
81. Grignani, F., et al., High-efficiency gene transfer and selection of human hematopoietic progenitor cells with a hybrid EBV/retroviral vector expressing the green fluorescence protein. Cancer Res, 1998. **58**(1): p. 14-9.

82. Roth, W., et al., Cathepsin L deficiency as molecular defect of furless: hyperproliferation of keratinocytes and pertubation of hair follicle cycling. FASEB J, 2000. **14**(13): p. 2075-86.

83. Klein, L., et al., CD4 T cell tolerance to human C-reactive protein, an inducible serum protein, is mediated by medullary thymic epithelium. J Exp Med, 1998. **188**(1): p. 5-16.

84. Wang, L., et al., Epitope-Specific Tolerance Modes Differentially Specify Susceptibility to Proteolipid Protein-Induced Experimental Autoimmune Encephalomyelitis. Front Immunol, 2017. **8**: p. 1511.

85. Weber, K.S., et al., Distinct CD4+ helper T cells involved in primary and secondary responses to infection. Proc Natl Acad Sci U S A, 2012. **109**(24): p. 9511-6.

86. Kaye, J., et al., Selective development of CD4+ T cells in transgenic mice expressing a class II MHC-restricted antigen receptor. Nature, 1989. **341**(6244): p. 746-9.

87. Rossi, S.W., et al., Keratinocyte growth factor (KGF) enhances postnatal T-cell development via enhancements in proliferation and function of thymic epithelial cells. Blood, 2007. **109**(9): p. 3803-11.

88. Zijlstra, M., et al., Germ-line transmission of a disrupted beta 2-microglobulin gene produced by homologous recombination in embryonic stem cells. Nature, 1989. **342**(6248): p. 435-8.

89. Cosgrove, D., et al., Mice lacking MHC class II molecules. Cell, 1991. **66**(5): p. 1051-66.

90. Mombaerts, P., et al., RAG-1-deficient mice have no mature B and T lymphocytes. Cell, 1992. **68**(5): p. 869-77.

91. Barnden, M.J., et al., Defective TCR expression in transgenic mice constructed using cDNA-based alpha- and beta-chain genes under the control of heterologous regulatory elements. Immunol Cell Biol, 1998. **76**(1): p. 34-40.

92. Klugmann, M., et al., Assembly of CNS myelin in the absence of proteolipid protein. Neuron, 1997. **18**(1): p. 59-70.

93. Mombaerts, P., et al., Mutations in T-cell antigen receptor genes alpha and beta block thymocyte development at different stages. Nature, 1992. **360**(6401): p. 225-31.

94. Kouskoff, V., et al., Cassette vectors directing expression of T cell receptor genes in transgenic mice. J Immunol Methods, 1995. **180**(2): p. 273-80.

95. Alamyar, E., et al., IMGT((R)) tools for the nucleotide analysis of immunoglobulin (IG) and T cell receptor (TR) V-(D)-J repertoires, polymorphisms, and IG mutations: IMGT/V-QUEST and IMGT/HighV-QUEST for NGS. Methods Mol Biol, 2012. **882**: p. 569-604.

96. Nazarov, V.I., et al., tcR: an R package for T cell receptor repertoire advanced data analysis. BMC Bioinformatics, 2015. **16**: p. 175.

97. Yang, S., et al., Development of optimal bicistronic lentiviral vectors facilitates high-level TCR gene expression and robust tumor cell recognition. Gene Ther, 2008. **15**(21): p. 1411-23.

98. Irla, M., et al., Autoantigen-specific interactions with CD4+ thymocytes control mature medullary thymic epithelial cell cellularity. Immunity, 2008. **29**(3): p. 451-63.

99. Moon, J.J., et al., Naive CD4(+) T cell frequency varies for different epitopes and predicts repertoire diversity and response magnitude. Immunity, 2007. **27**(2): p. 203-13.

100. Nelson, R.W., et al., T cell receptor cross-reactivity between similar foreign and self peptides influences naive cell population size and autoimmunity. Immunity, 2015. **42**(1): p. 95-107.

101. Correia-Neves, M., et al., The shaping of the T cell repertoire. Immunity, 2001. **14**(1): p. 21-32.

102. Pacholczyk, R., et al., Origin and T cell receptor diversity of Foxp3+CD4+CD25+ T cells. Immunity, 2006. **25**(2): p. 249-59.

103. Kouskoff, V., et al., A vector driving the expression of foreign cDNAs in the MHC class II-positive cells of transgenic mice. J Immunol Methods, 1993. **166**(2): p. 287-91.

104. Holst, J., et al., Generation of T-cell receptor retrogenic mice. Nat Protoc, 2006. **1**(1): p. 406-17.

105. Reinheckel, T., et al., The lysosomal cysteine protease cathepsin L regulates keratinocyte proliferation by control of growth factor recycling. J Cell Sci, 2005. **118**(Pt 15): p. 3387-95.

106. Potts, W., et al., Cathepsin L-deficient mice exhibit abnormal skin and bone development and show increased resistance to osteoporosis following ovariectomy. Int J Exp Pathol, 2004. **85**(2): p. 85-96.

107. Petermann, I., et al., Lysosomal, cytoskeletal, and metabolic alterations in cardiomyopathy of cathepsin L knockout mice. FASEB J, 2006. **20**(8): p. 1266-8.

108. Stypmann, J., et al., Dilated cardiomyopathy in mice deficient for the lysosomal cysteine peptidase cathepsin L. Proc Natl Acad Sci U S A, 2002. **99**(9): p. 6234-9.
109. Spira, D., et al., Cell type-specific functions of the lysosomal protease cathepsin L in the heart. J Biol Chem, 2007. **282**(51): p. 37045-52.
110. Funkelstein, L., et al., Unique biological function of cathepsin L in secretory vesicles for biosynthesis of neuropeptides. Neuropeptides, 2010. **44**(6): p. 457-66.
111. Yang, M., et al., Cathepsin L activity controls adipogenesis and glucose tolerance. Nat Cell Biol, 2007. **9**(8): p. 970-7.
112. Maehr, R., et al., Cathepsin L is essential for onset of autoimmune diabetes in NOD mice. J Clin Invest, 2005. **115**(10): p. 2934-43.
113. Honey, K., et al., Thymocyte expression of cathepsin L is essential for NKT cell development. Nat Immunol, 2002. **3**(11): p. 1069-74.
114. Symington, F.W. and J. Sprent, A monoclonal antibody detecting an Ia specificity mapping in the I-A or I-E subregion. Immunogenetics, 1981. **14**(1-2): p. 53-61.
115. Fung-Leung, W.P., et al., Antigen presentation and T cell development in H2-M-deficient mice. Science, 1996. **271**(5253): p. 1278-81.
116. Viret, C., et al., Thymus-specific serine protease contributes to the diversification of the functional endogenous CD4 T cell receptor repertoire. J Exp Med, 2011. **208**(1): p. 3-11.
117. Viret, C., et al., The T Cell Repertoire-Diversifying Enzyme TSSP Contributes to Thymic Selection of Diabetogenic CD4 T Cell Specificities Reactive to ChgA and IAPP Autoantigens. J Immunol, 2015. **195**(5): p. 1964-73.
118. Persaud, S.P., et al., Intrinsic CD4+ T cell sensitivity and response to a pathogen are set and sustained by avidity for thymic and peripheral complexes of self peptide and MHC. Nat Immunol, 2014. **15**(3): p. 266-74.
119. Mandl, J.N., et al., T cell-positive selection uses self-ligand binding strength to optimize repertoire recognition of foreign antigens. Immunity, 2013. **38**(2): p. 263-274.
120. Kim, H.O. and J.H. Cho, T Cell's Sense of Self: a Role of Self-Recognition in Shaping Functional Competence of Naive T Cells. Immune Netw, 2017. **17**(4): p. 201-213.
121. Rosenstreich, D.L. and S.B. Mizel, Signal requirements for T lymphocyte activation. I. Replacement of macrophage function with phorbol myristic acetate. J Immunol, 1979. **123**(4): p. 1749-54.

122. Ohigashi, I., et al., A human PSMB11 variant affects thymoproteasome processing and CD8+ T cell production. JCI Insight, 2017. **2**(10).
123. Nitta, T., et al., Human thymoproteasome variations influence CD8 T cell selection. Sci Immunol, 2017. **2**(12).
124. Bromme, D., et al., Human cathepsin V functional expression, tissue distribution, electrostatic surface potential, enzymatic characterization, and chromosomal localization. Biochemistry, 1999. **38**(8): p. 2377-85.
125. Tolosa, E., et al., Cathepsin V is involved in the degradation of invariant chain in human thymus and is overexpressed in myasthenia gravis. J Clin Invest, 2003. **112**(4): p. 517-26.
126. Sevenich, L., et al., Expression of human cathepsin L or human cathepsin V in mouse thymus mediates positive selection of T helper cells in cathepsin L knock-out mice. Biochimie, 2010. **92**(11): p. 1674-80.
127. Hagemann, S., et al., The human cysteine protease cathepsin V can compensate for murine cathepsin L in mouse epidermis and hair follicles. Eur J Cell Biol, 2004. **83**(11-12): p. 775-80.
128. Viken, M.K., et al., Polymorphisms in the cathepsin L2 (CTSL2) gene show association with type 1 diabetes and early-onset myasthenia gravis. Hum Immunol, 2007. **68**(9): p. 748-55.
129. Reiser, J., B. Adair, and T. Reinheckel, Specialized roles for cysteine cathepsins in health and disease. J Clin Invest, 2010. **120**(10): p. 3421-31.

6. Acknowledgements

This thesis is the product of four years of intense, at times frustrating, but also engaging and passionate work, which I definitely would repeat, if I had to go back. It's hard to decide where to start with acknowledgements, as many people contributed to the project with their precious friendship, help and guidance throughout this time. However, two people deserve to be acknowledged above all: **my parents**. *Grazie di tutto, Posi*. I feel extremely lucky to have a family that supported me in every decision, from studying in Milan to moving abroad. I really appreciate your constant presence and positive energy, which has always motivated me and will always do! If I think of the very beginning in Willibaldstrasse, I guess I would not have made it so far without your encouragement…

Now it's time to thank the ones who actively took part in my PhD project. First of all, **Ludger**, who convinced me to join his lab with his enthusiastic and open attitude, after hosting me twice in the Goethestrasse to avoid any kind of videocall. The first thing I learnt from you is the importance of face-to-face communication. Thanks for letting me always be independent, for treating me like a peer, for giving me the opportunity to travel to many international conferences and develop as a scientist, for teaching me that "less is more", for trusting me. I am very grateful for your supervision!

The third biggest "thanks" goes to **Sarina**, the friendliest collaborator I could ask for. Thanks for being always so patient throughout our endless emails, for your relaxed and practical attitude towards huge amounts of data, for taking the time to show me around in Hannover and to visit us in Munich, in spite of your small kids.

Thanks to **Jelena**, who conceived and started the project. Thanks for showing me that science can be extremely exciting and that reading is the most important part of a researcher´s work. Thanks to you, I also learnt to prioritize my private life over work. Needless to say, the project would not be where it is without you.

Danke **Ursula**, you were the first person I met at the Ifi and you immediately made me feel at home. Thanks for taking care of us all the time in such a sweet and loving way. You also taught me that speaking German can be nice! And of course, thanks for "the rocket"… it´s in safe hands now.

An enormous "thanks" goes to all the past and current Klein lab members. In particular: thanks, **Christine**, for your daily help in the lab and for teaching me how to ski (you did well, I was the problem!). Thanks, **Madlen** and **Lena**, for always being there to discuss science or life issues. Thanks, **Tomo**, for your intellectual help and mentoring. Thanks **Stefan**, **Sebi** and **Manu**: you were always helping when I needed it, and even when I didn´t. Thanks, **Lisa**, for being unofficially part of the Klein's: the office and the sorters would not be the same without you! Thanks **Barbara**, **Sabine** and **Jenny** for your friendly attitude in spite of the countless minis.

My gratitude goes also to the big **BIF** family, especially to **Claudia** and **Anja**, for the lovely and informal atmosphere you could create at any event I was attending. Thanks for choosing to support my project but also, and most importantly, for introducing to me amazing people like **Maria** and **Mirjam**!

The most important contribution to my mental health over the past years was certainly made by the "Italian crew" in Munich (**Gianlu**, **Giorgia M.**, **Benni**, **Nico**, **Vale**, **Giorgia P.**). Thanks for always letting me be myself, for sharing the same worries and complaints, for talking all at once and yet being able to listen… but, most of all, for being LOUD. *Vi voglio bene!*

Merci, **Aurore**, for accepting so many Italians around you, for always being so chilled and natural, for your constant presence and warm-heartedness… seeing you *pompette* was a rare but priceless experience.

*Grazie, **Nonna** e **Zia**, per avermi sempre sostenuta, coccolata e seguita sia da casa che in trasferta. Siete uniche!!! Grazie, **Nonno**, per l'interesse che mostri sempre nei confronti della mia ricerca e per essere l'esempio vivente che leggere e studiare mantiene giovani e attivi. Sono sicura che proverai a leggere questa tesi!*

My gratitude still goes to the "**Lab17"** in Milan, which brought me a lot of things but not bad luck. Thanks, **Super Vero**, for teaching me basically everything I know about bench work, for keeping contact after I moved to Munich and always finding time to meet me after all these years, especially on short notice. Thanks, **Anna**, for making me fall in love with immunology during your classes: you are the reason why I decided to work in this field.

Grazie, amici romagnoli, for being my reference point and never changing over the years! Thanks **Elly**, **Reby**, **Je**, **Marci**, **Arge** and **Ali** for making the 26th of December special

since “ten” years, for losing count of how long we’ve celebrated together, because it anyways feels like a lifetime. Thanks for being part of my family!

Second-last but not least, I’d like to thank my irreplaceable travel mates **Clau**, **Eli** and **Zambi**. No matter where we end up living, I will always count on our summer holidays and on our 6 o’-clock departures from Barcelona. Thanks to you, I know that true friendship knows no distance (although it can be suddenly disrupted by an alarm clock at 4 a.m.)!

As last, I would like to acknowledge the two most important people in my life. Thank you, **Tobi**, for generating the LLO tetramer “on the spot”, for your never-ending optimism and thoughtfulness, for being so spontaneous and creative, for always asking twice how I am, for the “clownyness” that makes you team up with Giorgio. I cannot imagine a scenario where you didn’t fall into my trap. *Grazie,* **Bosa**, for the countless calls when I needed to be cheered up or when I was bored. Thanks for all the amazing time we spent together in the last 26 years, for being as stupid as I am and for making me laugh, sometimes uncontrollably. Words cannot describe how much I love you and how grateful I am to have you both.

7. Appendix

7.1 List of abbreviations

Aire	autoimmune regulator
AmpR	ampicillin resistance
APC	antigen-presenting cell
β5	β5 subunit of the constitutive proteasome
β5i	β5 subunit of the immunoproteasome
β5t	β5 subunit of the thymoproteasome
BM	bone marrow
bp	base pair
C	constant gene
C2TAkd	C2TA knock-down
CD	cluster of differentiation
CDR	complementarity determining region
CFA	complete Freund adjuvant
CFSE	carboxyfluorescein succinimidyl ester
CLIP	class-II associated invariant chain peptide
cTEC	cortical thymic epithelial cell
C-terminal	carboxy-terminal
ctrl	control
Ctsl/CTSL	cathepsin L gene/protein
$Ctsl^{\Delta TEC}$	conditional knock-out of Ctsl in thymic epithelial cells
Ctsv/CTSV	cathepsin V gene/protein
D	diversity gene
DC	dendritic cell
DLL4	delta ligand like 4
dLN	draining lymph node
DN	double negative
dNTP	deoxyribonucleoside tri-phosphate
DP	double positive

EBV	Epstein-Barr virus
E_H	Shannon index evenness
ER	endoplasmic reticulum
ERAAP	ER aminopeptidase associated with antigen processing
FACS	fluorescence activated cell sorter (trademark of BD)
Fezf2	FEZ family zinc finger 2
FSC-A	forward scatter area
FTOC	fetal thymic organ culture
GWAS	genome wide association study
Gy	Gray
H	Shannon diversity index
hCD2	human CD2
hCRP	human C reactive protein
hIi	human invariant chain
Ii	invariant chain
IL	interleukin
i.p.	intra-peritoneal
ITAM	immunotyrosine activation motif
i.v.	intra-venous
J	joining gene
ko	knock-out
LLO	listeriolysin O
LN	lymph node
LTR	long-terminal repeat
M1	mature 1
M2	mature 2
MCC	moth cytochrome C
MESV	murine embryonic stem cell virus
MFI	mean fluorescence intensity
MHCI	major histocompatibility complex class I
MHCII	major histocompatibility complex class II
MHI	Morisita Horn index

MIIC	MHCII loading compartment
MMLV	Moloney murine leukemia virus
mTEC	medullary thymic epithelial cell
NK	natural killer
ns	not significant
N-terminal	amino-terminal
ori	origin of replication
OVA	ovalbumin
PCC	pigeon cytochrome C
PLP/Plp	proteolipid protein/gene
PMA	phorbol myristate acetate
pTα	pre T cell receptor α
PuroR	puromycin resistance
Rag/RAG	recombination activating gene/protein
SCF	stem cell factor
SD	standard deviation
self-pMHC	self-peptides on major histocompatibility complex
SEM	standard error of the mean
SLIP	small leupeptin-induced peptide
SM	semi-mature
SP	single positive
TAP	transporter associated with antigen processing
Tconv	T conventional cell
TCR	T cell receptor
TCR^{tg}	T cell receptor transgenic
TD	touch-down
TdT	terminal deoxyribonucleotidyl transferase
TRA	tissue restricted antigen
TRAC	T cell receptor α constant gene
TRAJ	T cell receptor α joining gene
TRAV	T cell receptor α variable gene
TRBC	T cell receptor β constant gene

TRBD	T cell receptor β diversity gene
TRBJ	T cell receptor β joining gene
TRBV	T cell receptor β variable gene
Treg	T regulatory cell
TSSP	thymus specific serine protease
UV	ultra-violet
V	variable gene
WT	wild type

7.2 List of figures

7.3 List of tables

7.4 List of plasmid maps

LMU LUDWIG-MAXIMILIANS-UNIVERSITÄT MÜNCHEN

Dekanat Medizinische Fakultät
Promotionsbüro

Affidavit

Petrozziello, Elisabetta

Surname, first name

Address

I hereby declare, that the submitted thesis entitled

The role of cathepsin L in shaping a functional CD4 T cell repertoire

is my own work. I have only used the sources indicated and have not made unauthorised use of services of a third party. Where the work of others has been quoted or reproduced, the source is always given.

I further declare that the submitted thesis or parts thereof have not been presented as part of an examination degree to any other university.

Munich, 26/02/2019
Place, Date

Elisabetta Petrozziello
Signature doctoral candidate